40201

National Library of Canada | Bibliothèque nationale du Canada

CANADIAN THESES ON MICROFICHE | THÈSES CANADIENNES SUR MICROFICHE

NAME OF AUTHOR/*NOM DE L'AUTEUR* DENNIS KIKUCHI

TITLE OF THESIS/*TITRE DE LA THÈSE* STRENGTH VARIABILITY OF BONDED PRESTRESSED CONCRETE BEAMS

UNIVERSITY/*UNIVERSITÉ* UNIVERSITY OF ALBERTA

DEGREE FOR WHICH THESIS WAS PRESENTED/*GRADE POUR LEQUEL CETTE THÈSE FUT PRÉSENTÉE* M.Sc.

YEAR THIS DEGREE CONFERRED/*ANNÉE D'OBTENTION DE CE GRADE* 1978

NAME OF SUPERVISOR/*NOM DU DIRECTEUR DE THÈSE* MacGregor

Permission is hereby granted to the NATIONAL LIBRARY OF CANADA to microfilm this thesis and to lend or sell copies of the film.

The author reserves other publication rights, and neither the thesis nor extensive extracts from it may be printed or otherwise reproduced without the author's written permission.

L'autorisation est, par la présente, accordée à la BIBLIOTHÈQUE NATIONALE DU CANADA de microfilmer cette thèse et de prêter ou de vendre des exemplaires du film.

L'auteur se réserve les autres droits de publication; ni la thèse ni de longs extraits de celle-ci ne doivent être imprimés ou autrement reproduits sans l'autorisation écrite de l'auteur.

DATED/*DATÉ* August 28, 1978 SIGNED/*SIGNÉ* Dennis Kikuchi

PERMANENT ADDRESS/*RÉSIDENCE FIXÉ* 12402 - 126 STREET
EDMONTON, ALBERTA
T5L 0X1

NL-91 (3-74)

National Library of Canada

Cataloguing Branch
Canadian Theses Division

Ottawa, Canada
K1A 0N4

Bibliothèque nationale du Canada

Direction du catalogage
Division des thèses canadiennes

NOTICE

The quality of this microfiche is heavily dependent upon the quality of the original thesis submitted for microfilming. Every effort has been made to ensure the highest quality of reproduction possible.

If pages are missing, contact the university which granted the degree.

Some pages may have indistinct print especially if the original pages were typed with a poor typewriter ribbon or if the university sent us a poor photocopy.

Previously copyrighted materials (journal articles, published tests, etc.) are not filmed.

Reproduction in full or in part of this film is governed by the Canadian Copyright Act, R.S.C. 1970, c. C-30. Please read the authorization forms which accompany this thesis.

THIS DISSERTATION
HAS BEEN MICROFILMED
EXACTLY AS RECEIVED

AVIS

La qualité de cette microfiche dépend grandement de la qualité de la thèse soumise au microfilmage. Nous avons tout fait pour assurer une qualité supérieure de reproduction.

S'il manque des pages, veuillez communiquer avec l'université qui a conféré le grade.

La qualité d'impression de certaines pages peut laisser à désirer, surtout si les pages originales ont été dactylographiées à l'aide d'un ruban usé ou si l'université nous a fait parvenir une photocopie de mauvaise qualité.

Les documents qui font déjà l'objet d'un droit d'auteur (articles de revue, examens publiés, etc.) ne sont pas microfilmés.

La reproduction, même partielle, de ce microfilm est soumise à la Loi canadienne sur le droit d'auteur, SRC 1970, c. C-30. Veuillez prendre connaissance des formules d'autorisation qui accompagnent cette thèse.

LA THÈSE A ÉTÉ
MICROFILMÉE TELLE QUE
NOUS L'AVONS REÇUE

THE UNIVERSITY OF ALBERTA

STRENGTH VARIABILITY OF BONDED PRESTRESSED CONCRETE BEAMS

by

© Dennis Kazuo Kikuchi

A THESIS

SUBMITTED TO THE FACULTY OF GRADUATE STUDIES AND RESEARCH

IN PARTIAL FULFILMENT OF THE REQUIREMENTS FOR THE DEGREE OF

Master of Science.

DEPARTMENT OF CIVIL ENGINEERING

EDMONTON, ALBERTA

FALL, 1978

THE UNIVERSITY OF ALBERTA

FACULTY OF GRADUATE STUDIES AND RESEARCH

The undersigned certify that they have read, and recommend to the Faculty of Graduate Studies and Research for acceptance, a thesis entitled STRENGTH VARIABILITY OF BONDED PRESTRESSED CONCRETE BEAMS submitted by DENNIS KAZUO KIKUCHI in partial fulfilment of the requirements for the degree of Master of Science.

J.G. MacGregor, Supervisor

S.H. Simmonds

J. Warwaruk

J.D. Whittaker

July 25, 1978

Date

ABSTRACT

The present safety theory for concrete structures is based on reducing the probability of failure to an acceptable value by the use of load and resistance factors. The purpose of this study was to obtain populations of the ratio of theoretical ultimate flexural moment to the ACI design strength for bonded prestressed concrete beams using the Monte Carlo technique. The results of this study will be used in the future to develop understrength factors for prestressed concrete beams in flexure.

Probability models for concrete strength, reinforcing steel strength, and cross section dimensions were obtained from papers on this subject. The probability models for prestressing steel and prestressing losses were developed in this study. Concrete properties, prestressing steel properties, losses, and dimensions of the cross section were varied in this study to examine the effect on the variability of the strength ratios. The type of prestressing strand, the depth of the beam, and the reinforcement index, ω_p, were also varied to see what effect they had on the strength ratios. The effects of construction quality, conventional reinforcing steel, and prestressing losses were also studied.

ACKNOWLEDGEMENTS

This investigation was made possible by a grant provided by the National Research Council of Canada.

The author wishes to express his appreciation to Dr. J. G. MacGregor under whose direction this study was performed.

The assistance of Dr. S. Ali Mirza in describing the probability models and in developing the Monte Carlo program is gratefully acknowledged.

TABLE OF CONTENTS

CHAPTER		Page
I	INTRODUCTION	1
	1.1 General	1
	1.2 Scope	2
II	LITERATURE REVIEW	4
	2.1 Flexural Theory	4
	2.2 Safety Theory	7
	2.3 Direct Calculation of Probability of Failure of Structural Members	12
	2.4 Monte Carlo Technique	15
III	THEORETICAL BEHAVIOUR OF PRESTRESSED CONCRETE SECTIONS	19
	3.1 Basic Assumptions in Analysis	19
	3.2 Stress-Strain Relationship for Concrete	21
	3.3 Stress-Strain Relationship for Reinforcement	24
	3.4 Stress-Strain Relationship for Prestressing Steel	24
	3.5 Method for Developing the Moment-Curvature Diagram	29
	3.6 Numerical Analysis Techniques	40
	3.7 ACI Calculation of Ultimate Moment	49
IV	PROBABILITY MODELS OF VARIABLES AFFECTING SECTION STRENGTH	57
	4.1 Concrete Variability	57

CHAPTER Page

4.2 Reinforcing Steel Variability 61

4.3 Prestressing Steel Variability 62

4.4 Variability of Prestressing Losses . . . 71

4.4.1 Preliminary Investigation 71

4.4.2 Method of Calculation of Losses 74

4.4.3 Summary of Losses and Comparison With Other Sources . . 89

4.5 Dimensional Variability 94

V COMPUTER PROGRAM FOR ANALYSIS 98

5.1 Description of the Monte Carlo Technique 98

5.2 Description of the Computer Program 98

5.3 Comparison of Theory With Test Results 103

5.4 In-batch Variability and Variability of the Theoretical Model 111

VI THE MONTE CARLO STUDY 116

6.1 Beams Studied 116

6.2 Results of the Monte Carlo Simulation 124

6.2.1 General 124

6.2.2 Effect of Variability of Individual Variables on the Variability of Section Strength 126

6.2.3 Effect of Type of Prestressing on Section Strength 132

6.2.4 Effect of Type of Strand on Section Strength 137

CHAPTER Page

6.2.5 Effect of Depth of Beam on Section Strength 138

6.2.6 Effect of ω_p on Section Strength 139

6.2.7 Effect of Construction Quality on Section Strength 144

6.2.8 Effect of Conventional Reinforcing Steel on Section Strength 147

6.2.9 Effect of Prestressing Losses on Section Strength 149

6.2.10 Shape of Probability Distributions of Results 150

VII SUMMARY AND CONCLUSIONS 155

REFERENCES 158

APPENDIX A COMPRESSIVE FORCE IN T-SECTIONS 163

APPENDIX B PRESTRESSING LOSS CALCULATIONS 173

APPENDIX C FLOW DIAGRAMS OF THE MONTE CARLO PROGRAM 183

APPENDIX D NOMENCLATURE 189

LIST OF TABLES

Table	Description	Page
4.1	Modulus of Elasticity	65
4.2	Ultimate Tensile Strength	66
4.3	Ultimate Strain	68
4.4	Values of Variables Used in Loss Calculations	83
4.5	Summary of Lesses Post-tensioned Beam with Stress Relieved Strand	85
4.6	Summary of Losses Post-tensioned Beam with Stabilized Strand	86
4.7	Summary of Losses Pretensioned Beam with Stress Relieved Strand	87
4.8	Summary of Losses Pretensioned Beam with Stabilized Strand	88
4.9	Stress at Transfer	90
4.10	Losses	90
4.11	Comparison of Loss Calculations with Lin's Losses	93
4.12	Recommended Distribution Properties of Beam Dimensions	95
5.1	Comparison of Measured and Computed Ultimate Moments	104
5.2	Coefficients of Variation or Standard Deviations Used for In-Batch Runs	113
5.3	Summary of Calculations for V_{theo}	114
6.1	Combinations of h and ω_p Studied	117
6.2	Nominal Properties of Beams Studied	118

List of Tables (Continued)

Table	Description	Page
6.3	Sensitivity Study (ω_p = 0.054, h = 16") . . .	127
6.4	Sensitivity Study (ω_p = 0.295, h = 16") . . .	128
6.5	Sensitivity Study (ω_p = 0.053, h = 12") . . .	129
6.6	Mean and Coefficient of Variation of Monte Carlo Populations for Pretensioned Beams With Stress Relieved Strand	133
6.7	Mean and Coefficient of Variation of Monte Carlo Populations for Pretensioned Beams With Stabilized Strand	134
6.8	Mean and Coefficient of Variation of Monte Carlo Populations for Post-Tensioned Beams With Stress Relieved Strand	135
6.9	Mean and Coefficient of Variation of Monte Carlo Populations for Post-Tensioned Beams With Stabilized Strand	136
6.10	Effect of Construction Quality	146
6.11	Effect of Varying Losses	151
B-1	Mean Losses for Post-Tensioned Beam with Stress Relieved Strand	181

LIST OF FIGURES

Figure	Description	Page
2.1	Definition of Probability of Failure and Safety Index, β	10
3.1	Distribution of Strain Assumed in Analysis	20
3.2	Stress-Strain Curve for Concrete	23
3.3	Stress-Strain Curve for Prestressing Steel	26
3.4	Typical Moment-Curvature Diagram for a Prestressed Concrete Beam	30
3.5	Basic Notation	32
3.6	Stress Distribution Divided Into Parts	33
3.7	Four Basic Cases of Compressive Stress Distribution	33
3.8	Strain and Stress Distributions at Ultimate Moment for One Particular Case	39
3.9	Typical P-ε_t-ϕ Curves	42
3.10	Changes in Stress Distribution as ε_t Increases and Decreases	43
3.11	Illustration of Newton-Raphson Technique	45
3.12	Problems With Incrementing Curvature	47
3.13	Cases Where Newton-Raphson Procedure Breaks Down	48
3.14	Trial and Error Procedure	50
3.15	Comparison of Assumed and ACI Stress Distributions	52
4.1	Effect of f_{se} on Prestressing Steel Stress at Ultimate	72

List of Figures, Continued

Figure	Description	Page
5.1	Ratio of Test Strength to Theoretical Strength vs. Reinforcement Index, ω_p	109
6.1	Reinforcement Location in Pretensioned Beam	123
6.2	Reinforcement and End Plate Location in Post-Tensioned Beam	123
6.3	Variation in Mean Strength Ratio with ω_p	140
6.4	Variation in Coefficient of Variation of Strength Ratio with ω_p	141
6.5	Variation in First Percentile of Strength Ratio with ω_p	142
6.6	Effect of Conventional Reinforcing Steel on Statistical Properties of Distributions	148
6.7	Probability Density Functions for Pretensioned Beams	153
6.8	Probability Density Functions for Post-Tensioned Beams	154

CHAPTER I

INTRODUCTION

1.1 General

The present safety theory for concrete structures is based on reducing the probability of failure to an acceptable value by the use of load and resistance factors. An understrength or resistance factor, ϕ, is applied to the strengths and an overload factor, λ, is applied to the loads. The development of an understrength factor requires that the distribution of ultimate strengths be calculated and compared with the strength that would be computed by the designer. This is described in more detail in Section 2.2.

This study is concerned with the calculation of ultimate moment for bonded prestressed concrete beams in flexure. The results are expressed in the form of the ratio of theoretical ultimate strength to the ACI design strength. It is hoped that these results can be used to develop understrength factors for prestressed concrete beams in flexure.

A large population of ultimate strength ratios was obtained for each beam studied through the use of computers and the method of random sampling, also called the Monte

Carlo technique. This technique requires that the probability distribution of every variable affecting the strength be known. Using these probability distributions, random values are generated for each variable using a random number generating subroutine. These values are used in the appropriate equations and a moment-curvature curve is generated. The maximum moment from this curve is determined and taken to be the ultimate moment. When this random sampling procedure is repeated a large number of times, a representative population of ultimate strengths is obtained.

1.2 Scope

Both pretensioned and post-tensioned prestressed concrete beams were studied. The beams were either rectangular beams or T-beams. Two types of prestressing strand were used—stress relieved strand and stabilized, or low relaxation, strand.

Only beams with straight, bonded strand were studied. The beams were all assumed to be simply supported and the section of maximum positive moment was studied.

The overall depth of the beams and the amount of steel was varied. A sensitivity study into the effect of each variable on section strength was conducted. The effects of construction quality, reinforcing steel, and prestressing losses were also investigated.

It was attempted to study practical beams that

are used in prestressed construction. In view of this, many of the beams studied were taken from the *PCI Design Handbook* (1971).

CHAPTER II

LITERATURE REVIEW

A literature review was conducted into flexural theory, safety theory, direct calculation of probability of failure of structural members, and the Monte Carlo technique. Because of the extensive literature in these fields, only a few representative papers will be discussed.

2.1 Flexural Theory

Warwaruk (1957) used a semi-empirical analysis in determining the ultimate strength of prestressed concrete beams. The following assumptions were made in that analysis:

1. Conditions of statics are valid.

2. Concrete fails by crushing at an ultimate strain, ε_u.

3. The strain in the steel can be related to the concrete strain at the extreme fiber in compression using a strain compatibility factor F and the depth to the neutral axis at ultimate, $k_u d$. This compatibility factor is required because strains may not be linearly distributed in the tension zone due to cracking and loss of bond of the

steel to the concrete in this zone. The variation of $F\varepsilon_u$ is mainly due to concentration of the strain near the cracks in bonded beams and to the lack of bond in unbonded beams. If the ultimate steel stress is in the elastic range of the stress-strain curve, variations in $F\varepsilon_u$ can cause large changes in resisting moment. In the inelastic range, however, the value of $F\varepsilon_u$ does not affect the resisting moment significantly.

4. The effective stress of the concrete in the compression zone, f_{cu}, is known. The actual distribution of stress is probably quite similar to the stress-strain curve of cylinders in compression. This distribution was approximated by an average or effective stress. A relationship between effective stress and compressive cylinder strength, f'_c, was found.

5. The ratio, k_2, of the depth to the resultant compressive force in concrete to the depth to the neutral axis was assumed to be equal to 0.42. This value is midway between the extremes of 0.5 and 0.33 for rectangular and triangular stress distributions, respectively. The value of k_2 does not affect the calculated ultimate moment significantly.

6. The stress-strain curve for the prestressing steel is known.

7. No tension is resisted by the concrete. Some tension is, in fact, resisted by the concrete but this ten-

sion force is usually quite small and, at ultimate moment, is insignificant compared to the other forces.

From strain compatibility and equilibrium, the following equations were derived:

$$\varepsilon_{su} = F\varepsilon_u \frac{(1-k_u)}{k_u} + \varepsilon_{se} + \varepsilon_{ce} \qquad (2.1)$$

$$k_u = \frac{\rho_p f_{su}}{f_{cu}} \qquad (2.2)$$

$$M_u = A_{sp} f_{su} d(1 - k_2 k_u) \qquad (2.3)$$

where:

ε_{su} = prestressing steel strain at ultimate moment;

ε_{se} = effective prestrain in steel after losses;

ε_{ce} = the compressive strain in the concrete due to the prestressing force.

If the ratio of prestressed reinforcement ρ_p, f_{cu}, ε_{se}, and the stress-strain curve for reinforcement are known, and $F\varepsilon_u$ is known or assumed, the first two equations can be solved. Once the steel stress at ultimate moment, f_{su}, is known, Equation 2.3 can be used to solve for the ultimate moment. Therefore the calculation of ultimate moment reduces to the determination of the steel stress at ultimate moment. Warwaruk, Sozen, and Siess (1962) suggest that the steel stress can be determined using trial and error, graphical, or algebraic means.

Rüsch (1960) studied the effects of loading rate on the stress-strain curves for concentric compression in concrete. On the basis of a series of such curves, he proposed a stress block for the compression zone in flexure.

Perhaps the most important thing suggested by Rüsch was the definition of failure of a beam in flexure in terms of $dM/d\varepsilon_{cmax} = 0$. That is, there is a maximum point in the curve of resisting moment versus strain in the extreme concrete fiber that corresponds to the ultimate moment capacity of that section.

From this concept, Rüsch also showed that ε_{cu}, the strain in the extreme fiber in compression at ultimate moment, is not a constant quantity for all cross sections but dependent on the shape of the cross section as well as on the position of the neutral axis. For example, the value of ε_{cu} for a T-beam is generally less than that for a rectangular beam and much less than that for a triangular beam.

The suggestion that the strain at ultimate moment varied according to concrete strength, rate of loading, position of neutral axis, and shape of cross section was a departure from previous ultimate strength design theories which assumed a strain at ultimate moment that was constant, or dependent only on concrete strength.

2.2 Safety Theory

MacGregor (1976) reviewed the reasons for re-

quiring safety factors, the techniques for establishing safety provisions, and the derivation of resistance factors (ϕ) and load factors (λ).

Safety factors are required in structural design for three reasons:

1. The strengths of materials or elements may be less than expected due to variability in strengths, rate of loading effects, or the reduction in strength due to *in-situ* effects. Also, the area of the reinforcing bars, the size of the member, or the depth to the steel may be less than what the designer assumes them to be.

2. There may be an overloading of the structure due to variations in load. Both dead and live loads may be more in the structure than was assumed in the design. Actual stresses may be different from the stresses obtained from analysis due to inaccurate assumptions or modelling errors.

3. The result of a failure could be costly not only in terms of repair or replacement but also in terms of the consequences of the failure including the loss of human lives.

One technique for establishing safety provisions is to limit the maximum probability of failure to an acceptable value. The probability of failure is the probability that the loads (U) exceed the strengths (R), that is, the probability that $(R - U) < 0$ or:

$$P_f = P[(R-U) < 0.0] \tag{2.4}$$

A distribution curve for the function Y = R - U is plotted in Figure 2.1. The probability of failure can be represented by the area under the curve in this figure. The probability of failure can also be expressed in terms of the number of standard deviations, $\beta\sigma_Y$, that the mean, $\overline{Y}$, is above zero. The term β is referred to as the safety index since, if the type of distribution is known, β is a measure of the probability of failure.

After some manipulation of Equation 2.4, the following equation is obtained (Cornell, 1969; Lind, 1971; summarized in MacGregor, 1976):

$$R\gamma_R[e^{-\beta\alpha V_R}] \geq U\gamma_u[e^{\beta\alpha V_u}] \tag{2.5}$$

This equation can be rewritten as:

$$\phi R \geq U\lambda \tag{2.6}$$

where:

$$\phi = \gamma_R e^{-\beta\alpha V_R} \tag{2.7}$$

$$\lambda = \gamma_u e^{\beta\alpha V_u} \tag{2.8}$$

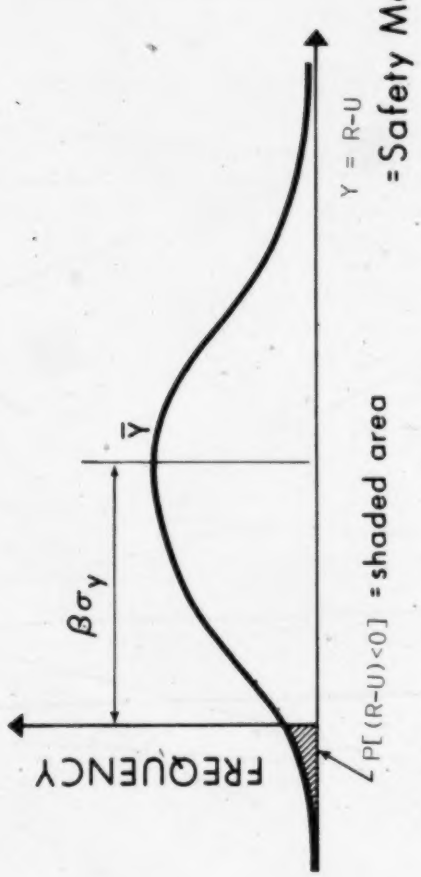

Figure 2.1 Definition of Probability of Failure and Safety Index, β

and:

ϕ = understrength factor;

λ = overload factor;

γ_R = ratio of actual mean strength to strength computed using the code procedures;

γ_u = ratio of actual mean load to the loads specified in the building code;

β = safety index, taken equal to:

3.5 for ductile structures with normal consequences of failure, and

4.0 for severe consequences of failure or brittle failures;

α = a separation factor taken equal to 0.75;

V_R = the coefficient of variation of the strength or resistance;

V_u = the coefficient of variation of the loads.

The values of β were chosen to obtain sufficiently low probabilities of failure, 10^{-4} in 30 years for ductile structures and 10^{-5} in 30 years for brittle structures.

The results from the present study will be values of γ_R and V_R which can be used in Equation 2.7 to calculate the understrength or ϕ factor for prestressed concrete beams.

2.3 Direct Calculation of Probability of Failure of Structural Members

Chandrasekar and Dayaratnam (1975) studied the probability of failure of prestressed concrete beams which were designed by the Indian Standards (IS) Code and the ACI Code. The strengths of materials were generated as random variables, the only restriction being that code specifications had to be met. The loads were treated as deterministic in one case and as having a probability distribution in the second. The probability of failure was then calculated using equations.

The probability of failure of the beams decreased as the amount of steel was increased. Varying the strength of concrete did not influence the probability of failure significantly because the beams were underreinforced. Very low probabilities of failure were obtained for the codes used; of the order of 10^{-14} for deterministic loads and of the order of 10^{-11} for probabilistic loads.

Ellingwood and Ang (1974) also used a probabilistic approach to failure. The level of risk was evaluated from an analysis of the uncertainties in the design. Uncertainties, Ω, in the variables are functions of the basic variabilities, δ, and the prediction errors, Δ, as given by $\Omega^2 = \delta^2 + \Delta^2$. The mean value and the basic variability (δ) for each variable were estimated from available data. The basic variabilities (δ) could exist even if the designer and fabricator took all due care.

The prediction error (Δ) accounts for inaccuracies in estimating the mean. Ellingwood attributes these prediction errors to modelling errors, insufficient information, and inaccurate calculations in design. If sufficient data on the variables are available, Δ can be set equal to the coefficient of variation. Otherwise, it may have to be estimated by estimating a range of values for the mean and then assuming a distribution over this range. In other cases, it may be necessary to use only judgment and past experience to choose Δ.

The uncertainties in f_y, f_c, b, d, and A_s were found using the basic variability and the prediction error for each variable. The uncertainty in the limiting strain, ε_{cu}, was also found since this variable was required to calculate the uncertainty in the balanced reinforcement ratio ρ_b. The uncertainties in the coefficients defining the concrete compressive stress distribution were also found.

The various uncertainties did not contribute equally to the uncertainty of M_T (the mean flexural capacity of a beam failing in tension). For lightly reinforced sections, the uncertainties of f_y, A_s, and d contributed greatly towards the uncertainty of M_T. As the amount of reinforcement increased, f_c, b, and the stress block parameters became more important which indicates that the moment at tension failure is more affected by crushing of the concrete for high amounts of reinforcement. Concrete

quality control (variability of f_c) and the mean value of the steel ratio were found to have little influence on the uncertainty of M_T. The uncertainty of M_C, the flexural capacity in compression, was higher than the uncertainty of M_T. Concrete quality control had more influence on the flexural strength for compression failures than for tension failures.

This probability approach was used to obtain the uncertainty in shear capacity. The uncertainties in shear capacity were considerably larger than those in flexure; however, the shear uncertainties were not affected by concrete quality control. The uncertainty of dead and live loads were also investigated.

The level of safety in the *ACI Building Code* (1971a) was evaluated using this risk analysis procedure. It was found that under the ACI restrictions, there is a probability of compressive failure as high as 25 percent for a steel ratio at the limit of 75 percent of the nominal balanced steel ratio. Also, the probability of shear failures (which are more dangerous than flexural failures because they give less warning) was higher than the probability of flexural failure for a wide range of the mean value of the steel ratio. The authors suggest lowering the reinforcement ratio limit to 50 percent of the mean balanced steel ratio to decrease the likelihood of a compression failure, and reducing the capacity reduction factor, ϕ, for shear to about 0.75 from its present value of 0.85,

to ensure that the risk of a shear failure is less than the risk of a flexural failure.

2.4 Monte Carlo Technique

The concept that strength is dependent on factors that are multivalued was used to determine a factor of safety for timber structures (Wood, 1958). Wood used frequency distributions to describe these factors. Although he called his procedure the method of random products, it is the same as the Monte Carlo technique. Wood stated that:

> The method of random products consists of taking a random value from the frequency distribution that represents each factor and multiplying these random values together to obtain a random product.

Warner and Kabaila (1968) described the concept of using a Monte Carlo technique in conjunction with high speed computers to evaluate structural safety. Their technique consisted of three steps.

1. Random values for the material properties and geometric parameters were generated in accordance with the density functions of these properties and parameters.

2. The structural response corresponding to these random values was calculated using a strength prediction equation.

3. Steps 1 and 2 were repeated until a large population of structural responses was obtained. From this

population, it would be possible to estimate the probability of the response falling below a particular value.

Warner and Kabaila present the variability of a short reinforced concrete column as an example. The results agree very well with the closed form solution.

The authors point out that very often only a small part of the distribution is of interest to the investigator. A few selective sampling techniques are suggested so that the desired information is obtained in a minimum number of simulations.

Allen (1970) has studied the variability of flexural failures for reinforced concrete beams reinforced in tension only. Allen's approach was very similar to that used in this study. He derived prediction equations for the ultimate moment and ductility ratio (ratio of curvature at ultimate to curvature at yield) for beams developing tension and compression failures. Probability distributions for the parameters involved in computing ultimate moment were obtained. A Monte Carlo analysis was then used to compute the probability distributions of the ultimate moment and ductility ratio.

The prediction equations were derived using the equivalent rectangular stress block for the compression zone and the assumption that plane sections remain plane. The concrete was assumed to have no tensile strength. The limiting strain in concrete and other parameters defining the concrete strength and the shape of the stress

block were determined from tests.

The prediction equations were found to predict the ultimate moment very accurately. The mean of the ratio of the ultimate test strength to the ultimate predicted strength was only 1.01 for tension failures and 1.00 for compression failures. The coefficient of variation of this ratio was 3.1 percent for tension failures and 5.7 percent for compression failures. Most of this dispersion could be attributed to variation of the actual test beam parameters from the measured values.

The effect of rate of loading on the compressive strength of concrete was taken into account by Allen. He also considered the rate effect in determining the probability model for yield strength for reinforcing steel. A normal distribution was used for yield strength.

Two levels of workmanship—minimum and good—were considered in the distributions for concrete strength and dimensions.

The results for ultimate moment were reported in the form of a ratio of predicted ultimate moment to the ultimate moment calculated using the 1963 ACI Code. The distribution of this ratio was close to being normal.

Allen concluded that there is a significant possibility that a section will have a compression failure even when it is underreinforced according to ACI318-63 due to variations in the concrete strength. This agrees with Ellingwood's observation mentioned earlier. He also

concluded that:

> The average ultimate moment [ratio] is more or less independent of depth to reinforcing, percentage of steel, and workmanship.

However, he found that the variability of the ultimate moment increased for shallow sections (i.e., thin slabs) or for high steel percentages whereas good workmanship decreased the variability. Rate of loading had little effect on the variability of the ultimate moment.

The distribution for ductility ratio was skewed positively. This ratio had a higher variability than did ultimate moment.

CHAPTER III

THEORETICAL BEHAVIOUR OF PRESTRESSED CONCRETE SECTIONS

3.1 Basic Assumptions in Analysis

In order to analyze a prestressed concrete section, several assumptions had to be made. These assumptions were:

1. Plane sections remain plane after loading. That is, the strains in the beam cross section are proportional to the distance from the neutral axis which leads to a linear strain distribution at the cross section.

2. The strain in the reinforcing steel was assumed to be equal to the strain in the concrete at the same point in the beam. In other words, perfect bond was assumed to exist and the strain compatibility factor, F, was equal to 1.0 (see Section 2.1).

3. The strain in the prestressing steel was assumed to be greater than the corresponding concrete strain due to the pretension strain that occurs in the steel before the concrete is bonded to the prestressing strands. Figure 3.1 shows that, relative to the unstressed state, this prestrain

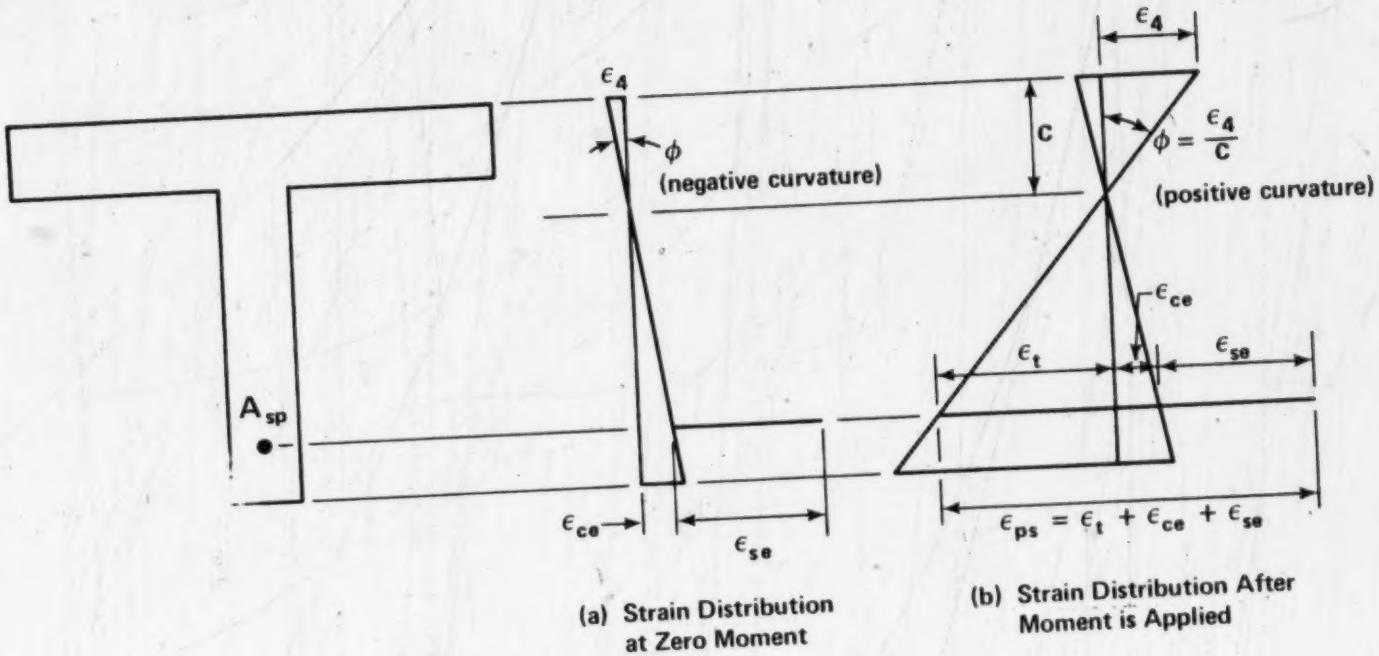

Figure 3.1 Distribution of Strain Assumed in Analysis

is made up of two parts—the effective prestrain in the steel after losses, ε_{se}, and the compressive strain in the concrete due to the prestressing force, ε_{ce}. After bonding occurred, however, any change in strain in the concrete was accompanied by the same change in prestressing steel strain. Hence, once a bond has occurred, this bond was assumed to be perfect.

4. The stress in the concrete could be determined from the strains using a modification of Hognestad's stress-strain curve in compression and an elastic line in tension (see Section 3.2).

5. The stress-strain relationship for the reinforcing steel was assumed to be elastic-plastic.

6. The stress in the prestressing steel was determined from the strains using a stress-strain curve composed of two straight lines and a parabola (see Section 3.4).

7. The forces acting on a cross section must be in equilibrium.

8. The maximum moment capacity of a given cross section corresponds to the maximum point in the moment-curvature diagram for that cross section (Rüsch, 1960).

3.2 Stress-Strain Relationship for Concrete

A variation of Hognestad's (1952) stress-strain curve for concrete was used in the theoretical analysis of

prestressed concrete sections. Hognestad's curve consists of a second order parabola up to a maximum stress of $f''_c = 0.85f'_c$ which occurs at a strain $\varepsilon_0 = 2f''_c/E_c$ where E_c is the initial tangent modulus of elasticity of concrete defined in Section 4.1. Beyond the maximum stress, the stress is assumed to decrease linearly with increasing strain to a value of $0.85f''_c$ at the ultimate strain, ε_u, taken by Hognestad as 0.0038. In this study, the same expression for ε_0 and the same value of ε_u was used. The stress-strain curve used in this study, shown in Figure 3.2, differed from Hognestad's curve only in that the maximum stress was set equal to the *in-situ* strength of concrete, adjusted for the effects of the rate of loading, f_{cstrR}. This particular strength is described more fully in Section 4.1.

The tensile strength of concrete was also considered in this study. The reason for its inclusion was the need for as high a degree of realism as possible in calculating forces and moments.

A linear relationship between tensile stress and strain in concrete was assumed up to the strain at which the concrete cracks, ε_r (see Section 4.1). At tensile strains greater than this cracking strain, the stress was zero as is shown in Figure 3.2. The modulus of elasticity was assumed to be equal in tension and compression.

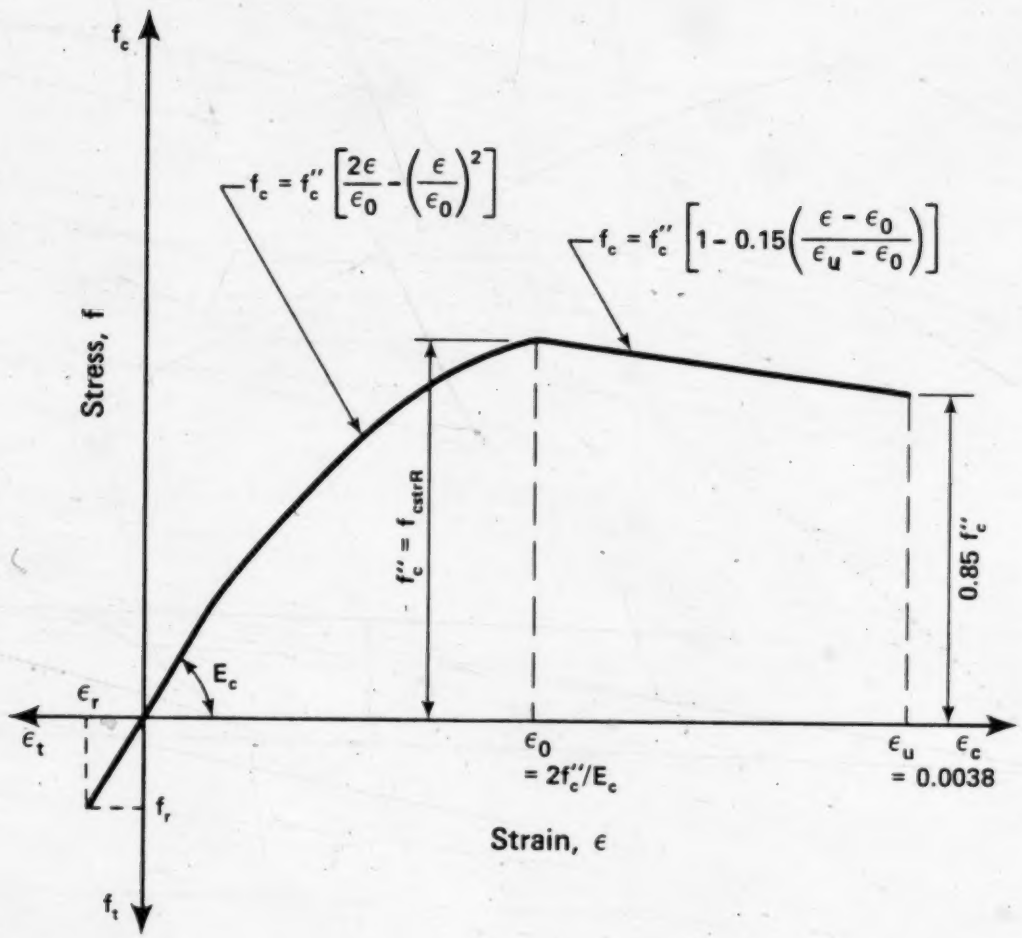

Figure 3.2 Stress-Strain Curve for Concrete

3.3 Stress-Strain Relationship for Reinforcement

The stress-strain relationship for conventional deformed reinforcement was assumed to be elastic for strains less than the yield strain, $\varepsilon_y = f_y/E_s$ where f_y and E_s are the yield strength and the modulus of elasticity, respectively, as defined in Section 4.2. At strains greater than the yield strain, the stress was equated to the yield strength. Because the onset of strain hardening in the reinforcement occurs at strains close to the failure strains of the prestressing tendons, strain hardening should have little effect on the strength and was ignored.

3.4 Stress-Strain Relationship for Prestressing Steel

Two types of prestressing steel strand were considered in this study, stress relieved and stabilized. The main difference between stress relieved and stabilized steel is that the stabilized steel has been further heat treated and subjected to high tension to reduce relaxation losses. As described in Section 4.3, the process of stabilization results in slightly improved stress-strain characteristics. This improvement is reflected in the stress-strain curve for stabilized strand used in this study. The assumed stress-strain curve for stress relieved strand will be described first, followed by a description of how the stress-strain curve for stabilized strand is different.

The stress-strain curve for stress relieved

strand was taken to be linear up to the elastic limit of 70 percent of the ultimate stress. From this point to the stress at 1 percent strain, the curve was defined by a second straight line as shown in Figure 3.3. The average value of the stress at 1 percent strain was found to be 89 percent of the ultimate stress although, as discussed in Section 4.3, it could be as high as 94 percent or as low as 84 percent of the ultimate stress. The part of the curve from 1 percent strain to the failure strain, point C to point D in Figure 3.3, was taken as a parabola. The equations for the three regions are:

Region I ($0 < \varepsilon \leq 0.7f_{pu}/E_{sp}$):

$$\sigma = E_{sp} \cdot \varepsilon \tag{3.1}$$

Region II ($0.7f_{pu}/E_{sp} < \varepsilon \leq 0.01$):

$$\sigma = 0.7f_{pu} + \frac{\left[\sigma_1 - 0.7f_{pu}\right]\left[\varepsilon - \frac{0.7f_{pu}}{E_{sp}}\right]}{\left[0.01 - \frac{0.7f_{pu}}{E_{sp}}\right]} \tag{3.2}$$

Region III ($0.01 < \varepsilon \leq \varepsilon_{up}$):

$$\sigma = \frac{-b + \sqrt{b^2 - 4ac}}{2a} \tag{3.3}$$

where:

$$a = \frac{\alpha}{f_{pu}^2}$$

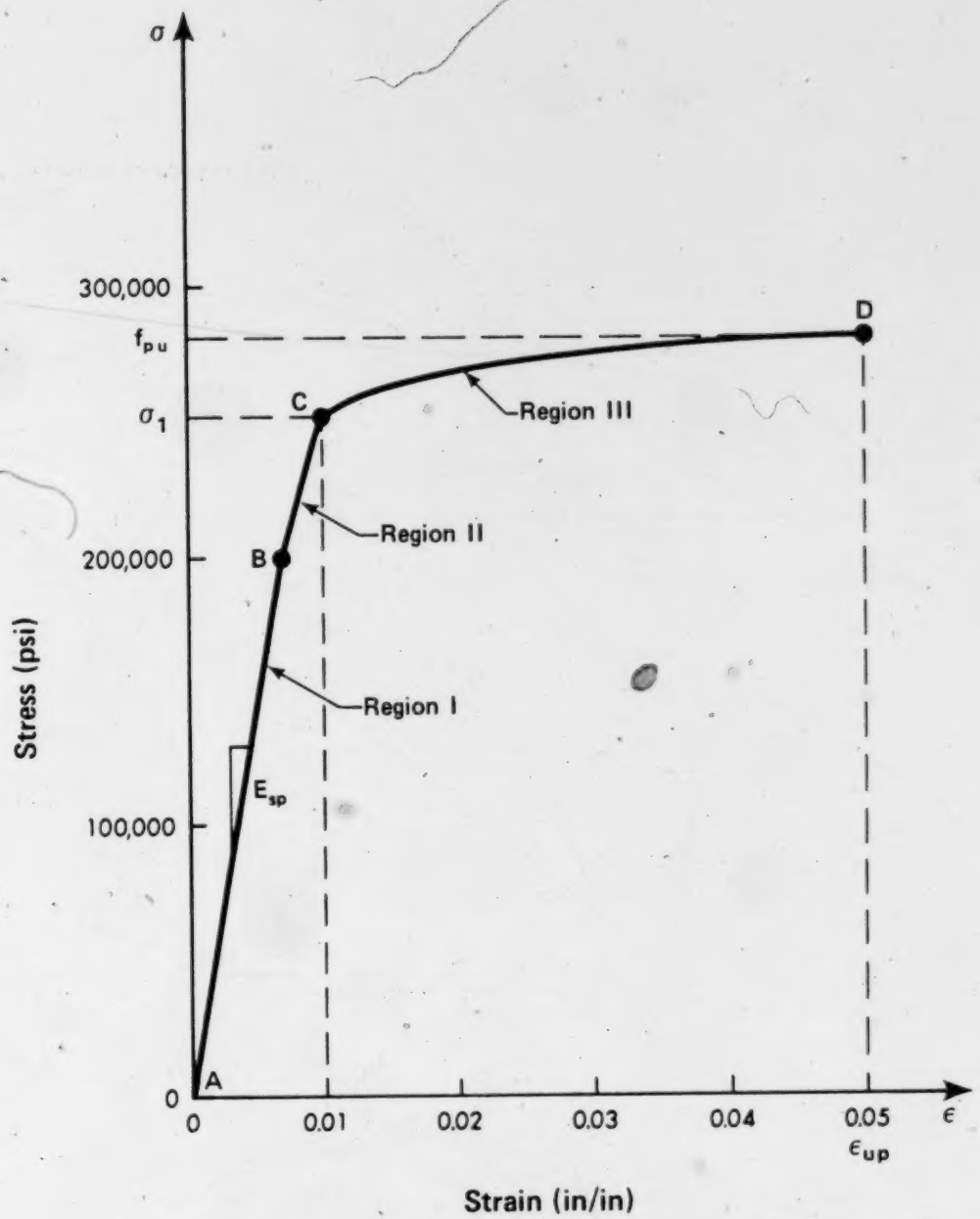

Figure 3.3 Stress-Strain Curve for Prestressing Steel

$$b = \frac{-2\alpha\beta}{f_{pu}}$$

$$c = \alpha\beta^2 + 0.01 - \varepsilon$$

$$\alpha = \frac{\varepsilon_{up} - 0.01}{(1 - \beta)^2}$$

$$\beta = \frac{\sigma_1}{f_{pu}}$$

σ_1 = stress at 1 percent strain

f_{pu} = ultimate tensile strength

ε_{up} = ultimate strain of prestressing steel

E_{sp} = modulus of elasticity of prestressing steel

The parabola used in this study was adapted from a stress-strain curve proposed by Murray and Epstein (1976). In that work, a parabola was used to describe the stress-strain curve between the elastic limit and the ultimate stress:

$$0.7f_{pu} < \sigma < f_{pu}$$

$$\varepsilon = \frac{\sigma}{E_{sp}} + 0.1\left(\frac{\sigma}{f_{pu}} - 0.7\right)^2 \qquad (3.4)$$

Equation 3.4 tended to underestimate the stress at small

strains where the curve started to bend over and reached the ultimate stress at too small a strain. This resulted in a straight, horizontal line from medium strains to the ultimate strain at the level of the ultimate stress. As can be seen in Figure 3.3, using the parabola between points C and D instead of between points B and D seems to overcome this problem. It should also be noted that in Murray's work, the stress was used in the parabola equation to solve for strain. On the other hand, the analysis in this study required that the strain be used to solve for the stress. This involved solving a quadratic equation, as can be seen in Equation 3.3. Since the root required was always the higher one, however, the solution was simplified somewhat.

The stress-strain curve for stabilized strand was assumed to be linear up to 75 percent of the ultimate stress, rather than 70 percent in the case of stress relieved strand. In addition, the stress at 1 percent strain was assumed to be a little higher for stabilized strand, averaging 90 percent of the ultimate stress, with a maximum and minimum of 95 percent and 85 percent, respectively. Thus, Equation 3.1 applies up the yield strain which is now defined as $0.75f_{pu}/E_{sp}$ and Equation 3.2 must be changed for stabilized strand:

Region II ($0.75f_{pu}/E_{sp} < \varepsilon \leq 0.01$):

$$\sigma = 0.75f_{pu} + \frac{\left[\sigma_1 - 0.75f_{pu}\right]\left[\varepsilon - \frac{0.75f_{pu}}{E_{sp}}\right]}{\left[0.01 - \frac{0.75f_{pu}}{E_{sp}}\right]} \qquad (3.5)$$

The term β, defined earlier, takes into account the magnitude of the stress at 1 percent strain in Region III.

Thus, the stress-strain curve for prestressing steel can be described using four parameters:

1. the modulus of elasticity,

2. the ratio of stress at 1 percent strain to ultimate stress,

3. the ultimate stress, and

4. the ultimate strain.

Values for these four terms are presented in Section 4.3 of this report.

3.5 Method for Developing the Moment-Curvature Diagram

The moment-curvature diagram was developed for a beam having the properties generated in each simulation in the Monte Carlo program. The maximum moment from the moment-curvature diagram was assumed to be the ultimate moment capacity of the section and was compared to the ultimate moment computed according to the ACI Building Code (1971a). A typical moment-curvature diagram for prestressed concrete beams is shown in Figure 3.4. Curvature is defined as the ratio of the strain at the extreme concrete fiber to the depth to the neutral axis.

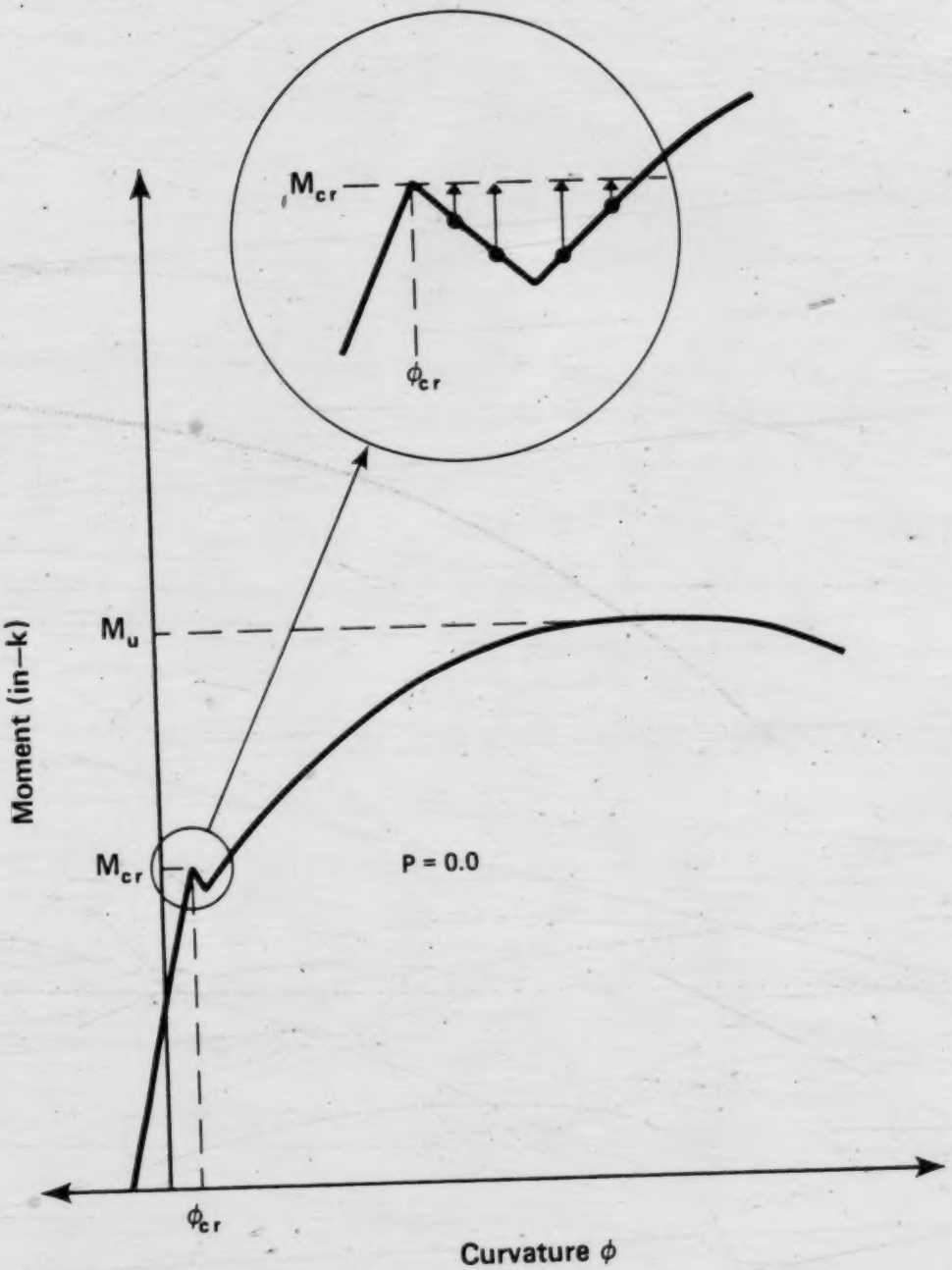

Figure 3.4 Typical Moment-Curvature Diagram for a Prestressed Concrete Beam

The moment-curvature diagram was developed by incrementing curvature. For a particular curvature, the strain at the top of the section was altered using either the Newton-Raphson procedure or a trial and error procedure until the compression and tension forces in the section were essentially equal. These procedures are further described in the balance of this section and in Section 3.6. Once the forces were balanced, the moment was calculated and thus one point on the moment-curvature diagram was determined. The curvature was then incremented and the above procedure of balancing the forces and calculating the moment was repeated. This was continued until the change in moment after an increment in curvature was so slight that for all practical purposes, the ultimate moment had been reached.

Before the calculation of the forces is described, a brief explanation of the notation and sign convention is in order. The basic notation for dimensions, strains, stresses, and forces is shown in Figure 3.5. The strain at the top of the section is ε_4, the strain at the bottom of the flange is ε_3, and the strain at the bottom of the section is ε_1. Compressive strains and forces were taken as positive. A positive moment was taken as counterclockwise as shown in Figure 3.5.

The compressive force in the concrete was calculated by splitting the stress distribution into three parts as shown in Figure 3.6. The area under the parabola could be calculated by integrating the equation for the parabola

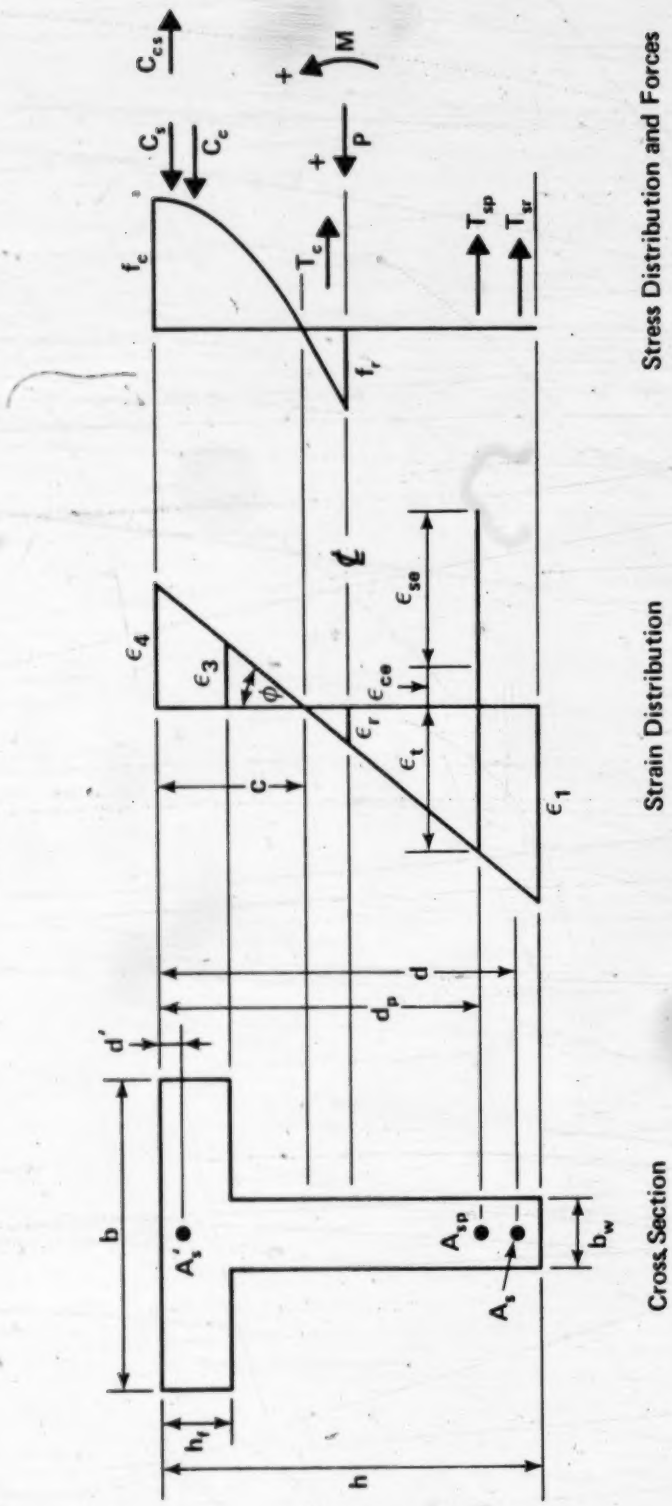

Figure 3.5 Basic Notation

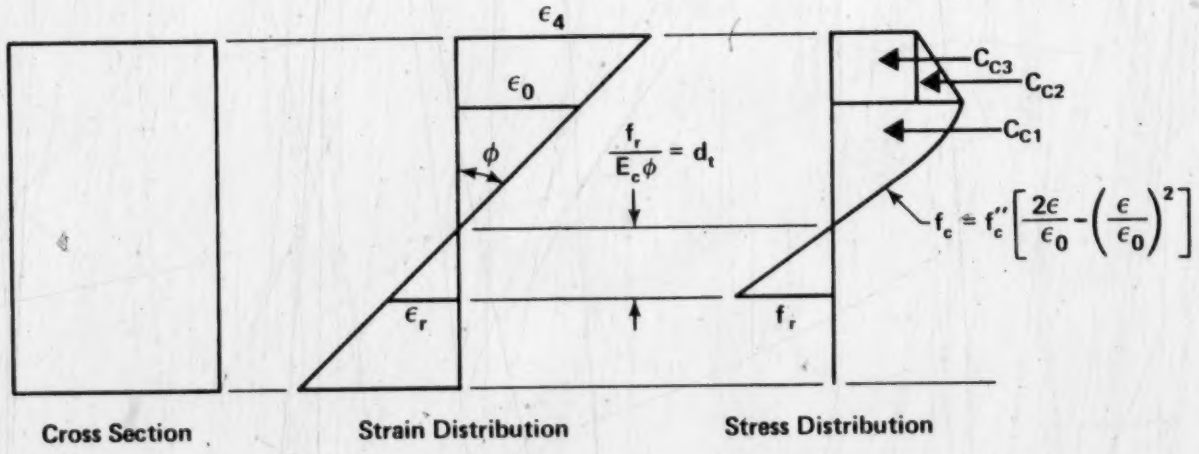

Figure 3.6 Stress Distribution Divided Into Parts

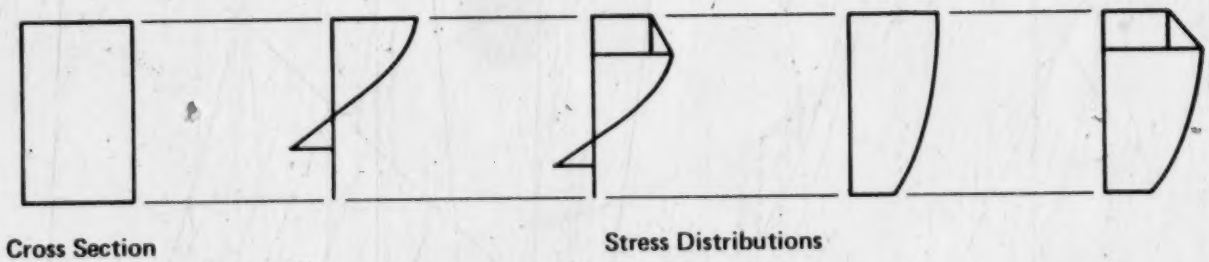

Figure 3.7 Four Basic Cases of Compressive Stress Distribution

as suggested by Gurfinkel and Robinson (1967):

$$\text{Area} = \frac{c}{\varepsilon_4} \int_0^{\varepsilon_4} f''c\left[\frac{2\varepsilon}{\varepsilon_0} - \left(\frac{\varepsilon}{\varepsilon_0}\right)^2\right] d\varepsilon \qquad (3.6)$$

The areas of the triangle and the rectangle could be calculated using simple geometric relationships. These areas are multiplied by the width of concrete that is influenced by this stress distribution to give the force in that part of the compression zone. For a rectangular cross-section, there were four basic cases as shown in Figure 3.7. For a T-section these basic cases had to be adjusted slightly to take into account the area of the flange. There are nine different cases to consider for a T-section. The various cases for rectangular and T-beams and the corresponding equations are summarized in Appendix A. The four cases for the rectangular section are included in the nine cases for the T-section since in a rectangular section, $b = b_w$ and some unnecessary terms drop out in the equations. It should be noted that some of these equations are not very accurate for very low values of ε_4 and ε_3 since these terms are taken to the third or fourth power at times. This inaccuracy did not affect the results of this study, however, since the critical ranges correspond to high values of ε_4.

The tension force in the concrete was calculated by multiplying the area under the triangular stress distribution by the width of the concrete influenced by this stress

distribution. This may be expressed as:

$$T_c = \left(\frac{1}{2} f_r \times \frac{f_r}{E_c \phi}\right) b_w \qquad (3.7)$$

where $\frac{f_r}{E_c \phi}$ is the distance shown in Figure 3.6.

For a given strain distribution, the strain in each reinforcing bar was obtained. The corresponding stress was obtained from the stress-strain curve. This stress, when multiplied by the bar area, gave the steel force.

Similarly, the strain at the level of the prestressing tendons, ε_t, could be determined for a given strain distribution. As explained in Section 3.1 and Figure 3.1, the total strain in the prestressing steel is:

$$\varepsilon_{ps} = \varepsilon_t + \varepsilon_{ce} + \varepsilon_{se} \qquad (3.8)$$

The load gradually reduces the compressive strain in the concrete due to the prestressing force, ε_{ce}, to zero strain before the concrete at the level of the prestressing steel goes into tension.

Once the strain in the prestressing steel was known, the stress was obtained from the stress-strain curve and the force was obtained by multiplying this stress by the tendon area.

Concrete that was displaced by the steel was taken into account by calculating the compressive force that this amount of concrete would have exerted, C_{cs}, and then sub-

tracting it from the compressive force. This displaced concrete was taken into account only when the steel was above the neutral axis.

The total force acting on the section was obtained by summing all of these forces:

$$P = C_c + T_c + T_{sr} + T_{sp} + C_s + C_{cs} \qquad (3.9)$$

As explained earlier, tensile forces are negative. These forces should add up to zero since this was a beam and there was no axial force on it. The computer program had a tolerance built into the force balancing procedure so that the sum of forces was close to, but not necessarily equal to, zero.

Once the forces were balanced within tolerance, the moment was calculated by multiplying the forces by their moment arms:

$$M = C_c \cdot y + T_c\left[\frac{h}{2} - \left(c + \frac{2}{3}d_t\right)\right] + T_{sr}\left[\frac{h}{2} - d\right] +$$

$$T_{sp}\left[\frac{h}{2} - d_p\right] + (C_s + C_{cs})\left[\frac{h}{2} - d'\right] \qquad (3.10)$$

The expressions for the moment arms for the compressive force in the concrete are given in Appendix A. All the moments were summed about midheight. This introduces a small error since the resultant force, P, acts at the centroid which is not at midheight for T-beams, and should thus con-

tribute to the total moment. However, the moment due to P would not significantly affect the total moment because the tolerance on P was small enough that P was close to zero.

Figure 3.4 shows that a prestressed concrete beam is initially subjected to negative curvature. This is caused by the prestressing force which makes the beam camber upwards before any load is applied. At this stage, the top of the beam is in tension (or at a small compression) and the bottom of the beam is in compression as shown in Figure 3.1(a).

Figure 3.4 also shows that for a small increase in curvature, the moment decreases slightly at the cracking moment, M_{cr}. The cracking moment is the bending moment at which the strain at the bottom of the section reaches the cracking strain. Up until this point, the tension force in the concrete increases as the strain in the concrete increases. As soon as the concrete cracks, however, the tension force in the cracked concrete disappears. As the cracking in the concrete progresses upward, the tension force in the concrete reduces in magnitude and moves toward the neutral axis causing a slight decrease in moment at this point. As the curvature increases, however, this reduction in moment is soon offset by an increase in the moment due to the increase in the reinforcement stress.

The decrease in calculated moments at cracking was found to stop the development of the full moment-curvature diagram in some cases. This problem was overcome

by finding the cracking moment and cracking curvature and then bringing the magnitude of the moment up to the level of the cracking moment if the curvature was greater than the cracking curvature. This is shown graphically in Figure 3.4. In effect, the dip in the curve was eliminated and was replaced by a horizontal line.

The cracking moment and cracking curvature were calculated using a trial and error procedure. The strain at the bottom of the section was assumed equal to the cracking strain and the curvature was incremented until the compression and tension forces were equal within a tolerance.

In a few cases, a second dip in the moment-curvature diagram was observed when the tension block in the concrete extended into the flange of a T-beam.

Generally, the ultimate moment was reached when either the strain in the concrete at the top of the section reached the ultimate strain, ε_u, or the strain in the prestressing steel reached the ultimate strain, ε_{up}. However, in some cases, the maximum moment was found to occur when the strains in the concrete and steel were less than the ultimate strains. The shape of the compressive stress block was partly responsible for this, as illustrated in Figure 3.8 for one particular case. The increase in ϕ and ε_4 results in a change in stress distribution, shown by the dotted lines. As ϕ and ε_4 increase:

1. ε_{ps} increases, resulting in increases in the steel stress, force and moment;

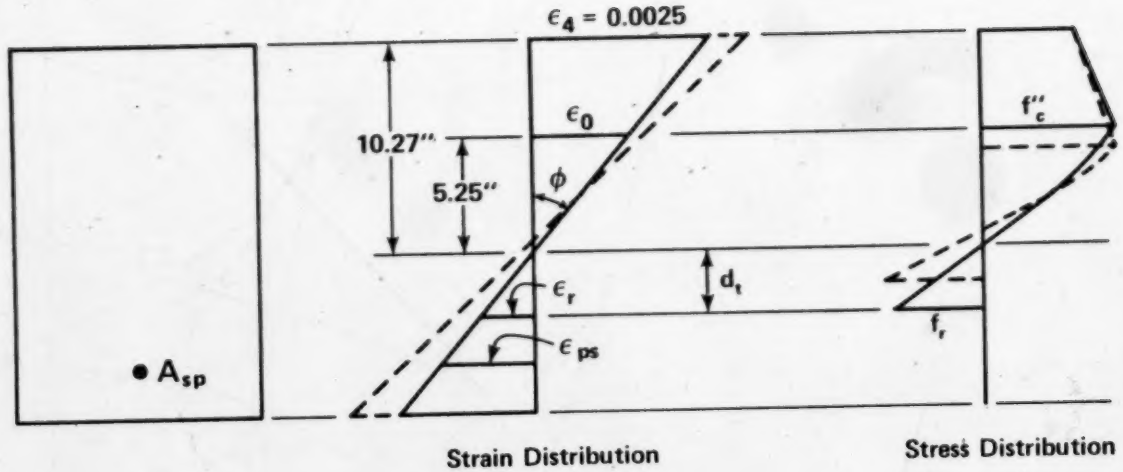

Dotted Lines Indicate Distributions as ϕ and ϵ_4 Increase

Figure 3.8 Strain and Stress Distributions at Ultimate Moment for One Particular Case

2. The tension force in the concrete decreases due to a decrease in d_t. Also, this force gets closer to mid-height, therefore, the moment due to the tension force decreases.

3. The compressive force in the concrete may decrease because the position of ε_0 moves down. There is less contribution from the parabola portion of the compressive block and slightly more from the trapezoidal part. The centroids of the parabola and trapezoid both move down resulting in smaller moment arms and a smaller moment due to the compressive force in the concrete.

If the decrease in the moments of the concrete forces is more than the increase in the moment of the steel force, the total moment will decrease. This beam was investigated at the ultimate moment condition assuming the concrete strain was at the ultimate strain and the moment was found to be less than the moment for the distributions shown in Figure 3.8. Thus, the ultimate moment may be reached before the strains in the concrete and steel reach their so-called ultimate strains.

3.6 Numerical Analysis Techniques

Two techniques were used to determine the strain at the top of the section, ε_t, that would balance the forces. The first technique was the extended Newton-Raphson method. This method was used by Gurfinkel and

Robinson (1967) to determine the strain distribution in a reinforced concrete section that was subjected to combined axial load and bending moment. In this study, the section is not subjected to a longitudinal load so the procedure is simplified somewhat. The Newton-Raphson technique converges on the correct value of ε_t very quickly. Thus, the computer program used in this study tries to use this method wherever possible. However, this technique does break down in a few cases, as discussed later in this section. When this happens, a trial and error technique is employed.

The Newton-Raphson procedure is used on nonlinear curves. In this case, it is used on the force-top strain ($P - \varepsilon_t$) curve which can have inflection points, as shown in Figure 3.9. There is one $P - \varepsilon_t$ curve for each curvature, ϕ. The upper part of the curve becomes flatter as ε_t increases (keeping ϕ constant) because the compressive stress in the concrete does not increase as fast as the strain due to the shape of the stress-strain curve for concrete. [See Section 3.2 and Figure 3.10(a).] As ε_t decreases, the compressive stress and hence the compressive force decreases as well. Eventually, as ε_t continues to decrease, the concrete cracks in tension and, because the $P - \varepsilon_t$ curve is plotted for a constant value of ϕ, the tension force remains constant while the compressive force continues to decrease as shown in Figure 3.10(b). Depending on the magnitude of the steel force, the resultant force, P,

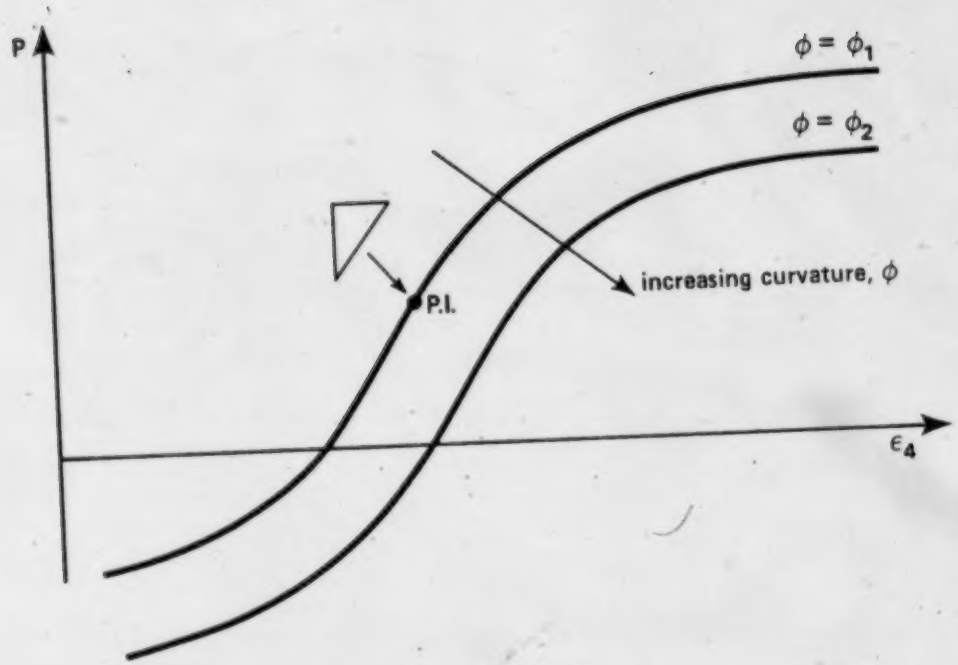

Figure 3.9 Typical P - ϵ_4 - ϕ Curves

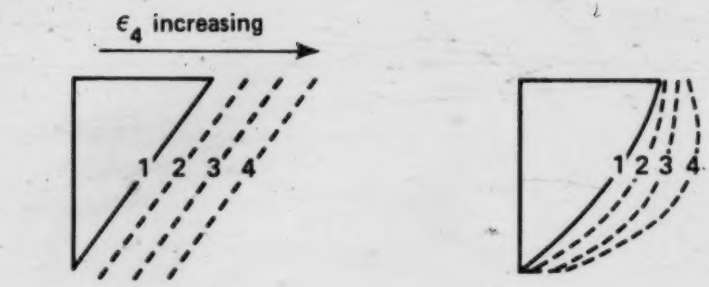

(a) ϵ_4 increasing

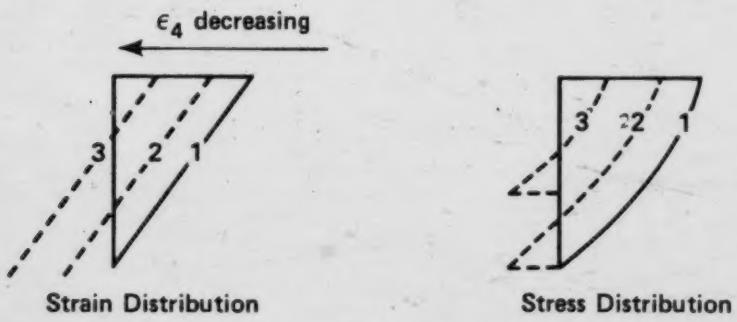

(b) ϵ_4 decreasing

Figure 3.10 Changes in Stress Distribution as ϵ_4 Increases and Decreases

could become negative as shown in Figure 3.9. The inflection point appeared to correspond to the condition of zero strain at the bottom of the section.

The strain distribution with zero strain on the tensile side was chosen as the starting reference point for the first curvature. The forces due to these strains as well as the resultant force, P_{ref}, were then calculated, as described in Section 3.5. Once the coordinates of the reference point are known, ε_4 is given a small increment, $\Delta\varepsilon_4$, as shown in Figure 3.11, and the coordinates of this point are calculated. The slope between these two points is then calculated using:

$$\frac{\delta P}{\delta \varepsilon_4} = \frac{P_a - P_{ref}}{\Delta \varepsilon_4} \qquad (3.11)$$

The correction to ε_4, ε_{cor}, is determined by going along this slope to the desired level of P as described by the following equation and as shown graphically in Figure 3.11.

$$\varepsilon_{cor} = \frac{P_{desired} - P_{ref}}{\delta P / \delta \varepsilon_4} \qquad (3.12)$$

For prestressed concrete beams, the desired P is zero since there is no external axial force on the beams. The value of P is calculated for this new corrected value of ε_4. This P is then compared to the tolerance level. If it is close enough to zero, no further iterations are required. If not, this corrected point is taken as the reference point

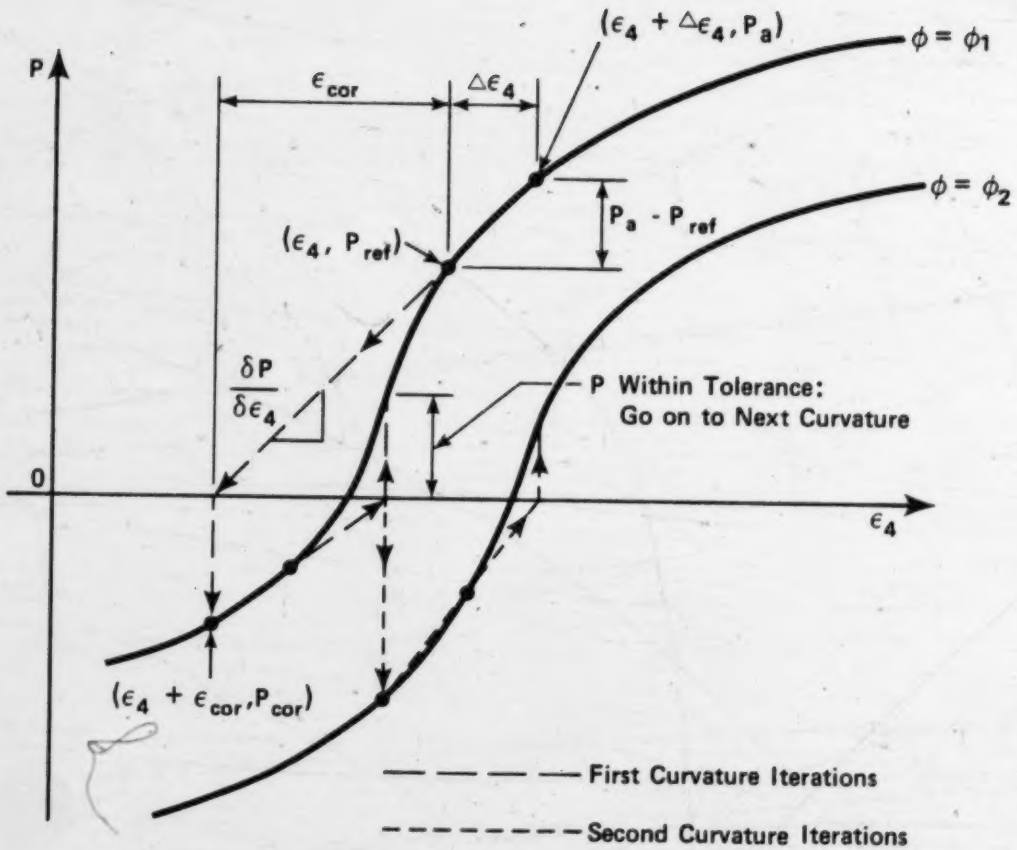

Figure 3.11 Illustration of Newton-Raphson Technique

and the process of incrementing ε_4, getting a slope, and then shooting along this slope is repeated.

Once the value of P is within the allowable tolerance, the moment due to this strain distribution can be found and thus one point on the M–ϕ curve has been determined. The curvature is then incremented and the "correct" ε_4 from the previous curvature is used as the starting point on this new P–ε_4 curve as shown in Figure 3.11.

Some problems were encountered with the Newton-Raphson procedure in connection with the incrementing of curvature. If the increment was too large, the Newton-Raphson procedure would tend to "shoot" to a corrected ε_4 that was close to, or greater than, the ultimate strain, ε_u. Due to the shape of the P–ε_4 curve in this region, the calculated slope for the next correction was either flat, as shown in Figure 3.12(a), or so slight that a negative value of ε_4 resulted, as in Figure 3.12(b). A reduction in the size of the increment in curvature corrected these problems, as shown by the dotted curves in these figures.

The Newton-Raphson technique was found to break down in a few other cases. These problems did not have anything to do with the increment of curvature. One case, shown in Figure 3.13(a), occurs when the corrected value of ε_4 corresponded to a P that was farther away from zero than the starting P. The value of ε_4 may not converge to the solution when this occurs. Another case occurs when the Newton-Raphson method oscillated back and forth between two points

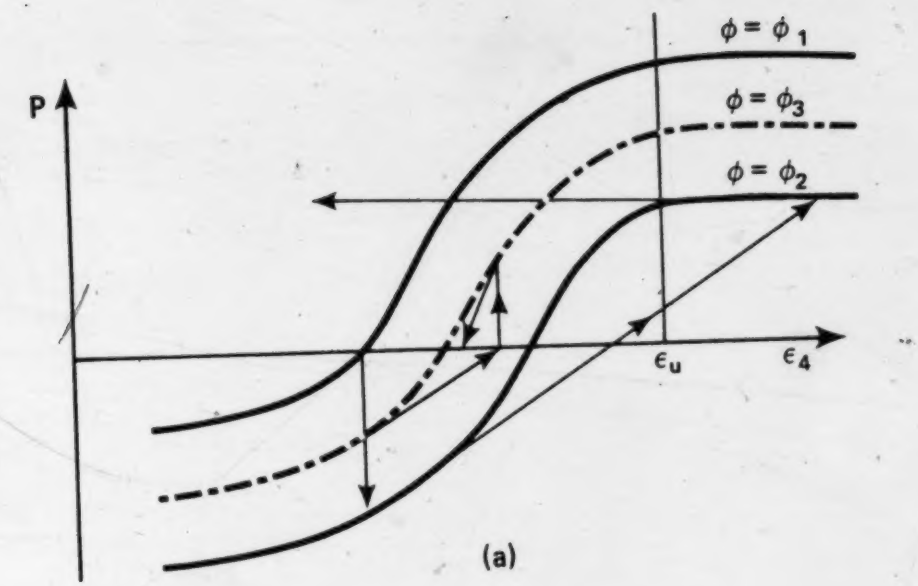

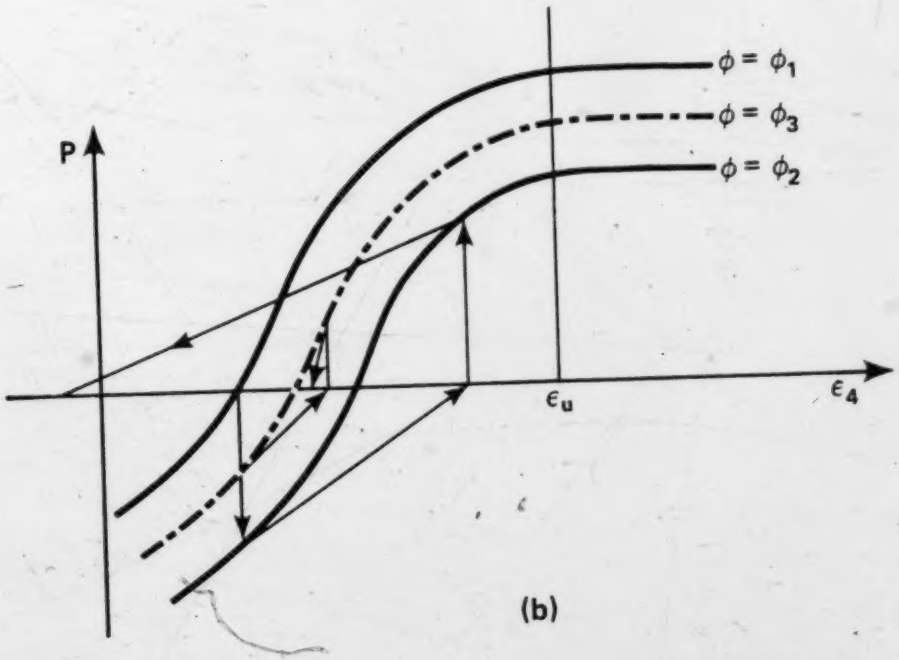

Figure 3.12 Problems with Incrementing Curvature

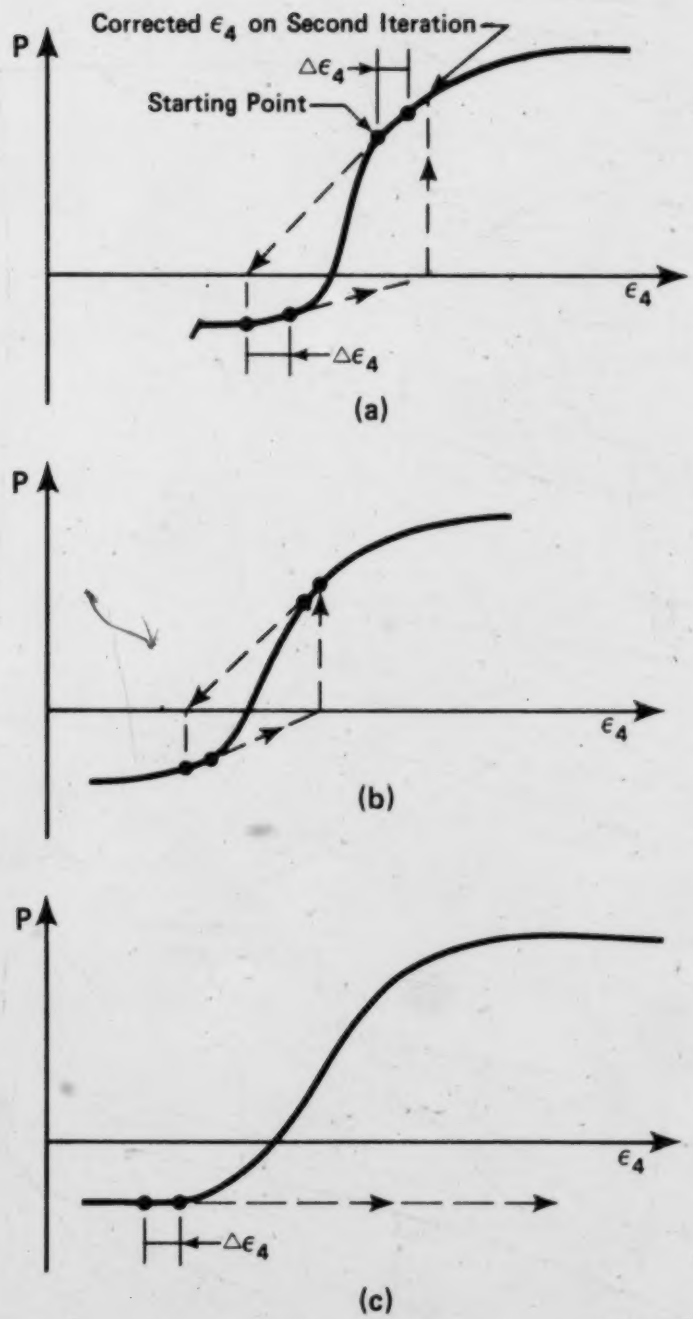

Figure 3.13 Cases Where Newton-Raphson Procedure Breaks Down

as shown in Figure 3.13(b). Yet another case where this technique cannot be used is when the value of P for ε_s and the value of P for $\varepsilon_s + \Delta\varepsilon_s$ are equal. The slope is thus calculated to be zero and the value of ε_{cor} cannot be calculated, as shown in Figure 3.13(c).

When the Newton-Raphson technique breaks down, a trial and error approach is used. This procedure basically increments ε_s until the forces balance within a specified tolerance. The increment is divided in two every time the sign of P changes and P is still outside the tolerance. Thus the increments become smaller as the method converges on the correct ε_s. This method is shown graphically in Figure 3.14. The value of P is calculated for point 1 first. Since P is outside the tolerance and is negative, the strain ε_s is increased by adding an increment, $\Delta\varepsilon_s$. Because P for point 2 is still outside the tolerance, $\Delta\varepsilon_s$ is added to the strain at point 2. Going from point 2 to point 3, the sign of P changes and the P at point 3 is still outside the tolerance so the increment is halved and subtracted from point 3. In the figure, point 4 is within the tolerance so the process is stopped. If the tolerance is small or the increments are large, the increment may be halved a number of times.

3.7 ACI Calculation of Ultimate Moment

The calculation of the ultimate moment capacity of prestressed concrete beams according to the ACI Building

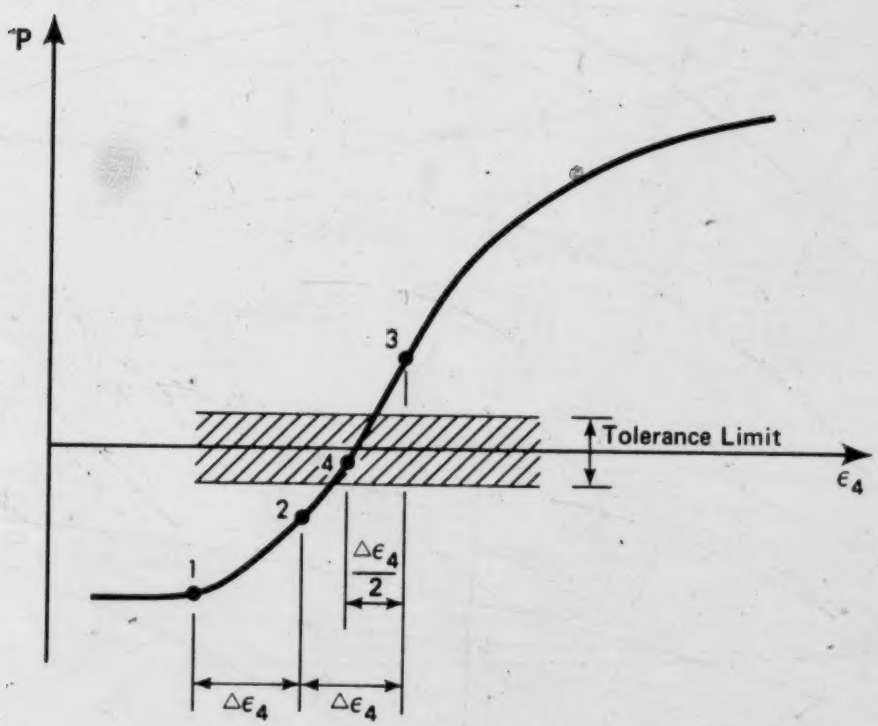

Figure 3.14 Trial and Error Procedure

Code (1971a) is required in this study. This calculation is basically the same as that for reinforced concrete beams. The only difference is that there is a force due to the prestressing steel, as shown in Figure 3.15.

The ACI calculation of ultimate strength is performed by the ACI subroutine in the computer program developed for this study. The rectangular concrete stress distribution as shown in Figure 3.15 is permitted in the ACI Code and was used in these calculations. The depth of the rectangular block was determined from $a = \beta_1 c$ where c is the depth to the neutral axis and β_1 is a constant defined in the ACI Code with a value of 0.85 for strengths, f'_c, up to 4000 psi and which is reduced continuously at a rate of 0.05 for each 1000 psi of strength in excess of 4000 psi. The maximum strain in the extreme concrete compression fiber was assumed to be 0.003 as specified in the ACI Code. The tensile strength of the concrete was neglected. It should be noted that the ACI calculation of ultimate moment in this study did not include any understrength (ϕ) factors.

The effect of conventional reinforcing steel on the ultimate moment was accounted for in the ACI subroutine. Tension reinforcing steel was always assumed to be yielded as allowed in Section 18.7.2 of the ACI Code. Following a check by hand calculations, this assumption was found to be true for all the beams investigated in this study. Any compression reinforcing steel was also assumed to be

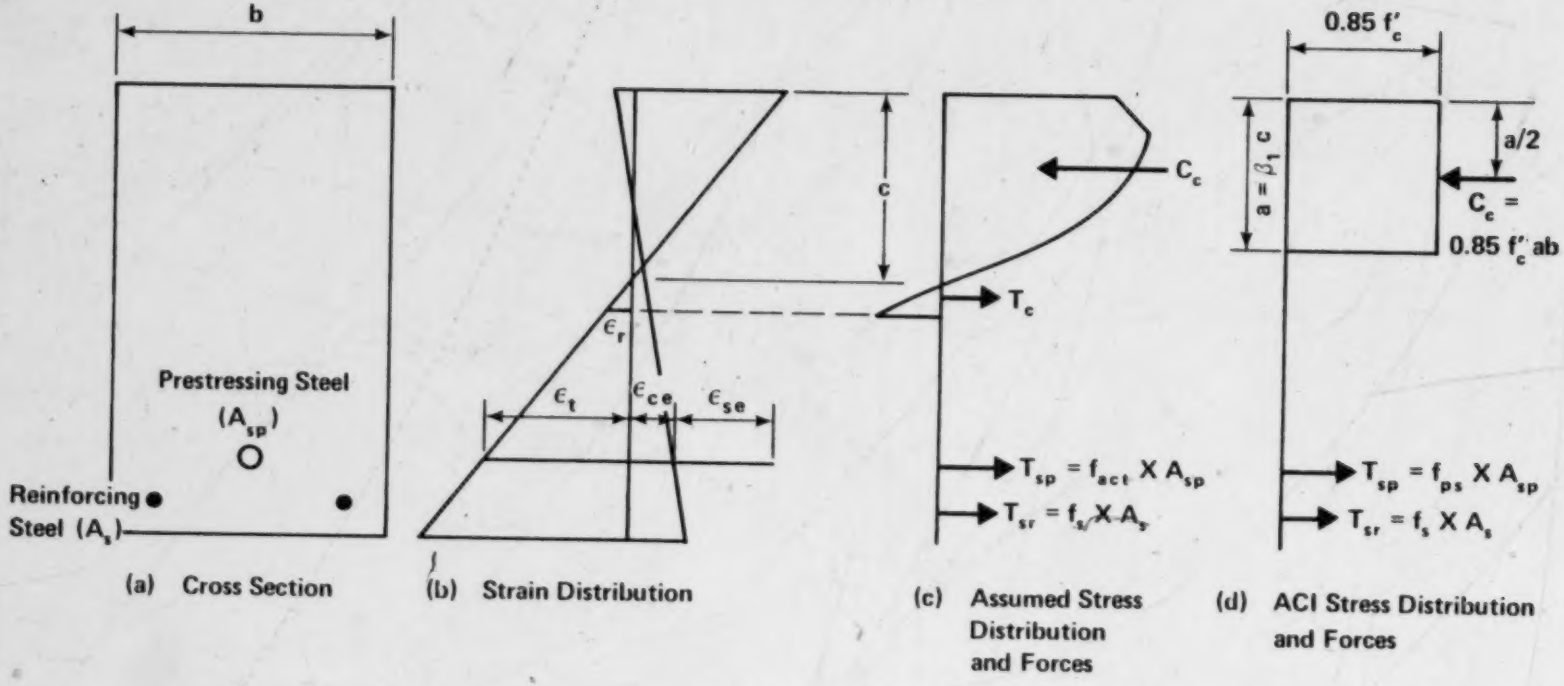

Figure 3.15 Comparison of Assumed and ACI Stress Distributions

yielded but, unlike the assumption for tension steel, this assumption is checked in the ACI subroutine using a strain compatibility analysis. If it was found that the compression steel had not yielded, the stress was set equal to the modulus of elasticity multiplied by the steel strain.

The stress in the prestressing steel at design load, f_{ps}, was determined by using Equation 18-3 of the ACI Code:

$$f_{ps} = f_{pu}\left(1 - 0.5\rho_p \frac{f_{pu}}{f'_c}\right) \qquad (3.13)$$

where:

f_{pu} = ultimate strength of the prestressing steel, psi

$\rho_p = A_{sp}/bd$
= ratio of prestressed reinforcement

f'_c = specified compressive strength of concrete, psi.

This equation is an approximation and can only be used if f_{se} is not less than $0.5f_{pu}$. However, the mean nominal value of f_{se} was always greater than $0.5f_{pu}$ for the beams investigated in this study. The above equation was used in lieu of a more exact strain compatibility analysis because

the designer would probably use that equation.

As written for this study, the ACI subroutine could handle only one layer of compression steel, one layer of prestressing steel, and one layer of tension reinforcing steel. Thus, if in reality there are three layers of prestressing steel, in the program the prestressing steel must be lumped at the centroid of the three layers.

If prestressing steel and normal tension reinforcing steel are both present, the combined centroid is calculated and the effective depth, d, is defined as the distance from the extreme compression fiber to the combined centroid (ACI Code, 1971a).

The ACI subroutine can determine the ultimate moment for either a rectangular beam or a T-beam. A beam is classified as a T-beam when the total maximum compressive force possible from the concrete in the flange and the compression steel is less than the tension force so that the neutral axis is forced down into the web.

When the compression steel lies within the equivalent rectangular stress block, the area of concrete that is displaced by the steel is accounted for in the program by subtracting the force due to this area from the total compressive force calculated assuming that no concrete is displaced by the steel.

A beam is classified as underreinforced and the ultimate moment is calculated in the normal way only if the steel ratio is less than or equal to 0.30:

$$\omega_p \leq 0.30 \qquad (3.14)$$

$$(\omega + \omega_p - \omega') \leq 0.30 \qquad (3.15)$$

$$(\omega_w + \omega_{pw} - \omega_w') \leq 0.30 \qquad (3.16)$$

where:

$\omega = \rho f_y / f'_c$ (tension reinforcement)

$\omega' = \rho' f_y / f'_c$ (compression reinforcement)

$\omega_p = \rho_p f_{ps} / f'_c$ (prestressing steel) and

$\omega_w, \omega_{pw}, \omega_w'$ = reinforcement indices for flanged sections computed as above except that b is the web width, and the steel area is that required to develop the compressive strength of the web only.

If the steel ratio is greater than 0.30, the beam is classified as overreinforced and the ultimate moment is calculated using the equation (ACI, 1971b):

$$M_u = 0.25 f'_c b d^2 \qquad (3.17)$$

This equation underestimates the ultimate moment because there are additional safety factors in this equation due to

the nature of failure of an overreinforced beam. This type of beam fails when the concrete crushes, which is a sudden and dangerous failure.

The ACI Code (1971a) requires that the area of prestressed and nonprestressed reinforcement be sufficient to develop a design load of at least 1.2 times the cracking load. This provision eliminates the possibility of a beam reaching the cracking moment and the ultimate moment simultaneously. This requirement was checked using another ACI program for all the beams studied here. This requirement was not inserted into the ACI subroutine of the Monte Carlo program because it is a design requirement, not an analysis requirement. If this requirement was not met, the section had to be adjusted by adding steel until it was satisfied. Only beams satisfying this requirement were used in the Monte Carlo studies.

CHAPTER IV

PROBABILITY MODELS OF VARIABLES AFFECTING SECTION STRENGTH

The strength of a cross section of a prestressed concrete beam is affected by the variability of the concrete, the reinforcing steel, the prestressing steel, the prestress force and losses, and the dimensions. A probability model is required for each of these variables for use in the Monte Carlo program.

4.1 Concrete Variability

The probability models for the compressive and tensile strengths of concrete and for the modulus of elasticity of concrete were taken from a statistical description of the strength of concrete prepared by Mirza, Hatzinikolas, and MacGregor (1978) and will not be derived here.

The mean 28-day strength of concrete in a structure for minimum acceptable curing was given as:

$$\bar{f}_{cstr_{35}} = 0.675f'_c + 1100 \leq 1.15f'_c \text{ psi} \qquad (4.1)$$

The subscript 35 denotes a rate of loading of 35 psi/sec.

which represents a typical testing rate for a concrete control cylinder.

The effect of different rates of loading should also be taken into account. The higher the rate of loading, the higher the apparent strength. Lower strengths at lower rates of loading are probably due to creep and microcracking effects which have more opportunity to develop when the specimen is loaded slowly. The mean value for the *"in-situ"* or "in-structure" compressive strength at a rate of loading of R psi/sec. was taken as:

$$\bar{f}_{cstrR} = \bar{f}_{cstr_{3s}}[0.89(1 + 0.08\log_{10}R)]\text{psi} \qquad (4.2)$$

The coefficient of variation of the *in-situ* strength at a given rate of loading was given by Mirza *et al.* (1978) as:

$$V^2_{cstrR} = V^2_{ccyl} - 0.04^2 + 0.10^2 = V^2_{ccyl} + 0.0084 \qquad (4.3)$$

where V_{ccyl} is the coefficient of variation of the compression test cylinders for a particular job. In the analyses reported in this thesis, pretensioned beams were assumed to be precast, and hence were assumed to have better-than-average to excellent control with V_{ccyl} equal to 10 percent. Post-tensioned beams, on the other hand, were assumed to be cast-in-place with average concrete control, for which V_{ccyl} was taken equal to 15 percent.

The tensile strength of concrete was represented by the model for flexural tensile strength proposed by Mirza *et al.* (1978) in lieu of that for splitting tensile strength. This was done because it was felt that the former better predicted the tensile strength of concrete in a beam. The following two equations were used to describe the tensile strength of concrete:

$$\bar{f}_{rstrR} = 8.3\bar{f}_{cstrss}^{\frac{1}{2}}[0.96(1 + 0.11\log_{10}R)]\text{psi} \qquad (4.4)$$

$$V_{rstrR} = 0.20 \qquad (4.5)$$

The model for the initial tangent modulus of elasticity used the following equations:

$$\bar{E}_{cistrR} = 60{,}400\bar{f}_{cstrss}^{\frac{1}{2}}(1.16 - 0.08\log_{10}t) \qquad (4.6)$$

where t is the loading duration in seconds

$$V_{cistrR} = 0.08 \qquad (4.7)$$

It can be seen from the above equations that the tensile strength and modulus of elasticity depend on the compressive strength. However, these equations by themselves do not prevent the Monte Carlo technique from generating a high value of compressive strength and low values of tensile strength and modulus of elasticity. This would be

unrealistic because, as can be seen from the above equations, a high compressive strength tends to be accompanied by a high tensile strength and a high modulus of elasticity. To prevent unrealistic combinations from occurring, the mean values of tensile strength and modulus of elasticity are set equal to values that depend on the generated value of compressive strength before the random number generating subroutine is used to generate values for tensile strength and modulus of elasticity as described by the following equations:

$$\bar{F}_{rstrss} = 8.3\sqrt{X_1} \qquad (4.8)$$

$$\bar{E}_{cistrss} = 60{,}400\sqrt{X_1} \qquad (4.9)$$

where X_1 is the generated value of compressive strength at a rate of loading equal to 35 psi/sec. for the particular beam under consideration.

Equations 4.2, 4.4, and 4.6 are then used to apply the rate of loading effects to the generated values. This procedure ensures that if a high value is generated for compressive strength, relatively high values would also be generated for the tensile strength and modulus of elasticity.

The cracking strain, ε_r, is equal to the tensile strength divided by the modulus of elasticity.

The distributions of compressive strength, ten-

sile strength, and modulus of elasticity of concrete were assumed to be normal.

4.2 Reinforcing Steel Variability

An elastic-plastic stress-strain curve was used for the reinforcing steel. Probability models of properties related to reinforcing steel were obtained from a paper on the variability of the properties of reinforcing bars by Mirza and MacGregor (1978a). It should be noted that only Grade 60 bars were considered in the present study.

The mean value and coefficient of variation of the mill test yield strength were 71,000 psi and 9.3 percent, respectively. The probability density function (PDF) of of the mill test yield strength was calculated using a Beta distribution described by:

$$PDF = 7.141\left\{\frac{f_y - 57}{51}\right\}^{2.02} \cdot \left\{\frac{108 - f_y}{51}\right\}^{6.95} \qquad (4.10)$$

where: $57 \leq f_y \text{ (ksi)} \leq 108$

The mill test yield strength is determined at a much greater rate of loading than is normally encountered in the structure. As a result, the yield strength is overestimated. This is corrected by subtracting df_{ys} from the mill test yield strength to get the static yield strength. The distribution of df_{ys} was assumed to be normal with a mean value of 3.5ksi and coefficient of variation of

13.4 percent.

The modulus of elasticity was assumed to be normally distributed with a mean of 29,000 ksi and a coefficient of variation of 3.3 percent.

The actual area of reinforcing steel is usually not equal to the nominal area. This is taken into account by multiplying the nominal area by the ratio of measured to nominal area, A_m/A_n. This ratio is normally distributed and truncated at 0.94 and 1.06. It has a mean value of 0.99 and a coefficient of variation of 2.4 percent.

Because reinforcing steel comes only in certain sizes, the furnished area of steel is usually not equal to the area of steel required by calculations. Therefore, the nominal area of steel is also multiplied by the ratio of furnished to calculated areas, A_f/A_c. A modified log-normal distribution with mean value 1.01, coefficient of variation 4 percent, and modification constant 0.91 was used for this ratio. This distribution was suggested by Mirza and MacGregor (1978b) in their paper "Variations in Dimensions of Reinforced Concrete Members."

4.3 Prestressing Steel Variability

Data pertaining to prestressing strand was obtained from the material test records of Con-Force Products Ltd., Edmonton for 1976 and 1977. This data included 99 and 100 samples, respectively, of Grade 270 stress relieved strand and Grade 270 stabilized strand. The strand was

from two sources in two countries and was in two diameters, 7/16 and 1/2 inch. This data was analyzed statistically as described in this section.

A number of correlation analyses were also performed using this data in an attempt to find interdependence between parameters. No correlation was found between the ultimate strain and the ultimate stress nor between the strain at 70 percent of the ultimate stress and the ultimate strain. A good correlation was found between the stress at 1 percent strain, σ_1, and the ultimate stress, f_{pu}, using a power regression analysis. However, a simpler, linear relationship was found between σ_1 and f_{pu} by dividing the mean value of stress at 1 percent strain by the mean value of ultimate stress to get the coefficient k in the following equation:

$$\sigma_1 = k\, f_{pu} \tag{4.11}$$

where: $k = \dfrac{\bar{\sigma}_1}{\bar{f}_{pu}}$

The results of the correlation analyses were used to help determine what parameters should be used in describing the stress-strain curve for prestressing steel. A number of different parameters with different equations were tried before the stress-strain curve described in Section 3.4 was selected. The stress-strain curve was described using four parameters: the modulus of elasticity, the ratio of the stress at 1 percent strain to the ultimate

stress, the ultimate stress, and the ultimate strain. The mean value and coefficient of variation of each of these four parameters was needed for use in the Monte Carlo program.

The coefficient k in Equation 4.11 was found to be 0.89 for stress relieved strand and 0.90 for stabilized strand. Equation 4.11 was found to fit the data very well; given the measured ultimate stress, this equation yielded values for the stress at 1 percent strain that averaged 0.997 times the measured values of σ_1 with a coefficient of variation 0.014. The coefficient of variation of σ_1/f_{pu} was taken equal to the coefficient of variation of the stress at 1 percent strain which was equal to 1.72 percent. The value of 0.90 for stabilized strand is a reasonable value, borne out by the fact that section 5.6.2 of CSA Standard G279 (1975) uses 90 percent of the minimum breaking strength of the strand as the minimum value for the stress at 1 percent extension for low relaxation strand.

Values for the other three parameters were obtained by comparing the statistical analysis of the Con-Force data with data from the other sources listed in Tables 4.1, 4.2, and 4.3.

It can be seen in Table 4.1 that the mean value of the reported modulus of elasticity from the Con-Force data was 27.58×10^6 psi which was low compared to the American data.* However, the modulus of elasticity calculated from

---

*Private communication not to be identified by company name.

Table 4.1

Modulus of Elasticity* (E_{sp})

TYPE	GRADE	DIAM. (in.)	NO. OF TESTS	MODULUS OF ELASTICITY MEAN ($\times 10^6$ psi)	MODULUS OF ELASTICITY COV+ (%)	SOURCE OF DATA
STRAND		3/8	25	28.92	2.06	
		7/16	25	29.38	2.11	
		1/2	25	28.52	1.86	American data
	270		9	28.26		
	250		9	28.12		
	250	1/2	20	28.06		
STRESS REL.	270	1/2 & 7/16	79	28.62	1.67	$0.7f_{pu}/\varepsilon_{0.7}$ Con-Force
STRESS REL.	270	1/2 & 7/16	51	27.58	1.50	Reported Con-Force
STABILIZED	270	1/2	100	28.25	1.01	$0.7f_{pu}/\varepsilon_{0.7}$ Con-Force

*Note: Based on Nominal Area
+Note: COV is Coefficient of Variation

RECOMMENDED
OVERALL
3/8"–1/2"

$\bar{E}_{sp} = 28.4 \times 10^6$ psi for Grade 270
$= 28.0 \times 10^6$ psi for Grade 250

COV = 2.0%

Table 4.2

Ultimate Tensile Strength (f_{pu})

TYPE AND SIZE	NO. OF TESTS	ULTIMATE TENSILE STRENGTH				REFERENCE
		MEAN	NOMINAL	MEAN/NOM.	COV+ (%)	
WIRE						
5 mm mill coil	100	1,552	1,530	1.0147	2.54	
5 mm stabilized	100	1,644	1,530	1.0749	3.10	
7 mm mill coil	100	1,674	1,580	1.0592	2.78	Bannister (MPa)
7 mm stabilized	100	1,691	1,580	1.0700	2.24	
7 mm	622	179.5	170	1.0559	2.67	BBR* (kg/mm^2)
Oval A-40	8265	165.12			1.38	Brenneisen and Baus (Germany and
12.2 mm	2698	144.98			1.45	Belgium)
7 mm	499	177.45	170	1.0438	3.16	(kg/mm^2)
7 mm stress rel.	514	163.1	150	1.0873	2.90	
STRAND						
9.5 mm	100	100,196	93,500	1.0716	3.22	
12.7 mm	200	178,062	165,000	1.0792	2.25	
15.2 mm	200	242,428	227,000	1.0680	2.17	Bannister (MPa)
17.8 mm	100	385,305	370,000	1.0414	1.44	
28.6 mm	25	948,360	822,000	1.1537	2.25	
3 x 2.4 mm	380	223	207.09	1.0768	5.83	Brenneisen and Baus (Belgium) (kg/mm^2)
1/2" & 7/16"	99	281,588	270,000	1.0429	1.57	Con-Force (Stress Relieved) (psi)
1/2"	100	279,473	270,000	1.0351	1.17	Con-Force (Stabilized) (psi)

(Continued ↓)

Table 4.2, continued

BARS						
14 mm	1832	107.26			4.1	Brenneisen and Baus (Russia and Germany) (kg/mm^2)
16 mm	195	106.26			3.58	
10 mm	110	112.92			5.0	
12 mm	231	109.46			4.12	
14 mm	275	108.83			5.12	
32 mm	605	109.0			1.92	

+NOTE: COV is Coefficient of Variation
* BBR refers to data provided by Canadian BBR Ltd.

RECOMMENDED OVERALL

$\bar{\sigma}_u$ = 1.04 x Nominal Strength

COV = 2.5%

Table 4.3

Ultimate Strain (ε_{up})

TYPE AND SIZE	NO. OF TESTS	ULTIMATE STRAIN		REFERENCE
		MEAN (IN/IN)	COV+ (%)	
WIRE				
Oval A-40	8265	0.0666	10.5	Brenneisen and Baus (Germany)
12.2 mm	2698	0.0823	8.0	
STRAND				
1/2" & 7/16"	51	0.0480	6.93	Con-Force (Stress Relieved)
BARS				
14 mm	1832	0.0964	18.0	
16 mm	195	0.0954	18.03	
10 mm	110	0.1152	20.06	Brenneisen and Baus (Russia and Germany)
12 mm	231	0.1001	17.8	
14 mm	275	0.0959	20.13	
32 mm	605	0.0980	8.7	

+NOTE: COV is Coefficient of Variation

RECOMMENDED OVERALL

$\bar{\varepsilon}_u$ = 0.05 in/in

COV = 7.0%

the Con-Force data by dividing 70 percent of the ultimate stress, $0.7f_{pu}$, by the corresponding strain, $\varepsilon_{0.7}$ agreed very well with that from the American data as shown in Table 4.1. Based on this, the mean value of the modulus of elasticity of Grade 270 strand was taken as 28.4×10^6 psi, with a coefficient of variation of 2.0 percent.

In order to facilitate comparison of ultimate strengths from different sources, the ratio of the mean ultimate strength to the nominal ultimate strength was computed and compared. Table 4.2 shows that this ratio varied from 1.035 to 1.154 for the strand. The Con-Force data fell at the low end of this range and also had slightly lower coefficients of variation than the other sources. The mean value of the ultimate strength was chosen to be 1.04 × nominal ultimate strength for both types of strand, representative of the Con-Force data. The coefficient of variation was chosen to be 2.5 percent. This value is roughly the average of the standard deviations of all of the tests of strand quoted in Table 4.2.

Not much data was available for ultimate strain (Table 4.3). The Con-Force data indicated a mean ultimate strain of 0.05 in/in and a coefficient of variation of 7.0 percent. These values were used for both types of strand.

Based on the data collected and the observation by Brenneisen and Baus (1968) that the mechanical characteristics of prestressing wires, bars, and cables were nor-

mally distributed, all prestressing steel properties were assumed to be normally distributed in this study. An upper and lower limit was set only for the ratio of stress at 1 percent strain to ultimate stress. This would result in a truncated normal distribution. The limits were set at three standard deviations away from the mean value resulting in an upper and lower limit of 0.94 and 0.84 for stress relieved strand, and an upper and lower limit of 0.95 and 0.85 for stabilized strand.

It should be noted that the coefficients of variation for the prestressing steel properties are less than those for the reinforcing steel properties. This is because the production of prestressing steel is a more continuous process than the batch process which is used for reinforcing steel (Bannister, 1968).

It is claimed that stabilized strand has improved stress-strain characteristics compared to stress relieved strand such as a higher modulus of elasticity (Stelco, 1976), a higher proportional limit (Stelco, 1976; Bannister, 1968), as well as a higher ultimate strength and ultimate strain (Bannister, 1968). Due to a lack of quantitative information, however, the same modulus of elasticity, ultimate stress, and ultimate strain were used for both stress relieved and stabilized strand. The data from Con-Force indicated that there was little difference between these values for the two types of strand. As described in Section 3.4, the proportional limit was increased from 70 per-

cent of the ultimate stress for stress relieved strand to 75 percent of the ultimate stress for stabilized strand. Bannister (1968) states that 75 percent is a minimum value for stabilized wire. As mentioned earlier, the ratio of the stress at 1 percent strain to the ultimate stress was increased to 0.90 for stabilized strand from 0.89 for stress relieved strand.

Since the Con-Force test data was based on the nominal areas of the strands, no correction was made to account for the variability of the areas of the strands.

4.4 Variability of Prestressing Losses

4.4.1 Preliminary Investigation

A preliminary investigation was carried out to determine if prestressing losses had a significant effect on the stress in the prestressing steel at ultimate, and hence on the ultimate moment. The stress-strain diagram used in this investigation was obtained from the mean values of the statistical analysis of the prestressing steel data (see Section 4.3). This mean curve was shifted in the negative direction by the initial prestrain, $\varepsilon_{se} + \varepsilon_{ce}$, as shown in Figure 4.1. The meanings of ε_{se} and ε_{ce} are explained in Section 3.1. The magnitude of $\varepsilon_{se} + \varepsilon_{ce}$ was calculated by arbitrarily assuming that losses of 22 percent of the initial transfer stress occurred. The calculation of ε_{se} and ε_{ce} is further described in Section 5.2.

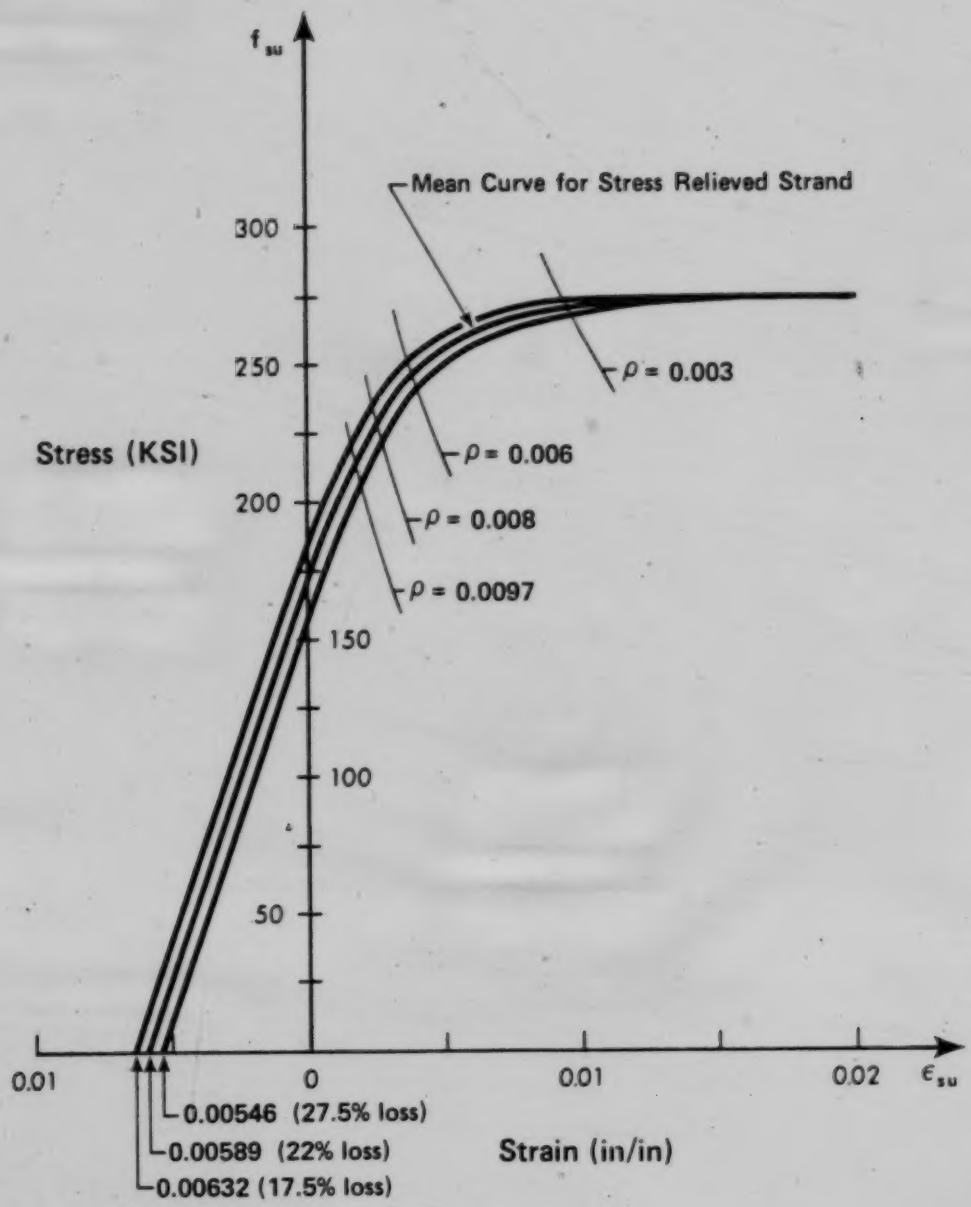

Figure 4.1 Effect of f_{se} on Prestressing Steel Stress At Ultimate

The effect of variations in the losses was arbitrarily studied by multiplying the assumed loss of 22 percent by 1.25 and 0.75 to get 27.5 percent and 16.5 percent losses, respectively. The different amounts of loss resulted in different values of $\varepsilon_{se} + \varepsilon_{ce}$. This in turn shifted the stress-strain curve to either side of the mean curve as shown graphically in Figure 4.1.

Also plotted in this figure is the locus of possible solutions for the stress in the prestressing steel at failure, f_{su}, for varying values of steel ratio, ρ_p. The range of ρ_p was obtained from a survey of the sections listed in the *PCI Design Handbook* (1971). The equation for these curves is:

$$f_{su} = \left(\frac{\beta_1 0.85 f'_c}{\rho_p}\right)\left(\frac{\varepsilon_{cu}}{\varepsilon_{cu} + \varepsilon_{su}}\right) \qquad (4.12)$$

where: β_1 = factor relating the depth of the equivalent rectangular stress block to the neutral axis depth (see Section 3.7).

ε_{cu} = limiting strain in concrete
= 0.003 in *ACI Building Code* (1971a)

ε_{su} = strain in the prestressing steel at failure.

This equation can be derived from strain compatibility and equilibrium (Warwaruk *et al.*, 1962), based on a rectangular stress block. The intersections give stresses at failure.

The difference between the high and low values of

steel stress due to the assumed variation in losses ranged from 1 percent for beams with a prestressing steel ratio $\rho_p = 0.003$ to as much as 6 percent for a steel ratio $\rho_p = 0.01$. Because the latter value appeared significant, prestressing losses were included as a random variable and a probability model for the losses was estimated.

4.4.2 Method of Calculation of Losses

The prestressing losses were calculated for a typical Prestressed Concrete Institute (PCI) beam (8DT 20 with a strand pattern 68-D1) (PCI, 1971) with a span of 50 feet. The strands were assumed to be jacked from one end. The mean loss, maximum loss, and minimum loss calculations were carried out for the four combinations of type of prestressing operation (pretensioned and post-tensioned) and type of prestressing steel (stress relieved and stabilized).

Anchorage loss, elastic shortening loss, and time dependent losses due to shrinkage, creep, and relaxation were all taken into account in these calculations.

Anchorage loss is the loss of stress in the prestressing steel due to the anchorage of the prestressing steel. In post-tensioned members, the anchors at the end of the tendons will slip slightly and locally deform the end of the beam as they set, thus reducing the stress slightly. Anchorage loss in pretensioned members is caused by slippage in the strand-holding devices.

Elastic shortening loss occurs when the pre-

stressing force is applied to the concrete. Under this compressive force, the concrete shortens a bit and the prestressing steel shortens the same amount. Thus, there is a reduction of stress in the steel. This loss occurs in both post-tensioned and pretensioned construction.

As the concrete loses water, it shrinks, resulting in loss of stress in the steel. This loss is called shrinkage loss.

Creep loss occurs as the concrete creeps. Creep is defined as the change in strain which takes place in concrete due to a constant stress. A prestressed beam is not subjected to a constant stress; the stress is always changing as the losses grow in magnitude. Partly for this reason, an incremental approach was used in the calculation of losses. The stress in the concrete at the center of gravity of the steel is the stress that is used in the creep calculations.

Relaxation of the prestressing steel also causes a loss of stress in the steel. Relaxation is defined as the change in stress that takes place due to a constant strain. Generally, relaxation increases as stress, time, and temperature increase. Only normal temperatures (20°C) were considered in this study. Thus, it was assumed that steam curing or any other process that increases the temperature was not used on the typical beam used for the loss calculations.

Due to the different sequence and method of pre-

stressing, the losses for a post-tensioned beam are different from those for a pretensioned beam. In a post-tensioned beam, ducts are placed in position and then the concrete is poured. The concrete is then cured until it is strong enough to withstand the jacking and anchoring of the tendons.

Shrinkage occurs in the concrete during this period of time between pouring and anchoring which was assumed to be fourteen days long in the loss calculations. This shrinkage does not affect the steel stress, however, because the concrete and the strands are still unbonded. When the tendons are jacked, there is a friction loss due to the lack of straightness (wobble) of the ducts. Since only straight tendons were used in this study, the curvature coefficient was omitted from the expression for friction loss:

$$P_s = P_x e^{Kl} \qquad (4.13)$$

where: P_s = steel force at jacking end

P_x = steel force at any point x

K = wobble friction coefficient per foot of prestressing steel

l = length of prestressing steel element from jacking end to any point x.

When the tendons are anchored, there is an anchorage loss due to the effect of wedge set. From a literature review,

the mean value of this movement was chosen to be 0.35 inch with a maximum of 0.5 inch and a minimum of 0.2 inch. The stress in the prestressing steel after the tendons are anchored is called the stress at transfer. The elastic shortening loss occurs at transfer. To develop bond between the tendons and the concrete, grout is injected into the ducts at this stage. The time dependent losses—shrinkage, creep, and relaxation—then take place.

In a pretensioned beam, the strands are first stressed in the pretensioning bed. Relaxation losses start from this point. An anchorage loss due to slippage in the strand-holding devices occurs. The Prestressed Concrete Institute (1971) suggests a maximum loss of 5 percent due to slippage and the effect of strand deflection devices. Since straight strands were used in this study, there would be no loss due to deflection devices. A mean anchorage loss of 2.5 percent was chosen, with a maximum of 4.5 percent and a minimum of 0.5 percent. The concrete is then poured around the tendons. After steam curing or a few days of normal curing, the concrete is bonded sufficiently to the strands and has sufficient strength to allow the strands to be released. Shrinkage occurs in the concrete during this period of time which was assumed to be three days long in the loss calculations. Unlike the post-tensioned beam, this preliminary shrinkage does reduce the steel stress because the concrete is bonded to the steel right from the start. An elastic shortening loss occurs at transfer. Time de-

pendent losses then take place.

There is essentially no difference between a post-tensioned beam and a pretensioned beam as far as the calculation of the elastic shortening and time dependent losses is concerned. A post-tensioned beam after anchoring and grouting behaves similarly to a pretensioned beam in which the strands are cut. In fact, Khachaturian and Gurfinkel (1969) suggest that losses measured from transfer may be taken as 25,000 psi for both post-tensioned and pretensioned beams.

The mean loss was calculated first. The mean properties of concrete and prestressing steel, described in Sections 4.1 and 4.3, respectively, were used in these calculations. It was assumed that the stress at transfer, $f_{transfer}$, was 70 percent of the specified ultimate stress, $f_{specified}$. Any losses that occur before transfer were compensated for by overtensioning the tendons to an initial jacking stress that was greater than the stress at transfer. The mean value of initial jacking stress in the prestressing steel was calculated by working backwards from the stress at transfer using a trial and error approach. In this calculation, the initial jacking stress was estimated. From this value, the mean friction loss (for post-tensioned beams), the mean shrinkage and relaxation losses during the period prior to transfer (for pretensioned beams), and the mean anchorage loss were subtracted to get the stress at transfer. This trial and error calculation was repeated

until $f_{transfer}$ was approximately 70 percent of $f_{specified}$.

Starting from $f_{transfer}$ and using common elastic theory, the elastic shortening loss was then calculated (PCI, 1971):

$$L_{es} = \frac{E_{sp}}{E_c}(f_{cs})$$

$$= \frac{E_{sp}}{E_c}\left(\frac{P_o}{A_c} + \frac{P_o e^2}{I_g} - \frac{M_{dl} e}{I_g}\right) \qquad (4.14)$$

where: L_{es} = loss of prestress due to elastic shortening

f_{cs} = concrete stress at the centroid of the strand

P_o = prestress force at transfer

A_c = area of concrete

e = eccentricity at point of consideration

I_g = gross moment of inertia of section

M_{dl} = moment due to dead load of the member

The elastic shortening loss for pretensioned beams can be calculated directly from this equation. For post-tensioned beams, the elastic shortening loss calculated in this manner must be adjusted to take into account the effects of stressing tendons one at a time. As each tendon is stressed, the concrete shortens a bit more, resulting in more elastic shortening loss in the steel. The first tendon that is stressed would have the highest elastic shortening loss since the stressing of each subsequent tendon contributes to its loss of prestress. On the other hand, the last tendon that is stressed would have no loss due to elastic

shortening because the shortening in the concrete and steel would have already occurred by the time the prestress was being measured in the last tendon. An average loss for all the tendons is generally used for post-tensioned beams.

The mean time dependent losses were calculated next. Creep and shrinkage losses were determined using the *Comité Européen du Bêton* prediction equations and curves (Neville, 1970). These curves give coefficients which allow one to calculate the 5th and 95th percentiles as well as the mean values of shrinkage and creep. A water cement ratio of 0.5 was assumed for all calculations. The creep and shrinkage calculations require the use of an equivalent thickness, d_m, defined as the ratio of cross sectional area to semi-perimeter. For T-sections, the equivalent thickness was based on the dimensions of the stems because that is where the prestressing steel is located. A relative humidity of 40 percent was assumed for the calculation of mean losses. As explained earlier, the age at transfer, which was taken to be the age at loading for the creep calculations, was taken as fourteen days for post-tensioned beams and three days for pretensioned beams.

The relaxation loss was determined using the graphs for the range of losses for stress relieved strand and stabilized strand given by Stelco (1976). The maximum and minimum values from these bands, as well as the mean value calculated from these values, were used because the customary relaxation formulae tend to overestimate the mean

relaxation losses for strand (Stelco, 1976).

Before maximum or minimum losses could be calculated, the maximum and minimum jacking forces had to be determined. Using data obtained from stressing records for the Edmonton plant of Con-Force Products Ltd., a statistical analysis of the ratio of the actual jacking pressure to the specified jacking pressure was carried out. A mean of 1.030 and a coefficient of variation of 0.0132 were obtained. The maximum and minimum jacking forces were calculated by adding and subtracting three standard deviations from the mean jacking force calculated earlier by trial and error.

A value that is three standard deviations from the mean corresponds to a chance of occurrence of about 1 in 1000. Because the jacking force is independent of the variability of the concrete and steel properties, the chance of getting the maximum or minimum jacking force is about 1 in 1000. On the other hand, the magnitude of the losses depend on both the concrete and steel properties. The maximum and minimum values for these properties were taken as the mean plus or minus 1.645 standard deviations corresponding to the 5th and 95th percentile values, or a chance of occurrence of 1 in 20. The chance of getting maximum (or minimum) concrete and steel properties at the same time is about $1/20 \times 1/20 = 1/400$. This is the same order of magnitude as the chance of getting the maximum or minimum jacking force. The values of the variables

used for the loss calculations are summarized in Table 4.4.

The maximum loss was calculated by using low values of the modulii of elasticity of concrete and steel. Minimum slip and friction losses were subtracted from the maximum jacking force in order to obtain a high stress at transfer and, as a result, the maximum time dependent losses. Mean values were used for all creep and shrinkage coefficients except that the 95th percentile values were taken for the effects of water cement ratios and relative humidity. A relative humidity of 40 percent was used for maximum loss calculations. The upper limit on relaxation losses was taken from the Stelco (1976) literature.

The higher strength properties of concrete and steel (i.e. mean plus 1.645 standard deviations) were used in the calculations for minimum loss. Starting at the minimum jacking force, higher slip and friction losses were subtracted in order to minimize time dependent losses. Mean values were used for all creep and shrinkage coefficients except that the 5th percentile values were used for the terms reflecting the effects of water cement ratio and relative humidity. A relative humidity of 90 percent was used for minimum loss calculations. The relaxation losses were based on the minimum losses suggested by Stelco (1976).

The strength gain of concrete with time was taken into account for pretensioned beams:

Table 4.4

Values of Variables Used in Loss Calculations

VARIABLE	MEAN LOSSES	MAXIMUM LOSSES	MINIMUM LOSSES
JACKING FORCE	31.47 k	32.71 k	30.23 k
STEEL PROPERTY E_{sp}	28.62×10^6 psi	27.83×10^6 psi	29.40×10^6 psi
CONCRETE PROPERTY E_{cc}			
(f'c = 4000 psi) (post-tensioned)	3.723×10^6 psi	2.995×10^6 psi	4.451×10^6 psi
(f'c = 4500 psi)	3.885×10^6 psi	3.125×10^6 psi	4.645×10^6 psi
(f'c = 5000 psi	4.04×10^6 psi	3.25×10^6 psi	4.83×10^6 psi
FRICTION LOSS k (post-tensioned)	0.00125	0.0005	0.002
ANCHORAGE LOSS SLIP			
(post-tensioned)	0.35"	0.2"	0.5"
(pretensioned)	2.5%	0.5%	4.5%
CREEP LOSS			
α_f	0.75	0.75	0.75
β_f	0.85	0.85	0.85
ϕ_0	3.2	3.8	1.25
ξ	1.2 for post-tensioned, 1.6 for pretensioned		
ρ_{time}	varies with time-used mean value line		
SHRINKAGE LOSS			
ψ	400×10^{-6}	550×10^{-6}	15×10^{-6}
α_r	0.76	0.76	0.76
B_r	1.2	1.4	0.95
RELAXATION LOSS	used Stelco Graphs (1976)		

f'c	days after pour
4000	3
4500	10
5000	17

The corresponding gain in modulus of elasticity can be seen in Table 4.4. Because post-tensioned beams were assumed to be cured for fourteen days before they were stressed, a constant strength and modulus of elasticity for concrete was used.

If steam curing was used, the strength gain of concrete would be accelerated so that the concrete would reach a higher fraction of final strength at an earlier period of time. This would tend to decrease the creep loss. Neville (1970) suggests that a fictitious age based on the maturity of the concrete be used in the calculation of creep loss. Steam curing would also raise the relative humidity of the storage which decreases the creep and shrinkage losses. Moist curing would raise the relative humidity so that creep and shrinkage losses would both decrease but would not accelerate the strength gain.

The losses were calculated using the numerical integration procedure presented by Libby (1971). The losses were calculated for a period of five years because most of the losses have occurred by this time and because the beam may be overloaded at any time in its life so that a forty-year loss would tend to overestimate losses at the hypothetical overloading. The results of the loss calculations are given in Tables 4.5, 4.6, 4.7 and 4.8. An

Table 4.5

Summary of Losses*
Post-Tensioned Beam with Stress Relieved Strand

TYPE OF LOSS	MAX.	MIN.	MEAN	$\frac{\text{MIN + MAX}}{2}$
EL. SHORTENING	1.69	0.87	1.24	1.28
SHRINKAGE	5.12	0.10	3.42	2.61
CREEP	9.40	1.68	5.88	5.54
RELAXATION	10.68	6.30	8.36	8.49
SUBTOTAL	26.90	8.95	18.91	17.92
FRICTION	1.42	5.08	3.34	3.25
ANCHORAGE	3.32	7.39	5.49	5.36
FRICTION + ANCHORAGE	4.74	12.48	8.83	8.61
ALL LOSSES	31.64	21.43	27.74	26.53

*All losses in percentage of nominal stress at transfer which is equal to $0.7f_{specified}$.

Table 4.6

Summary of Losses*
Post-Tensioned Beam with Stabilized Strand

TYPE OF LOSS	MAX.	MIN.	MEAN	$\frac{\text{MIN + MAX}}{2}$
EL. SHORTENING	1.69	0.87	1.24	1.28
SHRINKAGE	5.12	0.10	3.42	2.61
CREEP	10.51	1.83	6.50	6.17
RELAXATION	2.44	1.40	1.90	1.92
SUBTOTAL	19.76	4.20	13.07	11.98
FRICTION	1.42	5.08	3.34	3.25
ANCHORAGE	3.32	7.39	5.49	5.36
FRICTION + ANCHORAGE	4.74	12.48	8.83	8.61
ALL LOSSES	24.5	16.67	21.90	20.59

*All losses in percentage of nominal stress at transfer which is equal to $0.7f_{specified}$.

Table 4.7

Summary of Losses*
Pretensioned Beam with Stress Relieved Strand

TYPE OF LOSS	MAX.	MIN.	MEAN	$\frac{\text{MIN + MAX}}{2}$
EL. SHORTENING	1.80	1.08	1.36	1.44
SHRINKAGE	6.60	0.13	4.22	3.36
CREEP	12.01	2.77	8.09	7.39
RELAXATION	6.52	4.31	5.36	5.42
SUBTOTAL	26.93	8.29	19.04	17.61
RELAXATION + SHRINKAGE	5.59	2.42	4.13	4.00
ANCHORAGE	0.55	4.62	2.67	2.59
RELAX. + SHR. + ANCHORAGE	6.14	7.04	6.80	6.59
ALL LOSSES	33.07	15.33	25.84	24.20

*All losses in percentage of nominal stress at transfer which is equal to $0.7f_{specified}$.

Table 4.8

Summary of Losses*
Pretensioned Beam with Stabilized Strand

TYPE OF LOSS	MAX.	MIN.	MEAN	$\frac{\text{MIN + MAX}}{2}$
EL. SHORTENING	1.82	1.06	1.36	1.44
SHRINKAGE	6.60	0.13	4.22	3.36
CREEP	12.89	2.83	8.51	7.86
RELAXATION	1.34	0.86	1.10	1.10
SUBTOTAL	22.64	4.88	15.19	13.76
RELAXATION + SHRINKAGE	2.36	0.63	1.65	1.50
ANCHORAGE	0.54	4.51	2.61	2.52
RELAX. + SHR. + ANCHORAGE	2.90	5.14	4.26	4.02
ALL LOSSES	25.54	10.02	19.45	17.78

*All losses in percentage of nominal stress at transfer which is equal to $0.7f_{specified}$.

example calculation is given in Appendix B.

Because the loss computations were deterministic calculations, each based on a particular low or high value of each of the variables, the probability of the occurrence of the particular high or low losses computed is considerably less than the 1 in 20 assumed for some of the variables. The combinations chosen are felt to result in realistic upper and lower bounds for prestressing losses. For the purposes of computing the coefficient of variation of the losses, the high and low values were arbitrarily assumed to be plus and minus three standard deviations from the mean.

4.4.3 Summary of Losses and Comparison with Other Sources

A summary of the stress at transfer and mean losses occurring after transfer is given in Tables 4.9 and 4.10. For the Monte Carlo study, the mean stress at transfer was taken as 70 percent of the specified ultimate stress for all combinations of type of prestressing operation (pretensioned and post-tensioned) and type of strand (stress relieved and stabilized). The coefficient of variation of the stress at transfer varied only according to the type of prestressing operation, having values of 1.5 percent and 2.0 percent for pretensioned and post-tensioned beams, respectively. The mean losses and the coefficients of variation of losses were found to be

Table 4.9

Stress at Transfer

	STRESS RELIEVED	STABILIZED	RECOMMENDED (FOR STRESS RELIEVED AND STABILIZED)
MEAN STRESS AT TRANSFER	0.7 x specified ultimate	0.7 x specified ultimate	0.7 x specified ultimate
COV*—PRETENSION	0.0143	0.0142	0.015
—POST-TENSION	0.0193	0.0193	0.020

*Coefficient of Variation

Table 4.10

Losses

	PRETENSIONED	POST-TENSIONED	RECOMMENDED (FOR PRETENSIONED AND POST-TENSIONED)
STRESS RELIEVED			
MEAN LOSSES	0.190 x mean stress at transfer	0.189 x mean stress at transfer	0.19 x mean stress at transfer
COV*	0.163	0.159	0.16
STABILIZED			
MEAN LOSSES	0.152 x mean stress at transfer	0.131 x mean stress at transfer	0.14 x mean stress at transfer
COV*	0.195	0.198	0.20

*Coefficient of Variation

similar for pretensioned and post-tensioned beams when expressed as losses measured from transfer. This result supports Khachaturian's statement (1969) that there is no difference between losses measured from transfer for a pretensioned beam and a post-tensioned beam. There was a distinct difference between the losses for stress relieved strand and stabilized strand, however. Thus, the mean loss for stress relieved strand was taken as 19 percent of the mean stress at transfer with a coefficient of variation of 16 percent. The mean loss for stabilized strand was taken as 14 percent of the mean stress at transfer with a coefficient of variation of 20 percent. It should be noted that all losses in these tables are in terms of percent of mean stress at transfer—not initial jacking stress.

Based on a somewhat different method of analysis, Glodowski and Lorenzetti (1972) predicted total prestress losses in 40 years of 21.9 percent and 18 percent, respectively, for stress relieved and stabilized strand. If it is assumed that 90 percent of this would occur in the first five years, the corresponding five-year losses would be 19.7 and 16.2 percent which are close to the values of 19 and 14 percent in the last column of Table 4.10.

The ACI-ASCE Joint Committee 323 (1958) recommended using losses of 35,000 psi for pretensioned beams and 25,000 psi for post-tensioned beams. These losses do not include losses due to friction but they are measured from the time of tensioning—not from when the stress is trans-

ferred to the beam. Thus, the 35,000 psi for pretensioned beams includes relaxation and shrinkage losses that occur between the time of stressing and the time that the stress is transferred. This committee also states that the magnitude of the loss does not significantly affect the ultimate moment.

Lin (1955) gives prestressing losses for both pretensioned and post-tensioned beams with stress relieved strand. These losses are tabulated in Table 4.11. Lin's relaxation losses are quite a bit lower than the relaxation losses calculated in this study because Lin has assumed that the strands have been overtensioned to reduce relaxation losses. Lin (1955) states that ". . . creep may easily be cut in half if it is overtensioned by 5 to 10% and held there for 2 to 3 minutes." No overtensioning has been assumed for the calculations in this study. If the absence of overstressing was assumed to double the relaxation losses, Lin's final losses would be 18 percent for post-tensioned beams and 20 percent for pretensioned beams. This compares favorably with the loss calculations in this study which indicate a loss of 19 percent for both pretensioned and post-tensioned beams.

Overtensioning to reduce relaxation losses was not considered in this study because the effectiveness of this procedure is open to some doubt. The effect of overtensioning was investigated by Magura, Sozen and Siess (1962). After performing some tests of their own as well

Table 4.11

COMPARISON OF LOSS CALCULATIONS
WITH LIN'S LOSSES

TYPE OF LOSS	POST-TENSIONED		PRETENSIONED	
	CALCULATIONS	LIN	CALCULATIONS	LIN
EL. SHORTENING	1.24%	1%	1.36	3
SHRINKAGE	3.42	6	4.22	7
CREEP	5.88	5	8.09	6
RELAXATION	8.36	3	5.36	2
TOTAL	18.91	15	19.04	18

as looking at other investigators' results (Kajfasz, 1958; Dumas, 1958), they concluded that "prestretching is of little consequence if the prestretching period is limited to a matter of minutes."

4.5 Dimensional Variability

Probability models for dimensional properties proposed by Mirza and MacGregor (1978b) were used in this study and are tabulated in Table 4.12. The values for flange thickness were obtained from the recommended distribution properties of slab dimensions. In this table, a plus sign means that the mean value is greater than the nominal specified value whereas a negative sign means that the mean value is less than the nominal value.

The dimensional properties for precast members were used for all pretensioned beams because pretensioned beams are usually precast. *In-situ* dimensional properties were used for all post-tensioned beams. All dimensional properties were assumed to be normally distributed.

Unfortunately, no data for the effective depth to the prestressing steel was available. Although different factors may be involved in the placement of reinforcing steel and in the placement of prestressing steel, the same mean deviation was used for both types of steel, as shown in Table 4.12. The mean deviation of the effective depth to the prestressing steel for precast beams is positive whereas that for *in-situ* beams is negative. The

Table 4.12

Recommended Distribution Properties of Beam Dimensions

DIMENSION DESCRIPTION	IN-SITU BEAMS		PRECAST BEAMS	
	MEAN DEVIATION FROM NOMINAL (in.)	STANDARD DEVIATION (in.)	MEAN DEVIATION FROM NOMINAL (in.)	STANDARD DEVIATION (in.)
Width of Flange	--	--	+5/32	1/4
Width of Rib	+3/32	3/16	0	3/16
Depth of Flange	+1/32	15/32	0	3/16
Overall Depth	-1/8	1/4	+1/8	5/32
Effective Depth of Bottom Reinforcement	-3/16	1/2	+1/8	11/32
Effective Depth of Prestressing Steel	-3/16	1/4	+1/8	11/64

reason for this change in sign is that the mean deviaions of the overall depth reported by Mirza and MacGregor (1978b) change in sign and the effective depth is closely related to the overall depth.

For example, in a pretensioned (precast) beam, the prestressing steel is stressed in a prestressing bed. The position of the steel is determined by the position of the plates at the ends of this bed. These plates are fixed relative to the bottom of the bed when the concrete is poured. When the mean deviation of overall depth is 1/8 in. greater than the nominal depth, this extra depth is due to more concrete at the top of the form. As a result, the mean effective depth to the prestressing steel will tend to be greater than the nominal effective depth by about the same amount.

In a post-tensioned *(in-situ)* beam, the ducts are placed in position in the form and are secured by tying them to the reinforcing steel or to bolsters with wire ties, or by using chairs or other supports. If the ducts are tied to the reinforcing steel, the ducts will tend to float when the concrete is placed due to buoyancy effects. This effect, which reduces the effective depth, is more in evidence when the tubing is placed first without the tendons inside. If chairs are used, a mean deviation of effective depth of prestressing steel similar to that of reinforcing steel could be expected since chairs are also used in securing reinforcing steel in position.

Bolsters are horizontal bars that are usually attached to the form. Thus, in most of the securing methods, the position of the prestressing steel will be fixed relative to the bottom of the form when the concrete is poured. When the mean deviation of the overall depth is less than the nominal depth, this difference is due to not enough concrete at the top of the beam. As a result, the mean effective depth to the prestressing steel should be less than the nominal effective depth by about the same amount.

The standard deviation of the depth to the reinforcing steel was felt to be too large to be applied directly to the prestressing steel. For example, it seems extremely unlikely that a cast-in-place, post-tensioned beam would have a maximum variation (±3 standard deviations) in effective depth of ±1.5 inches. For this reason, and because prestressing steel is placed and held in position more carefully than reinforcing steel, the standard deviation for the depth to the prestressing steel was taken to be half of the corresponding values for reinforcing steel.

CHAPTER V

COMPUTER PROGRAM FOR ANALYSIS

5.1 Description of the Monte Carlo Technique

The Monte Carlo technique is a method of random sampling. In this study, random numbers from 0.001 to 0.999 are generated and the corresponding values from cumulative frequency functions for each of the variables are used to define strengths and dimensions to be used in a calculation of the strength of a prestressed concrete beam. A different random number is used to define each variable. This random number generation and strength calculation is repeated a sufficient number of times to obtain a stable distribution of ultimate strengths for prestressed concrete beams. The Monte Carlo technique has also been described in Chapters I and II.

5.2 Description of the Computer Program

The computer program developed for this study calculates the theoretical ultimate flexural strength of prestressed concrete beams by developing the moment-curvature diagram and picking the maximum point on this diagram. The Monte Carlo technique is used to obtain a

population of the ratio of the theoretical strength from this program to the strength predicted by the ACI Code (1971a) assumptions. The statistical properties of this population are then calculated.

The program consists of a MAIN program and eight subroutines—PROP, ACI, THEORY, MOM, AXIAL, FSTEEL, RANDOM, and STAT. A brief flow diagram outlining the general features of the program is given in Appendix C.

The MAIN program contains the Monte Carlo technique and puts all the subroutines together. First, it reads quantities needed for the Monte Carlo simulation. The PROP subroutine is then called, which reads and writes the nominal properties of the beam. The distribution properties of the variables that are used in the calculation of the theoretical ultimate moments are then read in and outputted in the MAIN program.

The ACI subroutine is used to calculate the ACI strength of the beam as described in Section 3.7. The nominal values of the variables are used in this calculation to give the strength that would be computed by the designer.

Each variable is then set equal to its mean value in the MAIN program. These values are used in the subroutine THEORY to calculate the mean theoretical ultimate flexural strength.

The THEORY subroutine first calculates section properties such as the centroid, gross and net areas, and

gross and net moments of inertia in order to calculate the prestress strains described in Section 3.1. The calculation of the net moment of inertia, used in calculating the prestress in post-tensioned beams, involves subtracting the moment of inertia of the holes in the concrete due to the prestressing ducts from the moment of inertia of the whole section. An elastic flexural analysis is used to calculate the stresses at the top and bottom of the section due to the prestressing force:

$$f_{top} = \frac{P}{A_{net}} - \frac{Pey_t}{I_{net}} \qquad (5.1)$$

$$f_{bot} = \frac{P}{A_{net}} + \frac{Pey_b}{I_{net}} \qquad (5.2)$$

where: P = prestressing force
$= f_{se} \times A_{sp}$
A_{net} = net area of concrete
e = eccentricity
y_t = distance from centroid to top of section
y_b = distance from centroid to bottom of section
I_{net} = net moment of inertia

It should be noted that although the net area and moment of inertia were used here, the transformed section was not. This is because the concrete is not bonded to the steel at the time of post-tensioning. Dividing the stresses in Equations 5.1 and 5.2 by the modulus of elasticity for

concrete gives the strain at the top and bottom of the section, respectively. Once the strain distribution is known, similar triangles are used to calculate the strain in the concrete due to the prestressing force, ε_{ce}. Since ε_{ce} is such a small number, it does not affect the strain in the prestressing steel or the ultimate moment very much (Warwaruk, Sozen and Siess, 1962). Therefore, the elastic analysis used should be accurate enough even though it is not an exact analysis.

The effective stress in the prestressing steel, ε_{se}, is calculated by dividing the effective prestress by the modulus of elasticity of the prestressing steel:

$$\varepsilon_{se} = \frac{f_{se}}{E_{sp}} \qquad (5.3)$$

This relationship is exactly true in this study, since the effective stress was found to be always in the intial linear portion of the stress-strain curve for prestressing steel.

The rest of the THEORY subroutine develops the moment-curvature diagram using the method described in Section 3.5. A flow diagram of this subroutine may be found in Appendix C. The THEORY subroutine uses three other subroutines—AXIAL, FSTEEL, and MOM. The AXIAL subroutine calculates the component forces and finally the resultant force for a given strain distribution as described in Section 3.5. Thus, given the curvature ϕ,

and the strain at the top of the section, ε_t, this subroutine calculates the compressive and tensile forces in concrete. The AXIAL subroutine makes use of the FSTEEL subroutine to calculate the force in the steel.

Subroutine MOM utilizes the Newton-Raphson procedure or the trial and error procedure to close in on the balanced condition which is the distribution of strain that gives a total axial force resultant close to zero. These procedures have been described in detail in Section 3.6. Once this balanced condition is reached, the MOM subroutine sums the moments due to the forces to give the total moment acting on the section.

As soon as the maximum moment is obtained from the moment-curvature diagram, the program returns to the MAIN program. The ratio of mean theoretical strength to ACI strength is calculated and outputted.

The program then starts the Monte Carlo simulations. Given the mean, standard deviation, and distribution properties for each variable, the RANDOM subroutine generates a random value for each variable. The THEORY subroutine uses these random numbers to calculate the theoretical ultimate strength of the beam as described above. The ratio of theoretical ultimate strength to ACI strength is obtained. The process of generating values, calculating the theoretical strength, and obtaining the above ratio is repeated for the number of simulations that is desired.

This simulated population of ratios is then analyzed statistically by STAT which finds the mean value, standard deviation, coefficient of variation, coefficient of skewness, coefficient of kurtosis, minimum and maximum values, and the median. Also calculated are the first and fifth percentiles, the second, third, and fourth moments of the distribution about the mean, and a cumulative frequency table for the population generated by this program.

5.3 Comparison of Theory With Test Results

In developing the computer program for this study, the THEORY, AXIAL, FSTEEL, and MOM subroutines were developed first. As described in the previous section, these subroutines find the theoretical ultimate moment using a theoretical model. The accuracy of the theoretical model was determined by comparing actual test beam results with results from the THEORY program. To make this comparison, the ratio of test strength to theoretical strength was calculated for 45 beams. The results are summarized in Table 5.1. The test strengths of these beams were obtained from other studies.

Most of the test beam results were taken from a study on the flexural strength of prestressed concrete beams (Warwaruk, Sozen, and Siess, 1962). These beams, with marks OB or RB in Table 5.1, were all rectangular, and were nominally 6"×12" in size. Most of the beams used

Table 5.1

COMPARISON OF MEASURED AND COMPUTED ULTIMATE MOMENTS

MARK	f'_c (psi)	ω_p	TEST (in. lb.)	THEORY (in. lb.)	TEST / THEORY
Warwaruk, Sozen, and Siess (1962)					
OB1	3530	0.070	111000	117,737.3	0.943
OB2	6330	0.146	408000	433,922.4	0.940
OB3	3910	0.224	415000	379,667.3	1.093
OB4	5550	0.305	501000	535,000.0	0.936
OB5	3750	0.332	394000	364,333.4	1.081
OB6	3750	0.414	444000	387,752.3	1.145
OB7	2890	0.140	156000	148,166.1	1.053
OB8	3450	0.330	387000	366,234.4	1.057
OB9	4280	0.290	434000	409,926.5	1.059
OB10	2500	0.290	270000	230,934.4	1.169
OB11	3760	0.064	136000	125,965.4	1.080
OB12	5420	0.086	258000	241,297.9	1.069
OB13	8320	0.091	372000	373,265.6	0.997
OB14	6560	0.102	302000	314,326.9	0.961
OB15	7180	0.166	559000	603,761.2	0.926
OB16	3820	0.164	281000	300,701.1	0.935
OB17	7630	0.166	592000	588,657.3	1.006
OB18	5490	0.172	443000	415,607.1	1.066
OB19	5650	0.173	482000	476,990.5	1.011
OB20	8200	0.244	707000	716,258.1	0.987
OB21	3440	0.252	389000	381,496.6	1.020
OB22	6120	0.257	577000	566,948.3	1.018
OB23	5910	0.317	646000	610,221.1	1.059
OB24	3270	0.368	432000	367,442.7	1.176
OB25	4590	0.374	588000	571,606.2	1.029
OB26	2950	0.414	424000	372,807.3	1.137
OB27	3280	0.462	572000	438,981.3	1.303
OB29	3330	0.075	122000	117,285.3	1.040
OB30	5710	0.160	426000	435,584.2	0.978
OB31	4580	0.200	408000	408,745.8	0.998
OB32	6220	0.280	635000	633,771.3	1.002
OB33	4100	0.307	462000	441,573.9	1.046
RB1	5280	0.080	198000	201,307.4	0.984
RB2	3970	0.217	362000	386,791.5	0.936
RB3	5230	0.279	569000	600,717.7	0.947
Brecht, Hanson and Hulsbos (1965)					
G2	6673	0.180	12,945,600	13,119,480	0.987
G4	7573	0.161	13,155,600	13,353,080	0.985

Continued ↓

Sozen, Zwoyer, and Siess (1959)					
B1	8260	0.054	341,000	321,224.0	1.062
B2	8400	0.054	334,000	320,829.6	1.041
B3	8560	0.053	334,000	321,059.4	1.040
A1	4840	0.310	547,000	506,999.6	1.079
A2	3350	0.363	494,000	454,400.1	1.087
A3	3665	0.186	321,000	312,520.6	1.027
Olesen, Sozen, and Siess (1965)					
BW1	2840	0.165	297,000	274,289.5	1.083
CW1	7620	0.121	526,624.4	520,687.6	1.011

from that study were post-tensioned and had the OB marking. The RB beams were pretensioned. All of these beams used bonded prestressing wire. Beam OB28 was omitted from the study because this test beam had a very low concrete strength and was not representative of the range of values of concrete strength that occur in reality. The ultimate test strength reported by Warwaruk *et al.* (1962) was the moment at which visible crushing of the concrete in the extreme fiber occurred. The maximum moment carried by the beam is usually a little higher than that corresponding to visible crushing.

Beams G2 and G4 are full-sized, 36" deep pretensioned I-beams taken from Brecht, Hanson and Hulsbos (1965). These beams were analyzed as T-beams since the lower flange was cracked at ultimate. Here again, the theoretical ultimate moments agreed very well with the measured test moments, as indicated by the ratios of test to calculated strength of 0.987 and 0.985. Stress relieved 270 ksi 7/16-inch diameter strand was used in these beams.

Beams with a mark A or B were taken from a study of shear strength of beams without web reinforcement (Sozen, Zwoyer and Siess, 1959). These particular beams failed in flexure. The beams with mark B were I-beams but were input into the program as T-beams. The beams with mark A were rectangular beams. All beams were 6"×12" overall. The reported measured moment was the maximum moment, not the moment corresponding to first visible crushing.

Beams with the mark BW1 and CW1 came from another study of shear strength (Olesen, Sozen, and Siess, 1965). Again, these beams failed in flexure. The beams were I-beams with overall dimensions of 6"×12" and they were treated as T-beams in this study. The reported measured moment was the maximum moment attained in the test.

In the comparison of theory with test results, it was assumed that the cylinder strength was equal to the *in-situ* strength since most of the test beams were relatively small and the curing of the beams and test cylinders was similar. Therefore, Equation 4.1 was not used in this comparison.

The effect of the rate of loading on the concrete properties was explained in Section 4.1. The higher the rate of loading, the higher the concrete strength and the theoretical strength of the beam. Thus, the test time that was chosen could have an effect on the comparison of theory with test results. Generally, the total time required to complete a test on a beam, including time taken for measurements, photographs, *et cetera*, was reported as 4 to 8 hours. What was required, however, was the actual rate of loading of the test beam. This was taken as 1 hour in the comparisons listed in Table 5.1.

The mean value of the ratio of test strength to calculated strength was 1.035 with a coefficient of variation of 0.0719. However, this includes the test to theory ratio of 1.303 for beam OB27 in Table 5.1. This ratio is

more than three standard deviations higher than the mean value. The test to theory result for this beam in the original study (Warwaruk, Sozen and Siess, 1962) was 2½ standard deviations higher than the mean. Although no reason could be found as to why this ratio was so high, it was found to have the highest value of ω_p (0.462) among the 45 beams investigated. The effect of high values of ω_p on the theoretical model used in this study is discussed later in this section. Because the ratio of test to theoretical strength was high for this beam in the original study as well as in this study, this ratio was considered to be an outlying point and was disregarded. The mean value and coefficient of variation without this point were 1.029 and 0.0611, respectively. These modified results were used in this study.

A mean value greater than 1.0 indicates that the test strength is greater than the theoretical strength. In other words, the theoretical model is on the safe side and underestimates the ultimate strength.

The data from Table 5.1 is plotted in Figure 5.1. The test data has been divided into underreinforced and overreinforced beams using the ACI (1971a) limit of ω_p of 0.30. Regression lines for the two parts suggest that the ratio of test to computed strength is more or less constant for ω_p less than 0.30, but increases rapidly as ω_p exceeds 0.30. Thus, the theoretical model predicts the ultimate strengths of underreinforced beams much more ac-

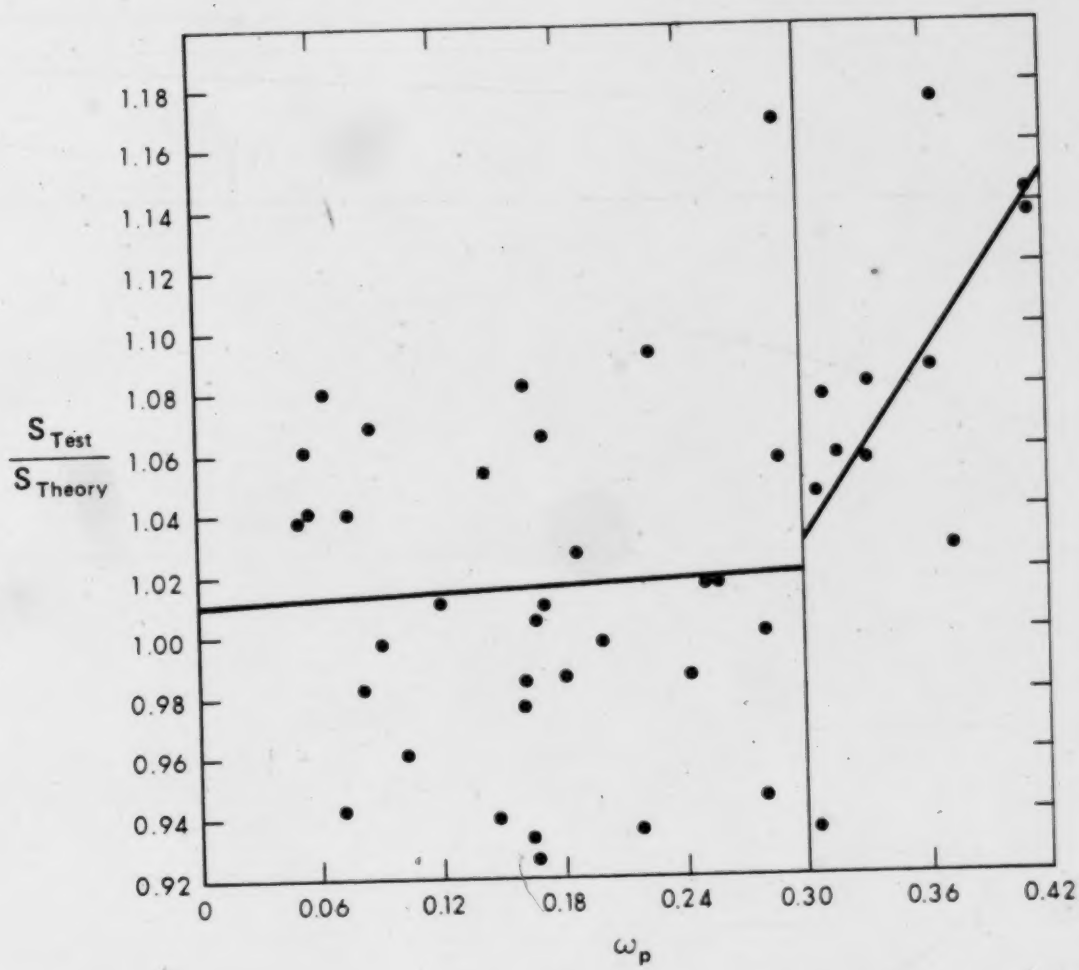

Figure 5.1 Ratio of Test Strength to Theoretical Strength vs Reinforcement Index, ω_p

curately than that of overreinforced beams. The mean ratios of test to computed strengths were 1.014 and 1.076 in the two ranges.

Some of this difference in accuracy can be attributed to the stress-strain curve for the prestressing steel used in the theoretical model. As described in Section 3.4, the assumed stress-strain curve has a straight line from the elastic limit to the stress at 1 percent strain, that is, from point B to point C in Figure 3.3. This line is a lower bound to the actual curve in this region. Consequently, the calculated stresses in this area are lower than the actual stresses. The maximum error in moment from this effect would be one percent or less. Generally, the stress in the prestressing steel is in this region at ultimate moment only for overreinforced beams.

Conversely, underreinforced beams have low amounts of steel resulting in higher stresses and strains in each tendon to obtain a certain amount of force in the steel. At higher strains, the assumed stress-strain curve agrees very closely to the actual stress-strain curve, as can be seen in Figure 3.3. Hence, this difference in accuracy between overreinforced and underreinforced beams is partly due to the assumed stress-strain curve for prestressing steel.

The lower accuracy for overreinforced beams can also be partly explained by the fact that the prestressing

steel stress at ultimate, f_{su}, is sensitive to a large number of variables including the prestressed reinforcement ratio ρ_p, the effective strength of the concrete f_{cu}, the effective prestrain in the steel ε_{se}, and the potential non-linear strain distribution.

5.4 In-batch Variability and Variability of the Theoretical Model

The coefficient of variation of the ratio of test strength to theoretical strength of 0.0611 mentioned in Section 5.3 is the result of three variabilities—variation due to different people performing the various tests, in-batch variability of the materials and dimensions, and variability of the theoretical model itself. This relationship is shown by the following expression:

$$V_s^2 = V_{test}^2 + V_{in\text{-}batch}^2 + V_{theo}^2 \qquad (5.4)$$

The variability due to different people testing and the errors implicit in the test itself were assumed to be 4 percent (Grant, 1978).

In-batch variability is the variability that exists even after material strengths and beam dimensions are controlled as closely as possible. In order to obtain a value for this variability, the Monte Carlo program developed in this study was run on beams B3, OB14, OB31, OB33 and OB26 to see the effect of in-batch variability. These

beams were selected because they represented a wide range of ω_p. The increased control of variability is reflected in the lower coefficients of variation or standard deviations used in these in-batch runs as can be seen in Table 5.2. The in-batch properties of concrete were from Mirza, Hatzinikolas, and MacGregor (1978). The in-batch variabilities of prestressing steel properties, effective stress, and dimensional properties were arbitrarily taken to be half of those in a beam with normal control which would have the variabilities presented in Sections 4.3, 4.4, and 4.5. It should be noted that the full variability for the depth to the prestressing steel was used since this variability was obtained by dividing the variability for the depth to the reinforcing steel arbitrarily by two.

The mean value of each variable was set equal to the corresponding measured value for these in-batch computer runs. Also, the effect of the variability of the analysis was eliminated by setting the mean value of the analysis factor equal to 1.0 and the coefficient of variation equal to 0.0.

Once $V_{in\text{-}batch}$ is known, the variability of the theoretical model, V_{theo}, can be calculated from Equation 5.4. The results from the in-batch runs and these calculations are summarized in Table 5.3. The in-batch variability increased as ω_p increased leading to a more or less uniform value of the computed V_{theo}. The average coefficient of variation of the theoretical model worked out

Table 5.2

COEFFICIENTS OF VARIATION OR STANDARD DEVIATIONS
USED FOR IN-BATCH RUNS

PROPERTIES	COEFFICIENT OF VARIATION	STANDARD DEVIATION
Concrete Properties		
Compressive Strength	0.05	
Tensile Strength	0.045	
Modulus of Elasticity	0.035	
Prestressing Steel Properties		
Stress @ 1% Strain/Ultimate Stress	0.005	
Ultimate Stress	0.01	
Ultimate Strain	0.03	
Modulus of Elasticity	0.01	
Effective Stress		
Stress at Transfer	0.01	
Prestressing Losses	0.08	
Dimensional Properties		
Width on Compression Face		0.125
Width on Tension Face		0.09375
Depth of Beam		0.07813
Flange Depth		0.09375
Depth to Prestressing Steel		0.17188
Variability of Analysis	0.00	

Table 5.3

SUMMARY OF CALCULATIONS FOR V_{theo}

Mark	ω_p	$V_{in\text{-}batch}$	$^*V_{theo} = \sqrt{V_s^2 - (0.04)^2 - (V_{in\text{-}batch})^2}$
B3	0.053	0.01872	0.042
OB14	0.102	0.02151	0.041
OB31	0.200	0.02362	0.040
OB33	0.307	0.03580	0.029
OB26	0.414	0.04028	0.023
			$\Sigma = 0.175$
			$\bar{\mu} = \frac{0.175}{5} = 0.035$

*NOTE: $V_s = 0.06111$

to 0.035 and this value was used to allow for the variability of the analysis in the Monte Carlo study described in Chapter VI.

CHAPTER VI

THE MONTE CARLO STUDY

6.1 Beams Studied

A wide range of beam sizes with varying amounts of prestressing steel were studied. The overall depths considered were 12", 14", 16", 24", 36", and 48". The values of reinforcement index, ω_p, that were investigated were 0.019, 0.054, 0.122, 0.228, 0.295, and 0.387. The combinations of overall depth and ω_p studied are shown in Table 6.1. The nominal properties of the beams that were studied are tabulated in Table 6.2. The beam with an overall depth of 16" and a reinforcement index of 0.054 was chosen as the basic beam used in sensitivity studies, etc. Only straight prestressing strand was used in these beams.

Some of the beam sections that were investigated were chosen directly from the *PCI Design Handbook* (1971). For example, the basic, pretensioned beam is designated as an 8DT16 beam with a strand pattern of 68-S in this handbook. Although it is a double T section in the handbook, this beam was analyzed as a single T in this study. This was accomplished by lumping the two stems of the double T together into a single stem. To investigate a

Table 6.1

COMBINATIONS OF h AND ω_p STUDIED*

h (in) \ ω_p	0.019	0.054	0.122	0.228	0.295	0.387
12	▪	▪			▪	
14		▪				
16	▪	▪	▪	▪	▪	▪
24		▪				
36		▪				
48	▪	▪			▪	

*▪ indicates combination studied

Table 6.2 Nominal Properties of Beams Studied

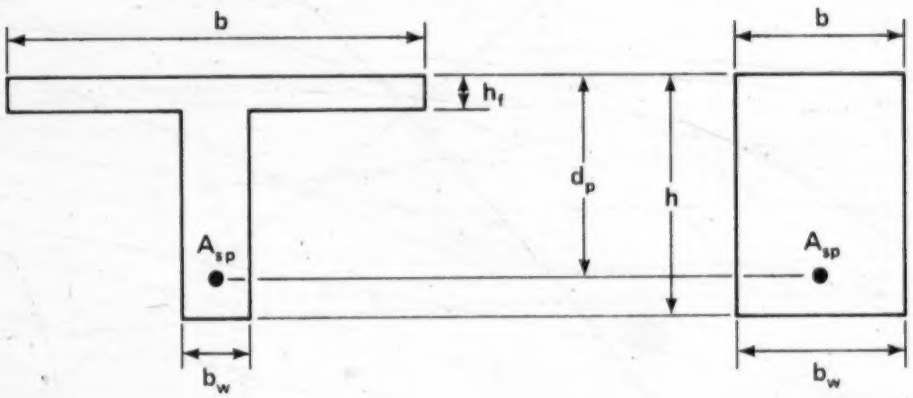

T-Beam Rectangular Beam

f'_c = 5,000 psi

f_{pu} = 270,000 psi

CODE*	ω_p	h (in)	h_f (in)	b (in)	b_w (in)	Asp (in^2)	d_p (in)
1	0.021	12.0	4.0	72.0	9.5	0.23	8.0
2	0.021	12.0	4.0	72.0	9.5	0.23	8.0
1	0.019	16.0	2.0	96.0	9.5	0.46	13.5
2	0.019	16.0	4.0	48.0	9.5	0.23	13.5
1	0.018	48.0	3.5	120.0	8.0	1.53	36.6875
2	0.018	48.0	7.0	60.0	8.0	0.765	36.6875
1	0.053	12.0	2.0	96.0	9.5	0.918	9.5
2	0.053	12.0	4.0	48.0	9.5	0.459	9.5
1	0.056	14.0	2.0	48.0	7.0	0.46	9.0
2	0.056	14.0	4.0	24.0	7.0	0.23	9.0
1	0.054	16.0	2.0	96.0	9.5	0.918	9.3125
2**	0.054	16.0	4.0	48.0	9.5	0.459	9.3125

*1 refers to pretensioned beams
2 refers to post-tensioned beams

**This section was used in the study of the effect of conventional reinforcing steel

Table continued ↓

1	0.056	24.0	2.0	96.0	9.5	1.836	18.0
2	0.056	24.0	4.0	48.0	9.5	0.918	18.0
1	0.054	36.0	3.0	96.0	8.0	2.754	28.0
2	0.054	36.0	6.0	48.0	8.0	1.377	28.0
1	0.055	48.0	3.5	120.0	8.0	4.59	36.6875
2	0.055	48.0	7.0	60.0	8.0	2.295	36.6875
1,2	0.122	16.0	0.0	12.0	12.0	0.306	10.5
1,2	0.228	16.0	0.0	12.0	12.0	0.612	10.5
1,2	0.292	12.0	0.0	12.0	12.0	0.612	7.75
1,2	0.295	16.0	0.0	12.0	12.0	0.918	11.5
1,2	0.297	48.0	0.0	16.0	16.0	3.978	37.0
1,2	0.387	16.0	0.0	12.0	12.0	1.224	10.5

particular combination of overall depth and ω_p, it was necessary at times to make up a beam by adjusting the amount of steel or the depth to the steel in the PCI section, or by adjusting the section dimensions.

No conventional reinforcing was included in the beams in the main investigation. A separate study on the effect of reinforcing steel was conducted on the basic beam, as described in Section 6.2.8.

Both rectangular beams and T-beams were studied. The T-beams were used to simulate both single T and double T stringers. T-beams were used to investigate the lower values of ω_p. For values of ω_p greater than or equal to 0.122, rectangular beams were used. This splitting of the beams into T-beams and rectangular beams came about because the expression for ω_p has b in the denominator:

$$\omega_p = \frac{A_{sp}}{bd} \frac{f_{ps}}{f'_c} \qquad (6.1)$$

where b is the cross section width on the compression face, A_{sp} is the area of the prestressing reinforcement, and f_{ps} is the calculated stress in the prestressing steel at design load (see Equation 3.13). Thus, for lower values of ω_p, a high value of b is required as in a T-beam. Conversely, for high values of ω_p, b is a low value requiring the use of rectangular beams.

For each combination of overall depth and ω_p, four different cases were considered to give all four pos-

sible combinations of pretensioning and post-tensioning with either stress relieved strand or stabilized strand. For rectangular beams, the same cross section and amount of reinforcement was used for both pretensioned and post-tensioned beams. In the case of most of the T-beams, however, the flange depth for the post-tensioned case was twice that of the pretensioned case and the flange width for the post-tensioned case was half that of the pretensioned case. Also, the amount of prestressing steel in these post-tensioned T-beams was half the amount in the corresponding pretensioned beams in order to keep the value of ω_p constant for both types of beams. (See Table 6.2.) This manipulation was done in the interest of practicality of the beam based on the assumption that the flange of a post-tensioned beam would be cast-in-place while pretensioned beams would be precast. The flange depth for pretensioned beams was nominally 2" in most cases. A variation of three standard deviations from the mean value for a precast (pretensioned) beam still results in a constructable flange depth of 1.438 inches. However, a variation of three standard deviations for an *in-situ* (post-tensioned) beam with the same nominal flange depth would result in a flange depth, h_f, of 5/8 inch and would be extremely unlikely. If the flange depth was nominally 4", however, the same variation would result in a beam that could possibly occur with h_f equal to 2 5/8 inches.

All post-tensioned T-beams were checked to ensure

that the 1971 ACI building code limit (Section 8.7.2) on the overhang of the flange was not exceeded.

It was also nececessary to adjust the depth to the prestressing steel when the Monte Carlo simulation could have put the steel below the bottom of the beam, which cannot happen in reality. For pretensioned beams, the bottom strand was checked to make sure that it had at least 1" of cover when the depth to the prestressing steel was at a maximum (about 3 standard deviations from the mean) and the overall depth was at a minimum. In this check, the spacing between the strands was assumed to be three times the diameter of a strand (Section 7.4.6 ACI Code), as shown in Figure 6.1. For post-tensioned beams, the bottom of the duct was checked to make sure it had at least 1½" of cover at all times. Also, the bottom of the end plate was checked to ensure that it did not extend below the bottom of the section. This is illustrated in Figure 6.2. These checks were introduced to ensure that the computer runs were on practical beams.

The information on duct diameters and anchor plate sizes for post-tensioned beams was obtained from the *PCI Post-tensioning Manual* (1972). It was assumed that the VSL multi-strand system was used for all post-tensioned beams. Up to 55 strands can be put in one duct in this system. None of the beams studied had more than 30 strands. It was assumed that the plate sizes could be altered to fit the cross section as long as the total area of the plate

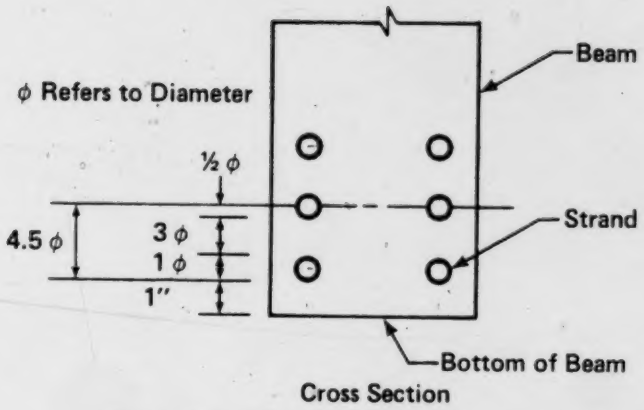

Figure 6.1 Reinforcement Location in Pretensioned Beam

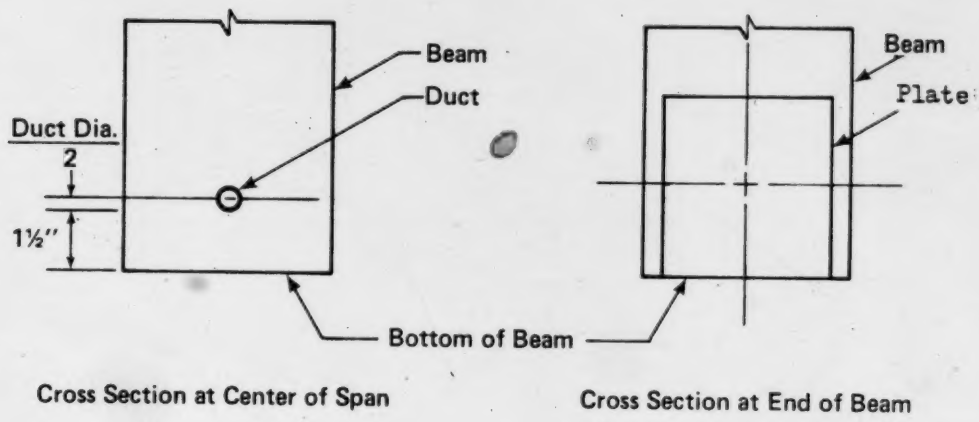

Figure 6.2 Reinforcement and End Plate Location in Post-tensioned Beam

remained the same.

After the location of the strands was checked to make sure that they remained within the cross section at all times, they were lumped together at one location for the Monte Carlo study. In doing this it was assumed that the position of the individual strands relative to one another within the span remains constant. For example, pretensioned strands move as a unit as the height of the end buttresses varies relative to the height of the forms. Similarly, the post-tensioned strands move as a unit as the duct moves within the beam. If there had been several post-tensioning ducts, the steel would have been lumped in several locations since each duct can move relative to the other ducts This possibility was not considered in this study due to the complete lack of data on these variations.

6.2 Results of the Monte Carlo Simulation

6.2.1 General

This Monte Carlo study was conducted to get a population of the ratio of theoretical ultimate strength to ACI ultimate strength for various prestressed concrete beams. The computer program analyzed the populations statistically. This information will be used in the future to calculate understrength (ϕ) factors for prestressed concrete beams once load factors have been selected.

Concrete properties, prestressing steel properties, losses, and dimensions of the cross section were varied to study the effect on section strength. The type of prestressing operation, the type of prestressing strand, the depth of the beam, and the reinforcement index, ω_p, were also varied to see what effect they had on the ultimate moment. The effects of construction quality, reinforcing steel, and prestressing losses were also studied.

The effect of rate of loading was not studied. One hour loading time was used for all beams.

It should be noted that although the degree of control of concrete strength was varied, the nominal strength was not varied. In this part of this study, f'_c was always equal to 5000 psi.

The computer runs to determine the in-batch variability discussed in Section 5.4 used 500 Monte Carlo simulations. The same seed, 65549, was used for all of these runs. The seed is any odd-numbered integer up to nine digits long that is used to initiate the random number generation in the RANDOM subroutine. The number of simulations was changed to 1000 in the final computer runs described in this chapter because the cost was not excessive. A different seed was used for every beam in the final runs. These seeds were chosen from a table for random selection (Kreyszig, 1970) so that a systematic influence would not be introduced into the results.

6.2.2 Effect of Variability of Individual Variables on the Variability of Section Strength

The effects of the variability of concrete strength, prestressing steel strength, prestressing losses, and geometric properties on the variabiltiy of the strength ratios were investigated for three combinations of overall depth and reinforcement index. The basic beam with h=16" and ω_p=0.054 was studied, as well as a beam with the same ω_p but with h=12", and a beam with h=16" and ω_p=0.295 (see Table 6.1). For each combination of h and ω_p, a pretensioned beam with stress relieved strand and a post-tensioned beam with stress relieved strand were considered. The results are summarized in Tables 6.3, 6.4, and 6.5. The coefficient of variation listed in these tables is the coefficient of variation of the population of the ratios of theoretical strength to ACI strength.

These sensitivity studies were carried out to determine the effect of each variable separately. Thus, if the effect of the variability of the concrete properties was being investigated, the compressive strength, tensile strength, and modulus of elasticity of concrete would be varied through the Monte Carlo technique and all other variables would be set equal to their mean values by setting their standard deviations to zero. It was found that the variability of the theoretical analysis itself represented a significant part of the overall variability. To examine the effects of the physical variables by them-

Table 6.3

Sensitivity Study (ω_p = 0.054, h = 16")

VARIABLE PROPERTIES	PRETENSIONED		POST-TENSIONED	
	COV*	$V_{px}^2/V_{p,all}^2$	COV	$V_{px}^2/V_{p,all}^2$
All Properties Variable Except Analysis Factor	0.033	1.00	0.042	1.00
Concrete Properties Variable	0.012	0.14	0.016	0.15
Prestressing Steel Properties Variable	0.023	0.52	0.023	0.30
Losses Variable	0.000	0.00	0.000	0.00
Geometric Properties Variable	0.020	0.36	0.029	0.49
$(V_{p,conc}^2 + V_{p,steel}^2 + V_{p,losses}^2 + V_{p,dim}^2)/V_{p,all}^2$	--	1.02	--	0.94

*COV is Coefficient of Variation

Table 6.4

SENSITIVITY STUDY (ω_p = 0.295, h = 16")

VARIABLE PROPERTIES	PRETENSIONED		POST-TENSIONED	
	COV*	$V_{px}^2/V_{p,all}^2$	COV	$V_{px}^2/V_{p,all}^2$
All Properties Variable Except Analysis Factor	0.075	1.00	0.095	1.00
Concrete Properties Variable	0.068	0.82	0.092	0.93
Prestressing Steel Properties Variable	0.013	0.03	0.013	0.02
Losses Variable	0.008	0.01	0.009	0.01
Geometric Properties Variable	0.025	0.11	0.035	0.13
$(V_{p,conc}^2 + V_{p,steel}^2 + V_{p,losses}^2 + V_{p,dim}^2)/V_{p,all}^2$	--	0.97	--	1.09

*COV is Coefficient of Variation

Table 6.5

Sensitivity Study (ω_p = 0.053, h = 12")

VARIABLE PROPERTIES	PRETENSIONED		POST-TENSIONED	
	COV*	$V_{px}^2/V_{p,all}^2$	COV	$V_{px}^2/V_{p,all}^2$
All Properties Variable Except Analysis Factor	0.032	1.00	0.040	1.00
Concrete Properties Variable	0.012	0.15	0.017	0.18
Prestressing Steel Properties Variable	0.023	0.51	0.023	0.34
Losses Variable	0.000	0.00	0.000	0.00
Geometric Properties Variable	0.019	0.38	0.030	0.57
$(V_{p,conc}^2 + V_{p,steel}^2 + V_{p,losses}^2 + V_{p,dim}^2)/V_{p,all}^2$	--	1.04	--	1.09

*COV is Coefficient of Variation

selves, the effect of the analysis factor was ignored by setting the analysis correction factor equal to 1.0 with coefficient of variation equal to zero for the sensitivity studies.

Tables 6.3 through 6.5 show that the overall coefficient of variation, as well as the coefficients of variation due to the concrete and geometric properties are greater for the post-tensioned beams than for the pretensioned beams. This is because the average control of concrete and dimensions assumed for post-tensioned beams was poorer than for pretensioned beams. The coefficients of variation due to the prestressing steel properties and losses were the same for pretensioned and post-tensioned beams.

The variability of the cross section strength can be empirically represented by:

$$V_{p,all}^2 = V_{p,conc}^2 + V_{p,steel}^2 + V_{p,losses}^2 + V_{p,dim}^2 \qquad (6.2)$$

where $V_{p,all}$ is the coefficient of variation of the section strength with all properties variable except for the analysis factor. The other terms are the coefficients of variation due to the concrete strength, prestressing steel strength, losses, and dimensions if these properties are varied one at a time. It can be seen in the tables that this expression was essentially satisfied.

A comparison of Table 6.3 and Table 6.5 shows

that when the overall depth, h, was reduced from 16 inches to 12 inches, the effects of the variabilities in concrete properties, prestressing steel properties, losses, and geometric properties on the variability of the cross sectional strength remained constant.

On the other hand, Table 6.3 and Table 6.4 show that ω_p considerably affects the relative contributions of the variabilities of the properties to the variability of the cross sectional strength. For small values of ω_p, the prestressing steel properties and geometric properties have the largest effect on the total variability. In one analysis, only the depth was varied. This gave almost identically the same variability as when all geometrical properties were varied which indicates that the effect of the geometric properties was almost entirely caused by the variability of the depth to the prestressing steel. The concrete properties have a small effect on the total variability and the losses have no effect at all.

For large values of ω_p, the concrete properties have the largest effect on the total variability, geometric properties have a small effect on the variability, and prestressing steel properties and losses have very little effect on the variability.

These results were expected. For low values of ω_p, there is not much prestressing steel in the beam and thus the beam fails when the steel strain is near the ultimate strain. Hence, the prestressing steel properties

should be important for low values of ω_p. Conversely, for high values of ω_p there is a lot of prestressing steel in the beam and the beam fails when the concrete crushes. Thus, the concrete properties should be important for high values of ω_p.

6.2.3 Effect of Type of Prestressing on Section Strength

The results of the Monte Carlo calculations showing the effect of type of prestressing, the effect of type of strand, the effect of depth of beam, and the effect of ω_p are tabulated in Tables 6.6, 6.7, 6.8 and 6.9. The mean values and the coefficients of variation (in brackets) of the populations of the ratios of theoretical strength to ACI strength are given in these tables.

It can be seen from these tables that the type of prestressing, pretensioned or post-tensioned, makes a significant difference in the strength of the section. Pretensioned beams have higher mean values of the ratio of theoretical strength to ACI strength than the post-tensioned beams. This difference decreases for larger values of overall depth h. Much of this difference can be attributed to the differences in effective depths to the prestressing steel. Pretensioned beams were assumed to have a mean effective depth of 0.125" greater than the nominal effective depth. On the other hand, post-tensioned beams had a mean effective depth of 0.1875" less than the nominal effective depth. Thus, the pretensioned beams had

Table 6.6

MEAN AND COEFFICIENT OF VARIATION OF MONTE CARLO POPULATIONS FOR PRETENSIONED BEAMS WITH STRESS RELIEVED STRAND

h (in.) \ ω_p	0.019	0.054	0.122	0.228	0.295	0.387
12	1.06* (0.047)**	1.07 (0.047)			1.03 (0.086)	
14		1.06 (0.049)				
16	1.06 (0.046)	1.07 (0.046)	1.05 (0.049)	1.05 (0.060)	1.03 (0.079)	1.19 (0.090)
24		1.06 (0.046)				
36		1.06 (0.046)				
48	1.05 (0.043)	1.05 (0.044)			1.02 (0.081)	

*Mean **Coefficient of Variation

Table 6.7

MEAN AND COEFFICIENT OF VARIATION OF MONTE CARLO POPULATIONS FOR PRETENSIONED BEAMS WITH STABILIZED STRAND

h (in.) \ ω_p	0.019	0.054	0.122	0.228	0.295	0.387
12	1.06* (0.048)**	1.07 (0.049)			1.05 (0.079)	
14		1.06 (0.048)				
16	1.06 (0.045)	1.07 (0.048)	1.05 (0.050)	1.06 (0.060)	1.05 (0.078)	1.22 (0.092)
24		1.06 (0.046)				
36		1.06 (0.044)				
48	1.05 (0.045)	1.05 (0.047)			1.04 (0.075)	

*Mean **Coefficient of Variation

Table 6.8

MEAN AND COEFFICIENT OF VARIATION OF MONTE CARLO POPULATIONS FOR POST-TENSIONED BEAMS WITH STRESS RELIEVED STRAND

h (in.) \ ω_p	0.019	0.054	0.122	0.228	0.295	0.387
12	1.02* (0.052)**	1.03 (0.053)			0.97 (0.113)	
14		1.02 (0.056)				
16	1.03 (0.047)	1.02 (0.055)	1.01 (0.058)	1.00 (0.085)	0.99 (0.105)	1.15 (0.118)
24		1.04 (0.047)				
36		1.04 (0.046)				
48	1.04 (0.044)	1.04 (0.046)			1.01 (0.094)	

*Mean **Coefficient of Variation

Table 6.9

MEAN AND COEFFICIENT OF VARIATION OF MONTE CARLO POPULATIONS FOR POST-TENSIONED BEAMS WITH STABILIZED STRAND

h (in.) \ ω_p	0.019	0.054	0.122	0.228	0.295	0.387
12	1.02* (0.056)**	1.03 (0.055)			0.99 (0.107)	
14		1.03 (0.054)				
16	1.03 (0.045)	1.03 (0.051)	1.02 (0.054)	1.02 (0.075)	1.01 (0.097)	1.16 (0.119)
24		1.03 (0.047)				
36		1.04 (0.046)				
48	1.04 (0.044)	1.04 (0.045)			1.03 (0.093)	

*Mean **Coefficient of Variation

a mean effective depth of 0.3125" greater than the mean effective depth for the post-tensioned beams. The concrete properties, prestressing steel properties, the stress at transfer, and the prestressing losses had the same mean values for both pretensioned and post-tensioned beams. As discussed in Section 6.1, the dimensions of the flange of the T-beams as well as the amount of steel was different for pretensioned and post-tensioned T-beams in most cases.

The coefficients of variation indicate that the post-tensioned beams have a greater variability in strength than the pretensioned beams. This can be attributed to the higher variability in concrete compressive strength, stress at transfer, and in dimensional properties, in particular effective depth, for post-tensioned beams.

6.2.4 Effect of Type of Strand on Section Strength

The results of the Monte Carlo analyses were analyzed statistically to see if there was a significant difference between beams with stress relieved strand and those with stabilized strand. The t-test and F-test were used to test the difference between the means and the difference between the variances, respectively, for groups of similar beams. It was found that there was no difference at the 5 percent significance level between the means and variances of the distributions for stress relieved strand and stabilized strand for low values of ω_p. Above ω_p = 0.1, there was a significant difference between the dis-

tributions for stress relieved strand and stabilized strand. For beams having $\omega_p \geq 0.1$, the ultimate moment with stabilized strand is greater than that with stress relieved strand because the strains in the prestressing steel are relatively low for higher values of ω_p, which allows the improved stress-strain characteristics of stabilized strand at low strains to be utilized. Another reason for the improved strength is that the prestressing losses are less for stabilized strand due to lower relaxation losses. The effect of prestressing losses is further discussed in Section 6.2.9.

The variability in strength is approximately the same for stress relieved strand and stabilized strand. This is to be expected since the coefficients of variation for the variables defining the stress-strain properties of the strand are only slightly different for the two types of strand.

6.2.5 Effect of Depth of Beam on Section Strength

Statistical tests (F and t-tests) were carried out to see if the overall depth, h, of the beam has a significant effect on the cross sectional strength ratios. Although it was possible to group certain sizes into representative populations, the hypotheses that the means and the variances were the same for the populations for the various values of h were rejected at the 5 percent significance level in most cases.

As shown in Tables 6.6 through 6.9, the mean value of the ratio of theoretical strength to ACI strength decreased slightly and the coefficient of variation stayed the same as h increased for pretensioned beams. The mean value increased and the coefficient of variation decreased as h increased for post-tensioned beams.

6.2.6 Effect of ω_p on Section Strength

The results were tested statistically to see if the reinforcement index, ω_p, has a significant effect on the strength ratios. At the 5 percent significance level there was no significant difference between beams with $\omega_p = 0.019$ and $\omega_p = 0.054$ in approximately 6 of the 12 pairs tested. On the other hand, there was a significant difference between beams with other values of ω_p. Therefore ω_p has a significant effect on the ultimate moment.

The results of Tables 6.6, 6.7, 6.8 and 6.9 are plotted against ω_p in Figures 6.3 and 6.4. The first percentile values are also plotted against ω_p in Figure 6.5. The results for pretensioned beams are plotted in the top half of the figures; those for post-tensioned beams are plotted in the bottom half. A best-fit line is drawn in each graph of Figures 6.3 and 6.4. In the case of post-tensioned beams, different lines fitted the data for beams with an overall depth less than or equal to 16" and those with an overall depth greater than 16". This was not true for pretensioned beams. The best-fit lines for the mean

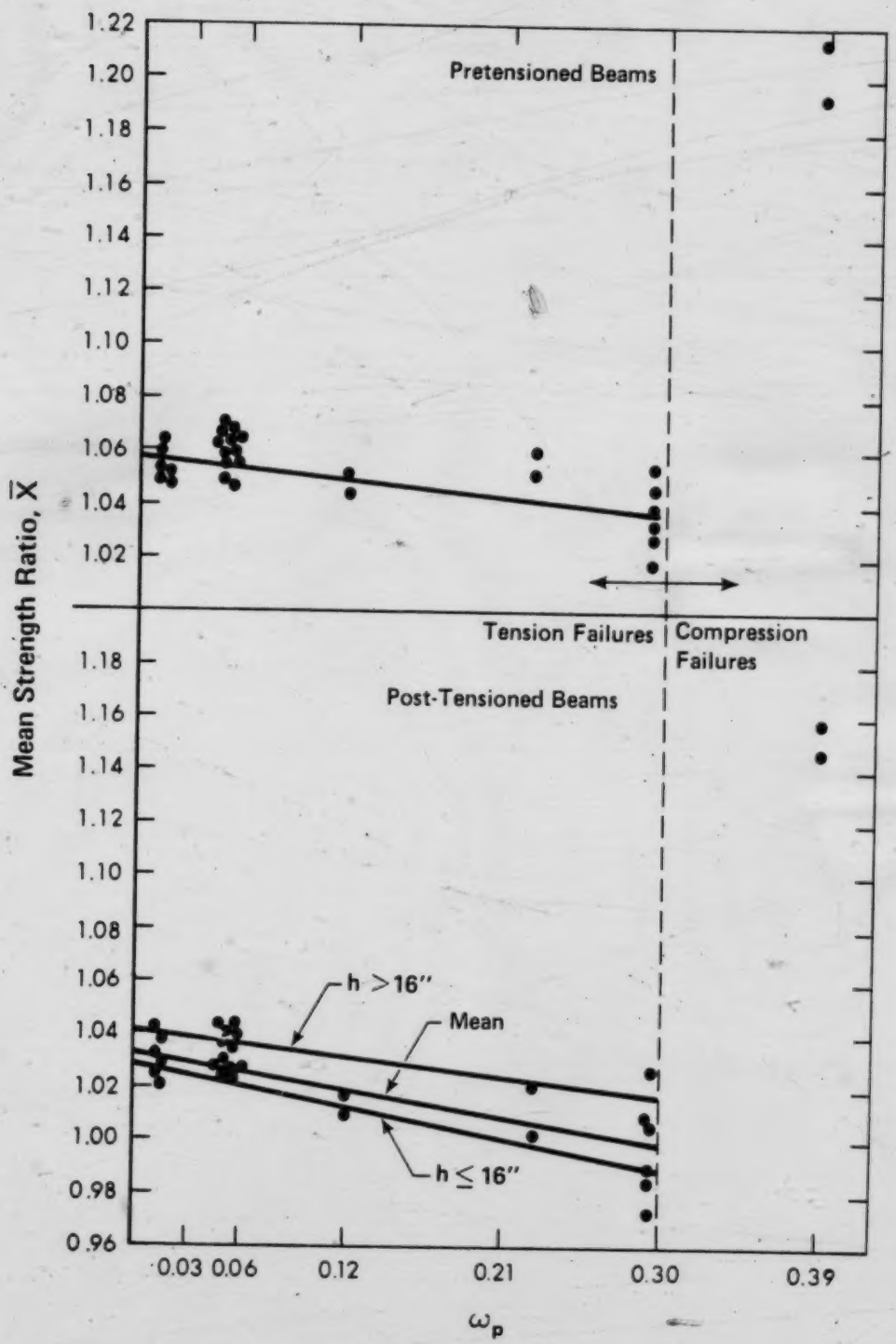

Figure 6.3 Variation in Mean Strength Ratio with ω_p

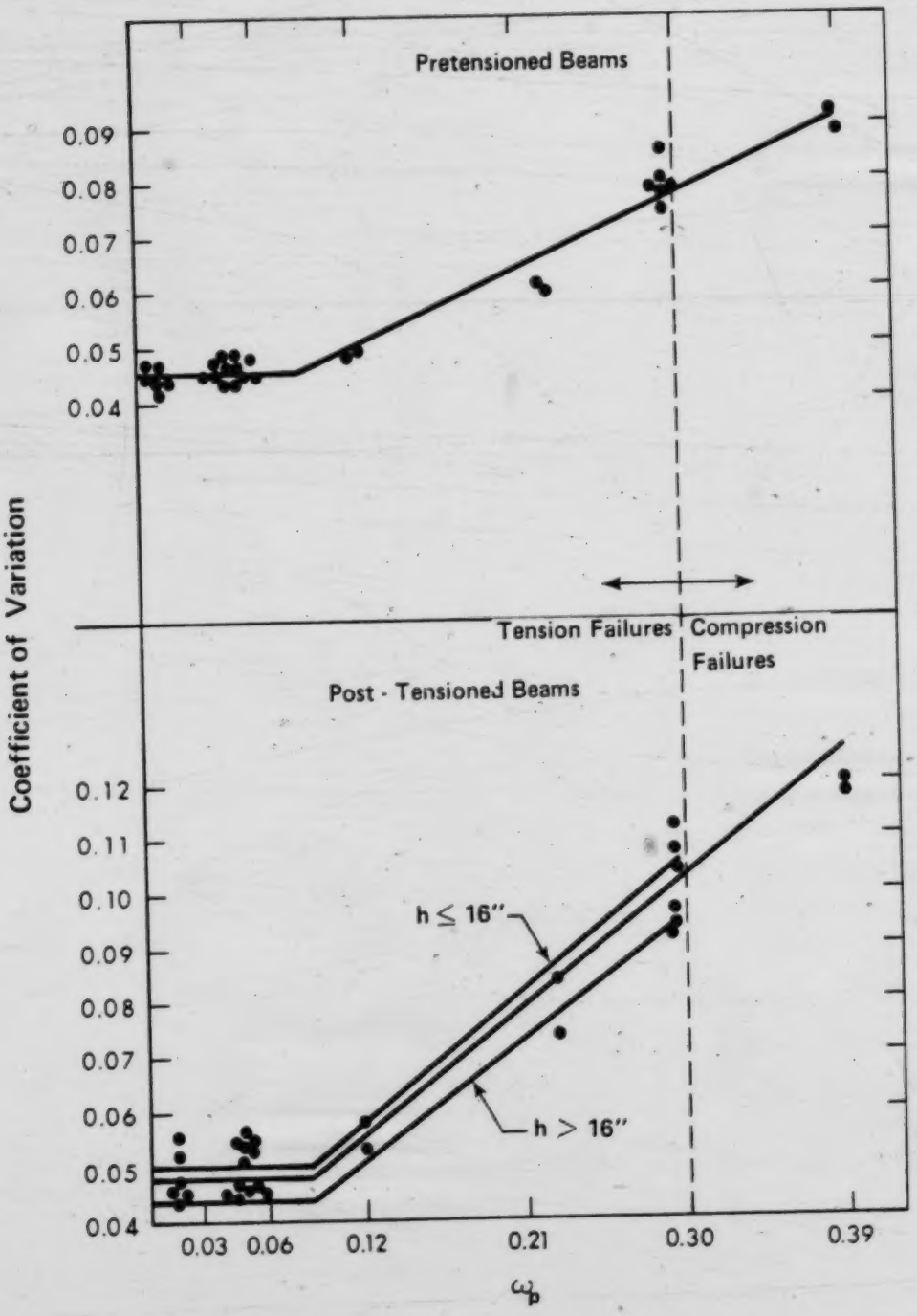

Figure 6.4 Variation in Coefficient of Variation of Strength Ratio with ω_p

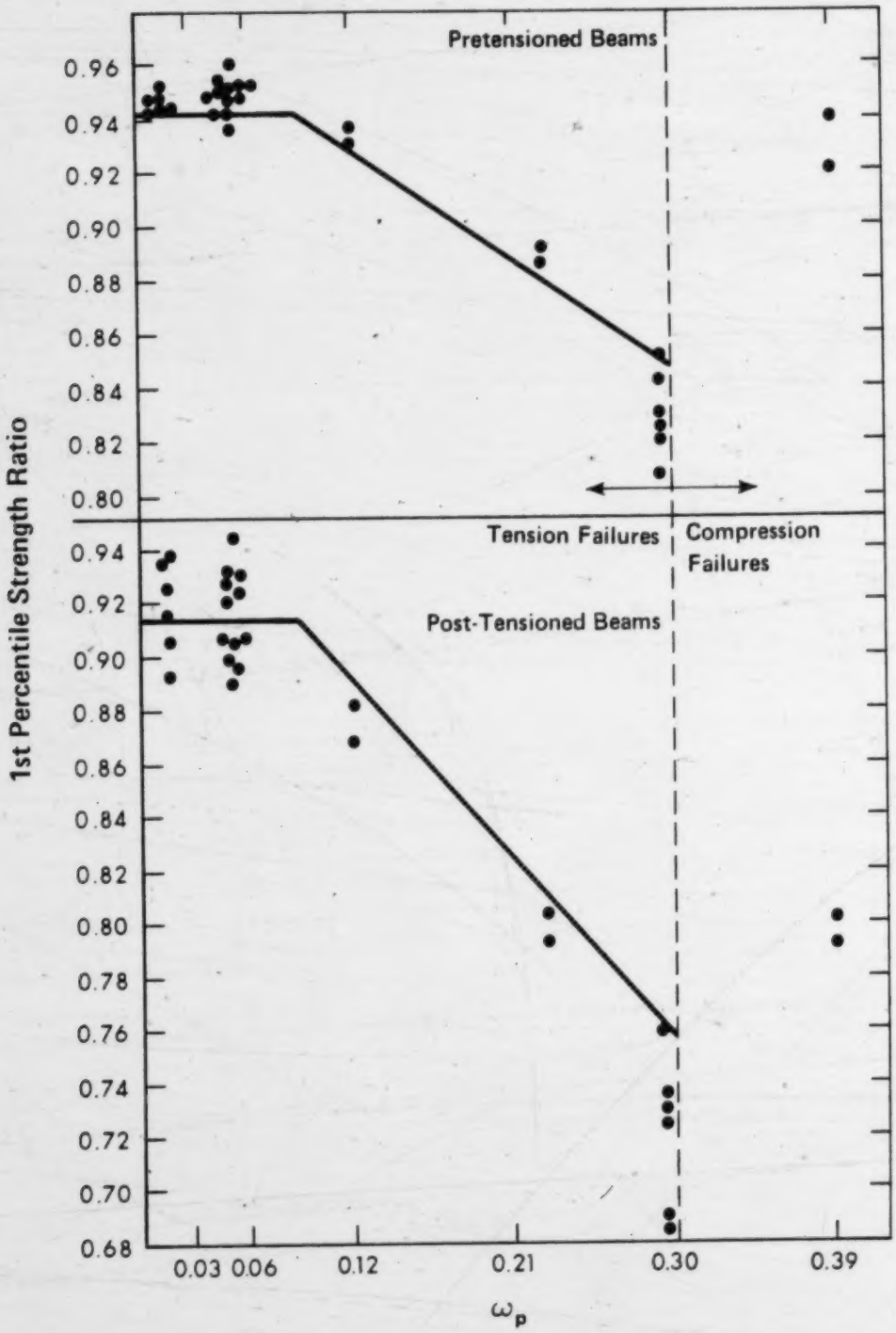

Figure 6.5 Variation in First Percentile of Strength Ratio with ω_p

and coefficient of variation were then used to calculate the first percentile values:

$$1st\ percentile = \bar{\mu} - 2.326\sigma \qquad (6.3)$$

where: $\bar{\mu}$ = mean value

σ = standard deviation.

The line in Figure 6.5 was plotted using these calculated values.

Figure 6.3 shows that the mean value of the ratio of the strengths decreases as ω_p increases up to 0.30, and then increases sharply. As ω_p approaches 0.30 from below, the percentage of the beams failing prematurely in compression increases, causing a reduction in the mean value of the ratio of the theoretical strength to the ACI strength because of the decrease in theoretical strength for over-reinforced beams. This decrease in theoretical strength has been discussed in Section 5.3 and is shown graphically in Figure 5.1. Part of the reason for this decrease is that the actual values of the variables may be quite different from the nominal values which are used in the expression for ω_p.

The variability of the strength ratio increases as ω_p increases. This too, can be explained by the fact that compression failures increase as ω_p increases. In other words, the variability of the beam strength for high

values of reinforcement index is more dependent on the variability of the strength of the concrete than for lower values of ω_p. As discussed in Section 6.2.2, the variability of the steel properties is more important for lower values of ω_p. Since concrete properties are more variable than steel properties, the variability of the beam strength increases as ω_p increases.

One beam section with ω_p greater than 0.30 was investigated. It can be seen from Tables 6.6, 6.7, 6.8 and 6.9 and Figures 6.3 and 6.4 that the mean value and coefficient of variation for this beam are considerably higher than the corresponding values for beams with ω_p less than 0.30. This is because this beam is classified as overreinforced. The variability of this beam was high because the ultimate steel strains fell on the steep rising part of the stress-strain curve and a small variation in properties caused a large variation in steel stress, and thus in ultimate moment. The mean strength ratio for this section was high because the ACI Commentary (1971b) equation for the ultimate moment of such a beam (Equation 3.17 in this thesis), tends to be conservative.

6.2.7 Effect of Construction Quality on Section Strength

The effect of construction quality on the strength ratios was studied by varying the degree of control of concrete quality and the degree of control of dimensions,

including the depth to the steel. The post-tensioned beam with stress relieved strand and h = 16" and ω_p = 0.054 was chosen as the basic test beam. This beam had already been studied in the original series using average control of concrete (V_{ccyl} = 15 percent) and average control of dimensions. Distributions were computed for the same beam for two more cases:

1. using excellent control of concrete and average control of dimensions, and
2. using poor control of concrete and poor control of dimensions.

In case 1, excellent control of concrete was achieved by setting V_{ccyl} equal to 10 percent as described in Section 4.1. The *in-situ* mean values and standard deviations described in Section 4.5 were used for average control of dimensions. In case 2, V_{ccyl} was set equal to 20 percent for poor control of concrete quality. Poor control of dimensions was simulated by multiplying the standard deviations for *in-situ* dimensions by 2. The results are tabulated in Table 6.10.

The F-test and t-test were carried out to compare the results of the basic beam with the results of case 1 and the results of case 2. These tests showed that construction quality had no significant effect on section strength when the control of concrete changed from average to excellent. Poor control of concrete and poor control of dimensions had a significant effect on the coefficient of

Table 6.10

EFFECT OF CONSTRUCTION QUALITY

CONSTRUCTION QUALITY	MEAN	COV*	CO-SKEWNESS+	KURTOSIS
Av. Control of Concrete Av. Control of Dimensions	1.02	0.055	-0.17	3.26
Ex. Control of Concrete Av. Control of Dimensions	1.02	0.052	0.09	2.87
Poor Control of Concrete Poor Control of Dimensions	1.02	0.079	-0.01	2.99

*Coefficient of Variation
+Coefficient of Skewness

variation in this case but there was no significant difference between the mean values. Therefore, it was concluded that construction quality, and in particular dimensional tolerances, did have a significant effect on the outlying values of the cross sectional strength ratios.

6.2.8. Effect of Conventional Reinforcing Steel on Section Strength

Once again, the basic section chosen was the post-tensioned beam with stress relieved strand and h = 16" and ω_p = 0.054. The amount or location of the prestressing steel was not changed in this part of the study. Various amounts of reinforcing steel, 2#4, 2#6, 2#9, 2#11 and 2#14, were added to the basic section at a nominal depth of 13.5" As mentioned in Section 4.2, the nominal yield strength and modulus of elasticity of reinforcing steel were 60,000 psi and 29,000,000 psi, respectively.

The location of the reinforcing steel was checked to make sure that the steel did not go below the bottom of the section in the Monte Carlo simulations. The relative positions of the prestressing steel and reinforcing steel were also checked to make sure that the bottom of the duct was never below the bottom of the reinforcing steel since it was assumed that there would be a stirrup across the bottom of the reinforcing bars.

The results are shown graphically in Figure 6.6. The independent variable in this plot is ω/ω_p, the ratio of the reinforcement index for prestressing steel plus reinforcing steel to the reinforcement index for the basic

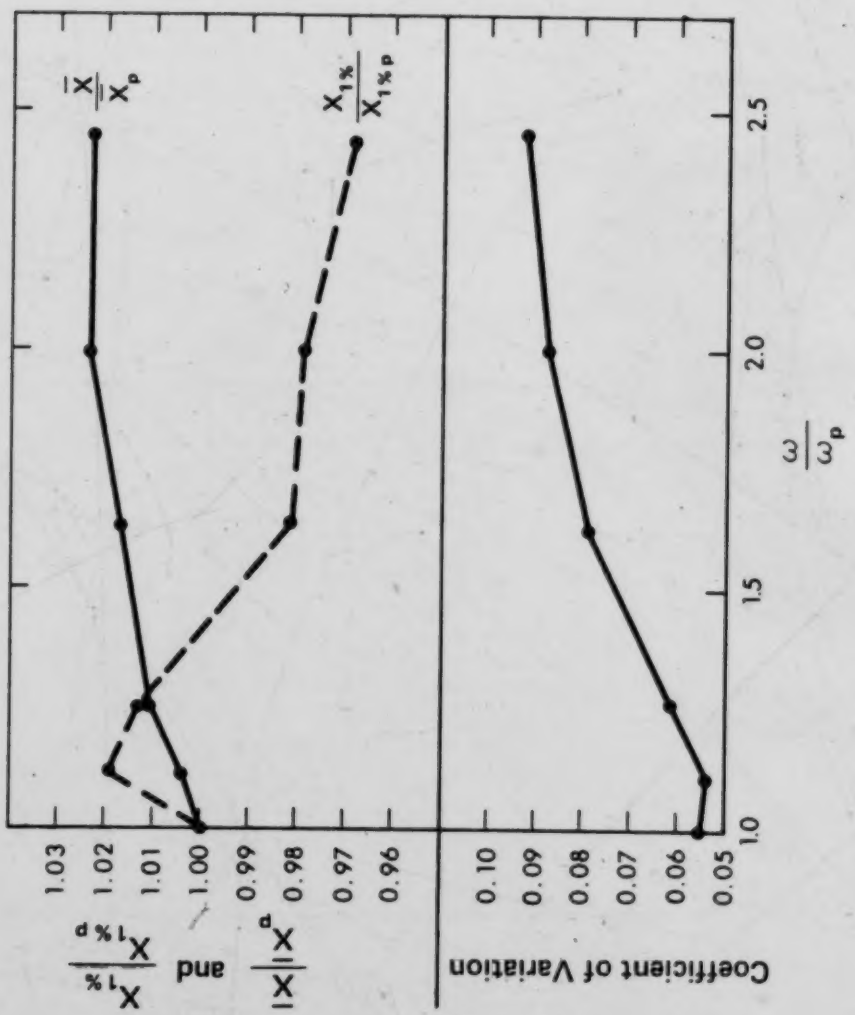

Figure 6.6 Effect of Conventional Reinforcing Steel on Statistical Properties of Distributions.

beam, which has prestressing steel only. Figure 6.6 shows the mean and first-percentile values as a ratio of the values for the beam with prestressing steel and reinforcing steel to the values for the basic beam. The values for the coefficient of variation are not shown as a ratio, rather the values plotted are those for the beam with prestressing steel and reinforcing steel. It can be seen from the figure that the section strength increases, and the variability of the section strength increases as the amount of conventional reinforcing steel increases. The ultimate moment increases because the ratio of actual to nominal yield strength is larger for conventional reinforcement than for prestressing tendons. The variability of the section strength also increases as the amount of reinforcing steel increases due to the relatively high variability of the properties of conventional reinforcing steel.

6.2.9 Effect of Prestressing Losses on Section Strength

The effect of prestressing losses on the section strength was studied by varying the losses for six beams. These beams all had an overall depth of 16". Three different values of ω_p were used—0.019, 0.054 and 0.295. For each value of ω_p, a pretensioned beam and a post-tensioned beam were investigated. The losses were varied by using:

1. 2/3 of the mean and standard deviation used in the basic computer runs:

$$\bar{\mu}_{losses} = 2/3 \times .19 \times 189000 = 23900. \text{ psi}$$

$$\sigma_{losses} = 2/3 \times .16 \times 23940 = 2550. \text{ psi}$$

2. 1½ times the mean and standard deviation used in the basic computer runs:

$$\bar{\mu}_{losses} = 1.5 \times .19 \times 189000 = 53900. \text{ psi}$$

$$\sigma_{losses} = 1.5 \times .16 \times 53865 = 12930. \text{ psi}$$

The results are tabulated in Table 6.11.

Statistical testing showed that for low values of ω_p (0.019 and 0.054), varying the amount of losses had no significant effect on the section strength ratios. This was expected since these beams failed with prestressing steel stresses at or near ultimate. For high values of ω_p (0.295), however, varying the amount of losses had a significant effect on the mean strength ratio of the section. The variability of the section strength ratio was not sifnificantly affected by varying the losses.

6.2.10 Shape of Probability Distributions of Results

Some typical probability density functions of the ratio of theoretical to ACI strengths for pretensioned and post-tensioned beams are shown in Figures 6.7 and 6.8, respectively. The probability density functions for a

Table 6.11

EFFECT OF VARYING LOSSES*

ω_p = 0.019

	MEAN	COV**	CO-SKEWNESS	KURTOSIS
PRETENSIONED				
BASIC BEAM	1.06	0.046	0.08	2.86
2/3 x Losses	1.05	0.045	0.04	2.90
1½ x Losses	1.05	0.045	0.13	2.85
POST-TENSIONED				
BASIC BEAM	1.03	0.047	0.08	3.19
2/3 x Losses	1.03	0.048	0.11	3.10
1½ x Losses	1.03	0.048	0.07	3.05

ω_p = 0.054

	MEAN	COV	CO-SKEWNESS	KURTOSIS
PRETENSIONED				
BASIC BEAM	1.07	0.046	0.04	3.36
2/3 x Losses	1.06	0.048	0.17	2.89
1½ x Losses	1.06	0.049	0.14	3.06
POST-TENSIONED				
BASIC BEAM	1.02	0.055	-0.09	2.94
2/3 x Losses	1.02	0.055	0.07	2.94
1½ x Losses	1.02	0.053	0.15	2.87

ω_p = 0.295

	MEAN	COV	CO-SKEWNESS	KURTOSIS
PRETENSIONED				
BASIC BEAM	1.03	0.079	-0.15	3.03
2/3 x Losses	1.04	0.076	-0.04	2.99
1½ x Losses	1.01	0.081	-0.16	3.20
POST-TENSIONED				
BASIC BEAM	0.99	0.105	-0.33	3.69
2/3 x Losses	1.00	0.097	-0.32	3.03
1½ x Losses	0.96	0.104	-0.28	3.10

*NOTE: All these beams have stress relieved strand
**NOTE: COV is Coefficient of Variation

reinforcement index, ω_p, of 0.054 are plotted in the top half of the figures; those for an ω_p of 0.295 are plotted in the bottom half.

These figures show that the probability distributions of the results were close to normal distributions. The higher coefficients of variation for beams with a higher value of ω_p is shown by the greater spread in results for the beam with $\omega_p = 0.295$. The shape of the distribution for a pretensioned beam was very similar to that for the corresponding post-tensioned beam, except that the distribution for the post-tensioned beam was shifted to the left due to the lower mean value for the post-tensioned beam. As discussed in Section 6.2.3, the lower mean values for post-tensioned beams were caused mainly by the assumed probability models for effective depths.

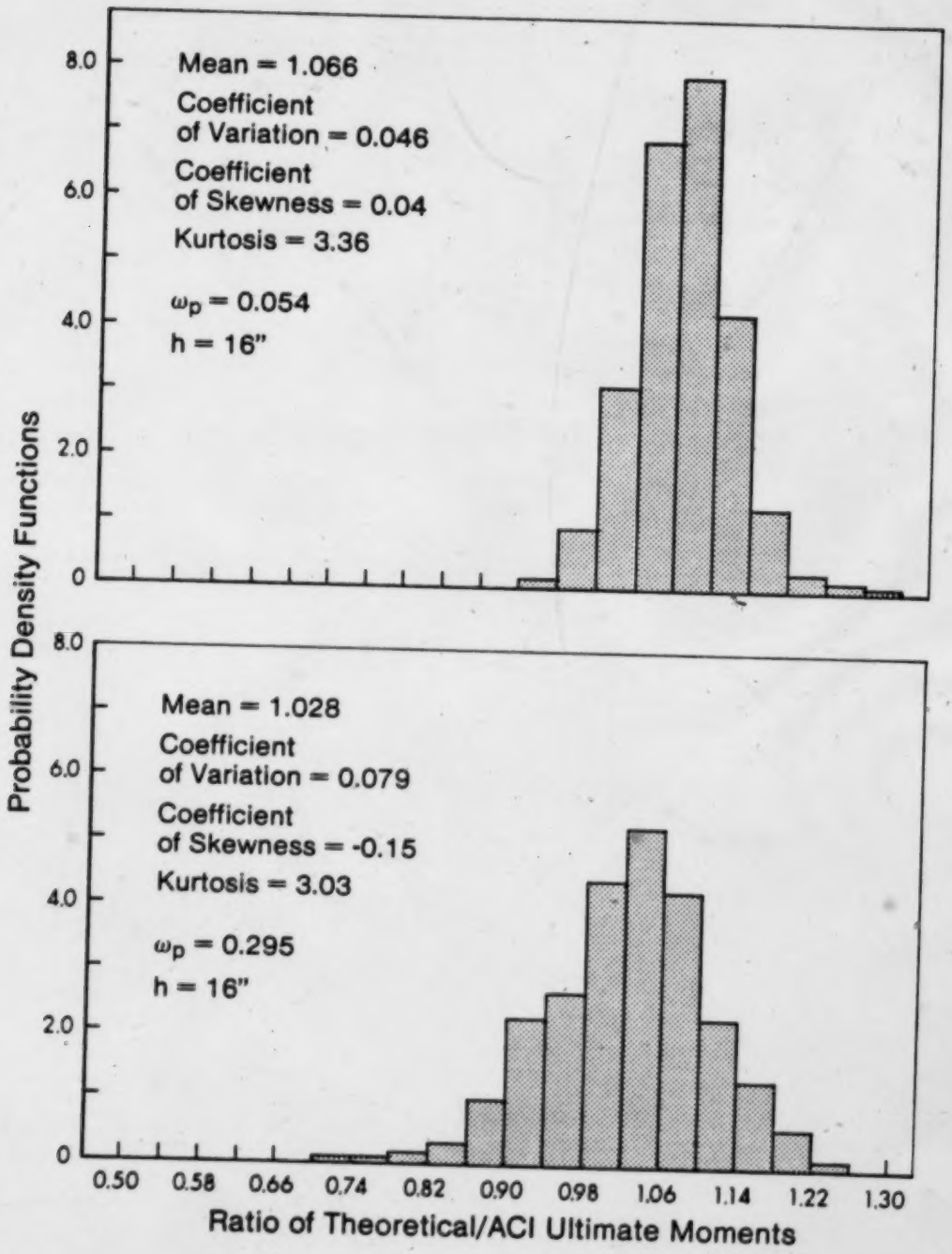

Figure 6.7 Probabiltiy Density Functions for Pre-Tensioned Beams

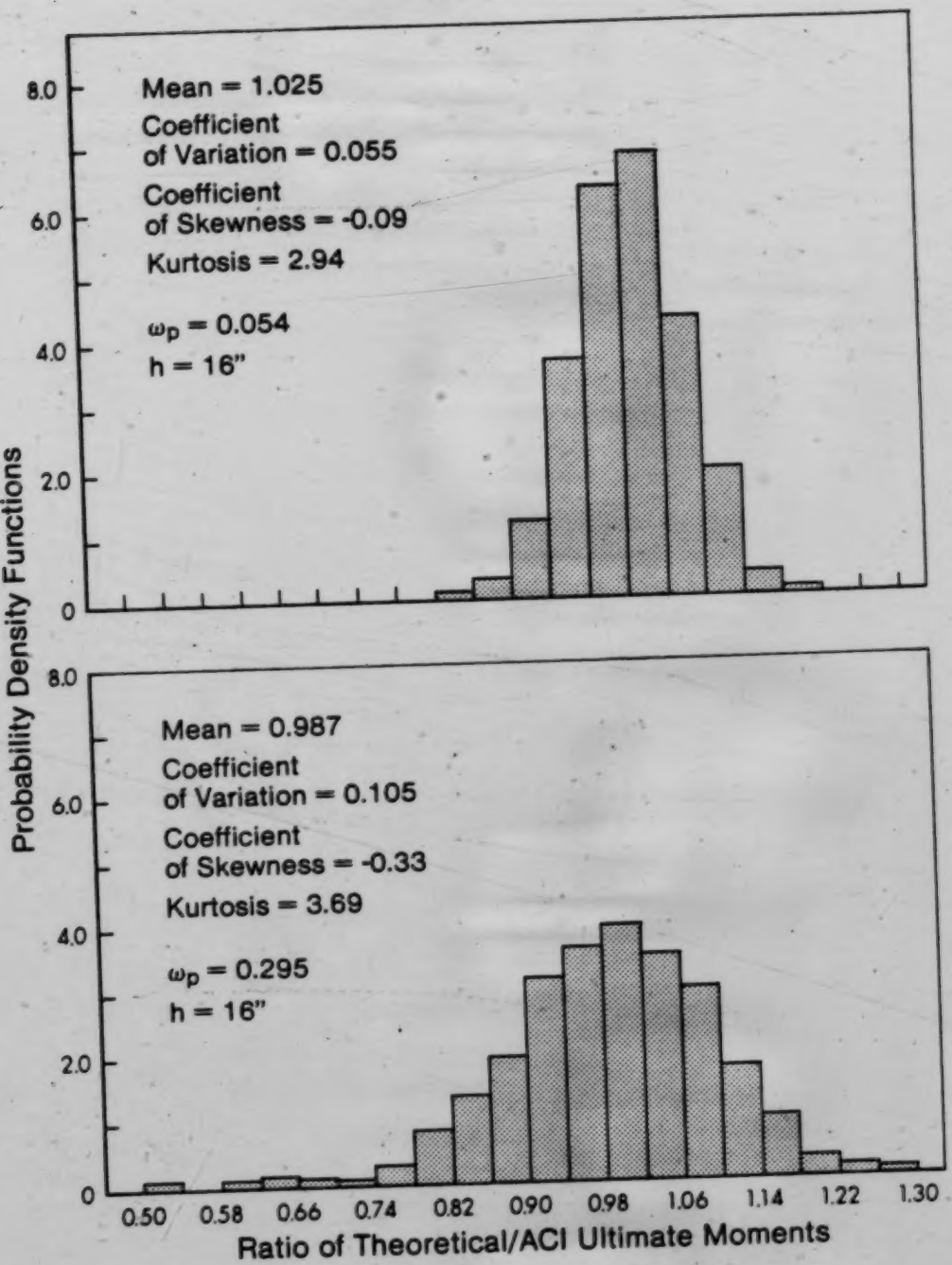

Figure 6.8 Probability Density Functions for Post-Tensioned Beams

CHAPTER VII

SUMMARY AND CONCLUSIONS

The ultimate flexural strength ratios of bonded prestressed concrete beams were determined in this study. A computer analysis using the Monte Carlo technique was performed. Probability models for concrete strength, reinforcing steel strength, and cross section dimensions were obtained from papers on this subject. The probability model for prestressing steel was obtained by analyzing data from a local prestressing firm as well as by conducting a literature review. The probability model for prestressing losses was obtained by calculating losses for a typical beam and then comparing these results with other sources.

Both pretensioned and post-tensioned beams were studied. Rectangular beams as well as T-beams were used. Both stress relieved and stabilized strand were used in this study. Only straight prestressing strand was used.

The sensitivity studies showed that prestressing steel properties and geometric properties were most important for low values of ω_p. The effect of the geometric properties was primarily due to the variation of the depth to the prestressing steel. For high values of ω_p, concrete properties were the most important variables.

The type of prestressing affected the section strength ratios at the 5 percent significance level. The flexural strength ratios for pretensioned beams were higher than for post-tensioned beams due to the greater ratio of actual to nominal effective depths assumed for the pretensioned beams. Post-tensioned beams were found to have a greater variability in strength. Again, this is due to the greater assumed variability in the variables contributing to strength.

The type of strand affected the strength ratios only for values of ω_p greater than about 0.1. For such beams, the ultimate strength was greater for stabilized strand due to the improved stress-strain characteristics and lower prestressing losses for stabilized strand. The variability in strength ratio was the same for both types of strand.

The overall depth of the beam, h, had some effect on the variability of the ultimate strength ratio of pretensioned beams but the effect was so small that for practical purposes, the effect of h on the strength ratio of pretensioned beams was neglected. Overall depth had a greater effect on the ultimate strength ratio of post-tensioned beams. The mean value of the strength ratios increased and the coefficient of variation decreased as h increased for post-tensioned beams.

The reinforcement index, ω_p, had a significant effect on the section strength ratios. For underreinforced

beams, the mean section strength ratios decreased and the variability of the strength ratios increased as ω_p increased.

Construction quality did not strongly affect the mean value of the strength ratio although it had a significant effect on the outlying values of the cross sectional strength.

Conventional reinforcing steel had a significant effect on the ultimate strength ratios. The mean section strength ratios and the variability of the section strength ratios both increased as the amount of reinforcing steel increased.

Prestressing losses affected the strength ratios of a section only for high values of ω_p. Smaller losses resulted in higher strength ratios and larger losses resulted in lower ratios. The variability of the section strength was not significantly affected by varying the losses.

REFERENCES

American Concrete Institute. 1963.
Building code requirements for reinforced concrete (ACI 318-63). Detroit, Michigan.

_____ 1971a.
Building code requirements for reinforced concrete (ACI 318-71). Detroit, Michigan.

_____ 1971b.
Commentary on building code requirements for reinforced concrete (ACI 318-71). Detroit, Michigan.

American Concrete Institute—American Society of Civil Engineers Joint Committee 323. 1958.
"Tentative recommendations for prestressed concrete." *Proceedings American Concrete Institute*, Vol. 54, January, pp. 545-578.

Allen, D. E. 1970.
Probabilistic study of reinforced concrete in bending. Technical Paper No. 311 of the Division of Building Research, National Research Council of Canada, January, Ottawa, Canada.

Bannister, J. L. 1968.
"Steel reinforcement and tendons for structural concrete, part 2: tendons for prestressed concrete." *Concrete*, Vol. 2, August, pp. 333-342.

Brecht, H. E., Hanson, J. M., and Hulsbos, C. L. 1965.
Ultimate shear tests of full-sized prestressed concrete beams. Prestressed Concrete Bridge Members, Progress Report No. 28, Lehigh University, Bethlehem, Pennsylvania.

Brenneisen, A. and Baus, R. 1968.
"Statistics and probabilities: steel for prestressing." Proceedings of Symposium, Inst. Eduard Torroja de la Construccion y del Cemento, June, Madrid, Spain.

Burns, N. H. 1964.
"Moment curvature relationships for partially prestressed concrete beams." *Prestressed Concrete Institute Journal*, Vol. 9, February, pp. 52-63.

Canadian Standards Association. 1975.
"Steel for prestressed concrete tendons." CSA Stand. G279-1975, Can. Stand. Assoc., October, Rexdale, Ontario.

Chandrasekar, P. and Dayaratnam, P. 1975.
"Analysis of probability of failure of prestressed concrete beams." *Building Science*, Vol. *10*, pp. 161-167.

Cornell, C. A. 1969.
"A probability based structural code." *Proceedings American Concrete Institute*, Vol. *66*, No. 12, December, pp. 974-985.

Dumas, F. 1958.
"The necessity for the use of the highest class materials in prestressed concrete construction." RILEM Symposium on Special Reinforcements for Reinforced Concrete and on Prestressing Reinforcements, Liege, Belgium.

Ellingwood, B. R. and Ang, A. H-S. 1974.
"Risk-based evaluation of design criteria." *Proceedings of the American Society of Civil Engineers, Journal of the Structural Division*, Vol. *100*, No. ST9, September, pp. 1771-1788.

Glodowski, R. J. and Lorenzetti, J. J. 1972.
"A method for predicting prestress losses in a prestressed concrete structure." *Prestressed Concrete Institute Journal*, Vol. *17*, No. 2, March/April, pp. 17-31.

Grant, L. H., Mirza, S. A., and MacGregor, J. G. 1978.
"Monte Carlo study of strength of concrete columns." To be published in *American Concrete Institute Journal*.

Gurfinkel, G. and Robinson, A. 1967.
"Determination of strain distribution and curvature in a reinforced concrete section subjected to bending moment and longitudinal load." *American Concrete Institute Journal*, Vol. *64*, July, pp. 398-403.

Hognestad, E. 1952.
"A study of combined bending and axial load in reinforced concrete members." University of Illinois Engineering Experiment Station Bulletin No. 399, Urbana, Illinois.

Kajfasz, S. 1958.
"Some relaxation tests on prestressing wire." *Magazine of Concrete Research*, Vol. *10*, No. 30, London, England.

Khachaturian, N. and Gurfinkel, G. 1969.
Prestressed concrete. McGraw-Hill Book Company, New York, N.Y.

Kreyszig, E. 1970.
Introductory mathematical statistics: principles and methods. John Wiley and Sons, Inc., New York, N.Y.

Libby, J. R. 1971.
Modern prestressed concrete: design principles and construction methods. Van Nostrand Reinhold Company, New York, N.Y.

Lin, T. Y. 1955.
Design of prestressed concrete structures. John Wiley and Sons, Inc., New York, N.Y.

Lind, N. C. 1971.
"Consistent partial safety factors." *Proceedings of the American Society of Civil Engineers,* Vol. *97,* No. ST6, June, pp. 1651-1670.

MacGregor, J. G. 1976.
"Safety and limit states design for reinforced concrete." *Canadian Journal of Civil Engineering,* Vol. *3,* No. 4, December, pp. 484-513.

Mack, C. 1967.
Essentials of statistics for scientists and technologists. Plenum Press, New York, N.Y.

Magura, D. D., Sozen, M. A., and Siess, C. P. 1962.
"Investigation of prestressed reinforced concrete for highway bridges: a study of stress relaxation in prestressing reinforcement." University of Illinois, Urbana, Illinois.

Mirza, S. A., Hatzinikolas, M., and MacGregor, J. G. 1978.
"Statistical descriptions of the strength of concrete." *American Society of Civil Engineers, Journal of the Structural Division,* Submitted for publication.

Mirza, S. A. and MacGregor, J. G. 1978a.
"Variability of the mechanical properties of reinforcing bars." *American Society of Civil Engineers, Journal of the Structural Division.* Submitted for publication.

_____ 1978b.
"Variations in dimensions of reinforced concrete members." *American Society of Civil Engineers, Journal of the Structural Division,* Submitted for publication.

Murray, D. W. and Epstein, M. 1976.
"An elastic stress analysis of a Gentilly type containment structure." Vol. *1,* A Technical Report to the Atomic Energy Control Board, University of Alberta, Edmonton, Alberta.

Neville, A. M. 1970.
Creep of concrete: plain, reinforced, and prestressed. North-Holland Publishing Company, Amsterdam, The Netherlands.

Olesen, S. E., Sozen, M. A. and Siess, C. P. 1965.
Investigation of prestressed reinforced concrete for highway bridges, part IV: strength in shear of beams with web reinforcement. University of Illinois, Urbana, Illinois.

Prestressed Concrete Institute. 1971.
PCI design handbook: precast and prestressed concrete. PCI, Chicago, Illinois.

_____ 1972.
PCI post-tensioning manual. PCI, Chicago, Illinois.

Rüsch, H. 1960.
"Researches toward a general flexural theory for structural concrete." *Proceedings American Concrete Institute,* Vol. *57,* July, pp. 1-28.

Sozen, M. A., Zwoyer, E. M., and Siess, C. P. 1959.
Investigation of prestressed concrete for highway bridges, part I: strength in shear of beams without web reinforcement. University of Illinois Engineering Experiment Station Bulletin No. 452, Urbana, Illinois.

Stelco. 1976.
"Stabilized strand and stress-relieved strand and wire for prestressed concrete." Hamilton, Ontario.

Warner, R. F. and Kaballa, A. P. 1968.
"Monte Carlo study of structural safety." *Proceedings of the American Society of Civil Engineers, Journal of the Structural Division,* Part 2, Vol. *94,* No. ST12, December, pp. 2847-2859.

Warwaruk, J. 1957.
"Strength in flexure of bonded and unbonded prestressed concrete beams." Thesis, Issued as a Part of the Sixth Progress Report of the Investigation of Prestressed Concrete for Highway Bridges, University of Illinois, Urbana, Illinois.

Warwaruk, J., Sozen, M. A., and Siess, C. P. 1962.
Investigation of prestressed reinforced concrete for highway bridges, part III: strength and behavior in flexure of prestressed concrete beams. University of Illinois Engineering Experiment Station Bulletin No. 464, Urbana, Illinois.

Wood, L. W. 1958.
"The factor of safety in design of timber structures."
Proceedings of the American Society of Civil Engineers, Journal of the Structural Division, Part 2, Vol. *84*, No. ST7, November, pp. 1838-1 to 1838-18.

APPENDIX A

Compressive Force in T - Sections

CASE A:

$(h_f < c \leq h;\ \varepsilon_3 < \varepsilon_0;\ \varepsilon_4 \leq \varepsilon_0)$

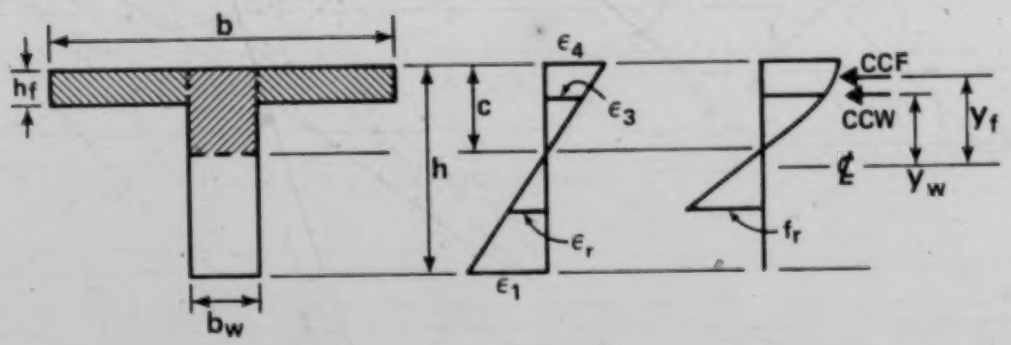

CROSS SECTION | STRAIN DISTRIBUTION | STRESS DISTRIBUTION

$$CCW = \frac{b_w}{\phi} f''_c \left[\frac{\varepsilon_4^2}{\varepsilon_0} - \frac{\varepsilon_4^3}{3\,\varepsilon_0^2}\right]$$

$$CCF = \frac{(b - b_w)\, f''_c}{\phi\, \varepsilon_0} \left[\varepsilon_4^2 - \varepsilon_3^2 + \frac{\varepsilon_3^3 - \varepsilon_4^3}{3\,\varepsilon_0}\right]$$

$$y_w = \frac{1}{\phi}\left[\frac{8\,\varepsilon_4\,\varepsilon_0 - 3\,\varepsilon_4^2}{12\,\varepsilon_0 - 4\,\varepsilon_4}\right] + \frac{h}{2} - c$$

$$y_f = \frac{\dfrac{(b - b_w)^2 f''_c}{\phi^2\,\varepsilon_0}\left\{\dfrac{2\,(\varepsilon_4^3 - \varepsilon_3^3)}{3} + \dfrac{\varepsilon_3^4 - \varepsilon_4^4}{4\,\varepsilon_0}\right\}}{CCF} + \frac{h}{2} - c$$

CASE B:

$(h_f < c \leq h;\ \varepsilon_3 < \varepsilon_0;\ \varepsilon_4 > \varepsilon_0)$

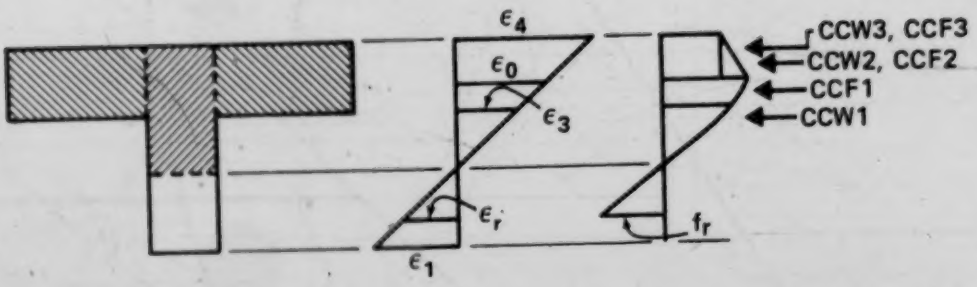

$$CCW1 = \frac{b_w f''_c}{\phi} \left[\frac{2}{3} \varepsilon_0\right]$$

$$CCW2 = \frac{b_w f''_c}{\phi} \times 0.075 \frac{(\varepsilon_4 - \varepsilon_0)^2}{\varepsilon_u - \varepsilon_0}$$

$$CCW3 = \frac{b_w f''_c}{\phi} \left[1 - 0.15 \left(\frac{\varepsilon_4 - \varepsilon_0}{\varepsilon_u - \varepsilon_0}\right)\right] \times (\varepsilon_4 - \varepsilon_0)$$

$$CCF1 = \frac{(b - b_w) f''_c}{\phi} \left[\frac{2}{3} \varepsilon_0 - \frac{\varepsilon_3^2}{\varepsilon_0} + \frac{\varepsilon_3^3}{3 \varepsilon_0^2}\right]$$

$$CCF2 = \frac{(b - b_w) f''_c}{\phi} \times 0.075 \frac{(\varepsilon_4 - \varepsilon_0)^2}{(\varepsilon_u - \varepsilon_0)}$$

$$CCF3 = \frac{(b - b_w) f''_c}{\phi} \left[1 - 0.15 \left(\frac{\varepsilon_4 - \varepsilon_0}{\varepsilon_u - \varepsilon_0}\right)\right] \times (\varepsilon_4 - \varepsilon_0)$$

CASE B (continued):

$$y_{w1} = \frac{5}{8} \times \frac{\varepsilon_0}{\phi} + \frac{h}{2} - c$$

$$y_{f1} = \frac{(b - b_w) f''_c}{CCF1 \times \phi^2} \left[\frac{.5\ \varepsilon_0^2}{12} - \frac{2\ \varepsilon_3^3}{3\ \varepsilon_0} + \frac{\varepsilon_3^4}{4\ \varepsilon_0^2} \right] + \frac{h}{2} - c$$

$$y_{w2} = y_{f2} = \frac{\varepsilon_4 + 2\ \varepsilon_0}{3\ \phi} + \frac{h}{2} - c$$

$$y_{w3} = y_{f3} = \frac{\varepsilon_4 + \varepsilon_0}{2\ \phi} + \frac{h}{2} - c$$

CASE C:

$(h_f < c \leq h;\ \varepsilon_3 \geq \varepsilon_0;\ \varepsilon_4 > \varepsilon_0)$

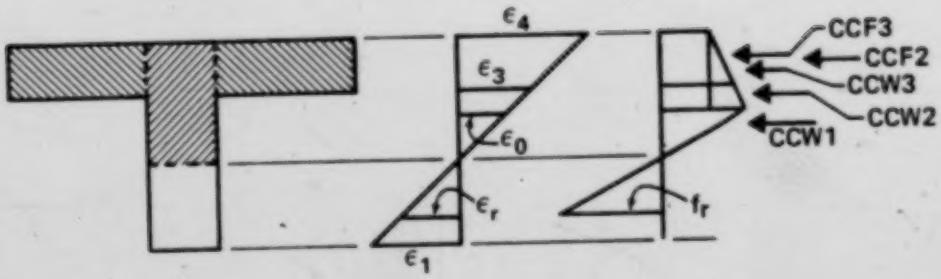

CCW1
CCW2
CCW3
y_{w_1}
y_{w_2} } SAME AS CASE B
y_{w_3}

$$CCF1 = 0.0$$

$$CCF2 = \frac{(b - b_w)\, f''_c}{\phi} \times 0.075\, \frac{(\varepsilon_4 - \varepsilon_3)^2}{(\varepsilon_u - \varepsilon_0)}$$

$$CCF3 = \frac{(b - b_w)\, f''_c}{\phi} \left[1 - 0.15\left(\frac{\varepsilon_4 - \varepsilon_0}{\varepsilon_u - \varepsilon_0}\right)\right] \times (\varepsilon_4 - \varepsilon_3)$$

$$y_{f_1} = 0$$

$$y_{f_2} = \frac{\varepsilon_4 + 2\,\varepsilon_3}{3\,\phi} + \frac{h}{2} - c$$

$$y_{f_3} = \frac{\varepsilon_4 + \varepsilon_3}{2\,\phi} + \frac{h}{2} - c$$

CASE A1:

($c > h$; $\varepsilon_3 < \varepsilon_0$; $\varepsilon_4 \leq \varepsilon_0$)

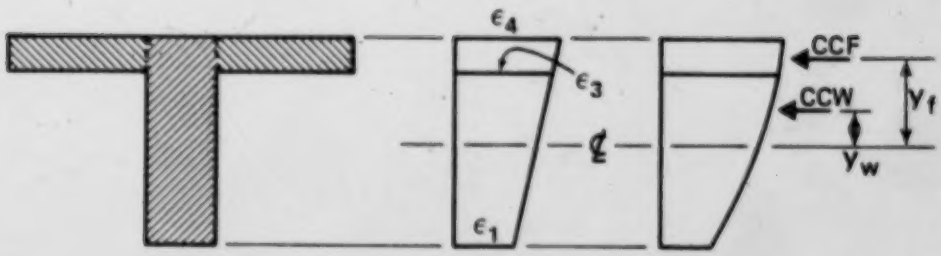

CROSS SECTION | STRAIN DISTRIBUTION | STRESS DISTRIBUTION

$$CCW = \frac{b_w f''_c}{\phi \varepsilon_0} \left[\varepsilon_4^2 - \varepsilon_1^2 + \frac{\varepsilon_1^3 - \varepsilon_4^3}{3 \varepsilon_0} \right]$$

$$y_w = \frac{\frac{b_w f''_c}{\phi^2 \varepsilon_0} \left\{ \frac{2 (\varepsilon_4^3 - \varepsilon_1^3)}{3} + \frac{\varepsilon_1^4 - \varepsilon_4^4}{4 \varepsilon_0} \right\}}{CCW} + \frac{h}{2} - c$$

$\left.\begin{matrix} CCF \\ y_f \end{matrix}\right\}$ SAME AS CASE A

CASE B1:

($c > h$; $\varepsilon_3 < \varepsilon_0$; $\varepsilon_4 > \varepsilon_0$)

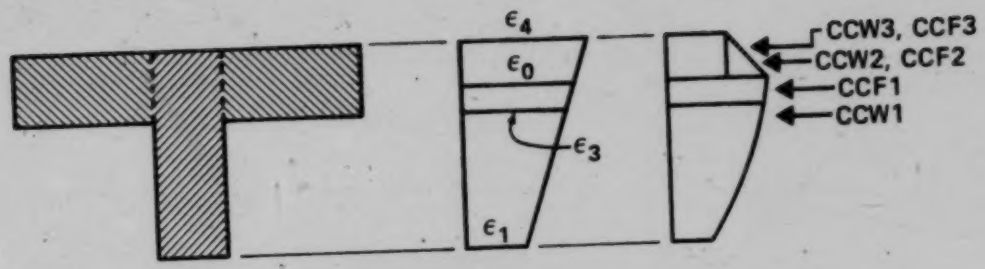

CCW2
CCW3
CCF1
CCF2
CCF3
y_{f1}
$y_{w2} = y_{f2}$
$y_{w3} = y_{f3}$

} SAME AS CASE B

$$CCW1 = \frac{b_w f''_c}{\phi} \left\{ \frac{2}{3} \varepsilon_0 - \frac{\varepsilon_1^2}{\varepsilon_0} + \frac{\varepsilon_1^3}{3 \varepsilon_0^2} \right\}$$

$$y_{w1} = \frac{b_w f''_c}{CCW1 \times \phi^2} \left[\frac{5 \varepsilon_0^2}{12} - \frac{2}{3} \frac{\varepsilon_1^3}{\varepsilon_0} + \frac{\varepsilon_1^4}{4 \varepsilon_0^2} \right] + \frac{h}{2} - c$$

CASE B1a:

($c > h$; $\varepsilon_1 \geq \varepsilon_0$, $\varepsilon_3 > \varepsilon_0$, $\varepsilon_4 > \varepsilon_0$)

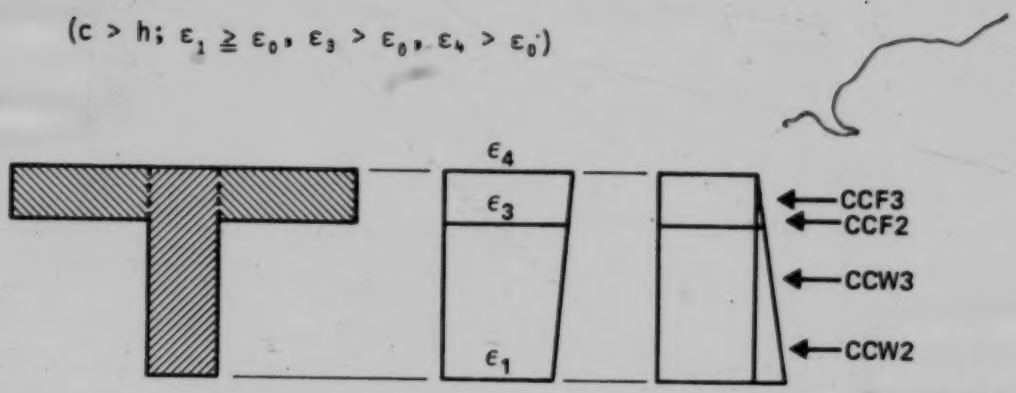

$CCW1 = 0.0$

$$CCW2 = \frac{b_w f''_c}{\phi} \times 0.075 \frac{(\varepsilon_4 - \varepsilon_1)^2}{(\varepsilon_u - \varepsilon_0)}$$

$$CCW3 = \frac{b_w f''_c}{\phi} \left[1 - 0.15 \left(\frac{\varepsilon_4 - \varepsilon_0}{\varepsilon_u - \varepsilon_0} \right) \right] \times (\varepsilon_4 - \varepsilon_1)$$

$y_{w1} = 0.0$

$$y_{w2} = \frac{\varepsilon_4 + 2\,\varepsilon_1}{3\,\phi} + \frac{h}{2} - c$$

$$y_{w3} = \frac{\varepsilon_4 + \varepsilon_1}{2\,\phi} + \frac{h}{2} - c$$

CCF1
CCF2
CCF3
y_{f1}
y_{f2}
y_{f3}

} SAME AS CASE C1 AND CASE C

CASE C1:

$(c > h;\ \varepsilon_3 \geq \varepsilon_0,\ \varepsilon_4 > \varepsilon_0)$

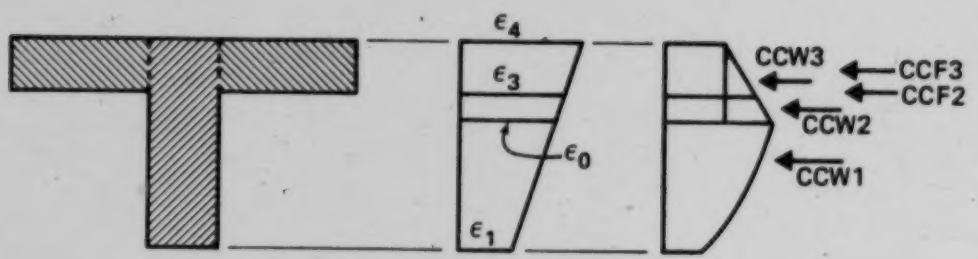

CCW1
CCW2
CCW3
y_{w1}
y_{w2} } SAME AS CASE B1
y_{w3}

CCF1
CCF2
CCF3
y_{f1}
y_{f2} } SAME AS CASE C
y_{f3}

CASE D:

$(c \leq h_f;\ \varepsilon_3 < \varepsilon_0;\ \varepsilon_4 \leq \varepsilon_0)$

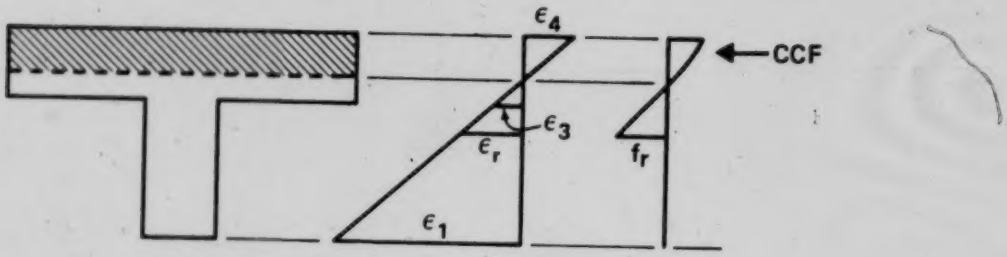

$$CCF = \frac{b\, f''_c}{\phi}\left[\frac{\varepsilon_4^2}{\varepsilon_0} - \frac{\varepsilon_4^3}{3\,\varepsilon_0^2}\right]$$

$$y_f = \left[\frac{8\,\varepsilon_4\,\varepsilon_0 - 3\,\varepsilon_4^2}{\phi\,(12\,\varepsilon_0 - 4\,\varepsilon_4)}\right] + \frac{h}{2} - c$$

TENSION BLOCK MAY BE PARTLY IN WEB, AS SHOWN HERE, OR COMPLETELY IN FLANGE.

CASE E:

$(c \leq h_f;\ \varepsilon_4 > \varepsilon_0)$

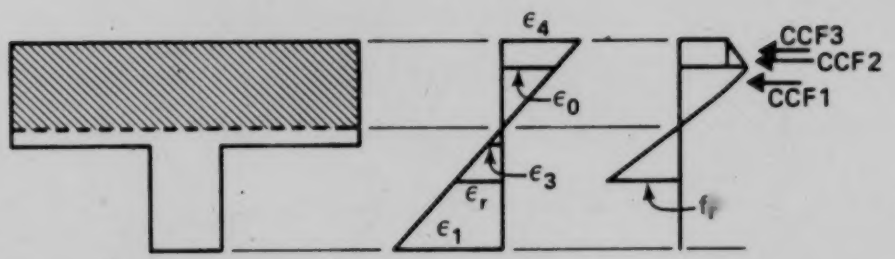

$$CCF1 = \frac{b}{\phi} f''_c \left[\frac{2}{3} \varepsilon_0\right]$$

$$CCF2 = \frac{b\ f''_c}{\phi} \times 0.075 \frac{(\varepsilon_4 - \varepsilon_0)^2}{(\varepsilon_u - \varepsilon_0)}$$

$$CCF3 = \frac{b\ f''_c}{\phi} \left[1 - 0.15 \left(\frac{\varepsilon_4 - \varepsilon_0}{\varepsilon_u - \varepsilon_0}\right)\right] \times (\varepsilon_4 - \varepsilon_0)$$

$$y_{f_1} = \frac{5}{8} \times \frac{\varepsilon_0}{\phi} + \frac{h}{2} - c$$

$$y_{f_2} = \left(\frac{\varepsilon_4 + 2\ \varepsilon_0}{3\ \phi}\right) + \frac{h}{2} - c$$

$$y_{f_3} = \left(\frac{\varepsilon_4 + \varepsilon_0}{2\ \phi}\right) + \frac{h}{2} - c$$

TENSION BLOCK MAY BE PARTLY IN WEB, AS SHOWN HERE, OR COMPLETELY IN FLANGE.

APPENDIX B

PRESTRESSING LOSS CALCULATIONS

Example: Mean Losses for Post-tensioned Beam with Stress Relieved Strand

Calculations done for beam from *PCI Design Handbook* (1971):

Strand Pattern 8 DT 20 68-D1

(6-½" DIA Strand)

$A_g = 363 \text{ in}^2$

$I_g = 12{,}551 \text{ in}^4$

$r^2 = \frac{I}{A} = 34.5758$

$y_b = 14.59 \text{ in.}$

$y_t = 5.41 \text{ in.}$

$Z_b = 860 \text{ in.}^3$

$Z_t = 2320 \text{ in.}^3$

$e = 12.09 \text{ in.}$

$S_e = \frac{I}{e} = \frac{12551}{12.09} = 1038.1 \text{ in.}^3$

wt = 378plf = 47psf

Superimposed dead load = 100plf

$A_{sp} = 6 \times 0.153 = 0.918 \text{ in.}^2$

$\rho_p = \frac{A_{sp}}{bd} = \frac{0.918}{96(5.41 + 12.09)}$

$= 5.464 \times 10^{-4}$

Mean Steel Properties

$E_{sp} = 28.617 \times 10^6 \text{ psi}$

Mean Concrete Properties

$f'_c = 5000 \text{ psi}$

$$f_{cstress} = 0.675 \times 5000 + 1100 \leq 1.15f'_c$$
$$= 4475\text{psi}$$
$$E_c = 60400\sqrt{4475}$$
$$= 4.04 \times 10^6 \text{ psi}$$

Assume $f_{transfer} = 0.70 \times 270 = 189$ ksi

From trial and Error, $f_{jacking} = 205.7$ ksi $= 31.47$ kips

$\therefore P_o = 31.47$ kips

Friction Loss

$$P_o = P_x e^{(Kl + \mu\alpha)}$$

$\mu\alpha = 0$ (straight tendons used)

$$\text{Av.K} = \frac{0.0005 + 0.002}{2} = 0.00125$$

$$P_o = P_x e^{(0.00125 \times 25)}$$

$$P_o = P_x e^{0.03125}$$

$$\frac{P_o}{P_x} = 1.03174$$

$$P_o = \frac{31.47}{1.03174} = 30.504$$

$$P_o - P_x = 0.9661$$

Anchorage Loss

Max. slip used = 0.5" @ one end

Min. slip used = 0.2" @ one end

$\therefore$ Av. slip $= \frac{0.5 + 0.2}{2} = 0.35$" @ one end

$$\frac{PL}{AE} = \frac{\frac{1}{2}[\Delta P_x + (\Delta P_x + 2(0.9661)] \ 50 \times 12}{0.153 \times 28.617 \times 10^3}$$

$$2\Delta P_x + 2(0.9661) = 5.10813$$

$$\Delta P_x = 1.588$$

$$P'_o = 31.47 - 1.588 - 2(0.9661) = 27.95 \text{ K } (182.7 \text{ ksi})$$

$$P'_x = 30.50 - 1.588 = 28.916 \text{ K } (188.99 \text{ ksi} \approx 189 \text{ ksi})$$

Elastic Shortening Loss

$$\frac{6P'_o}{A_g} = \frac{6 \times 27.95}{363} = 0.462$$

$$\frac{6P'_x}{A_g} + \frac{6P'_x e^2}{I_g} - \frac{M_{d1} e}{I_g} = \frac{6(28.92)}{363} + \frac{6(28.92)(12.09)^2}{12551} - \frac{(0.378)50^2 \times 12 \times 12.09}{8 \times 12551}$$

$$= 0.478 + 2.021 - 1.365$$

$$= 1.134 \text{ ksi}$$

Average loss on any previously stressed tendon due to stressing one additional tendon:

$$\Delta P = \frac{1}{n}\left(\frac{0.462 + 1.134}{2}\right)\left(\frac{E_{sp}}{E_c}\right) A_{sp}$$

$$\Delta P = \frac{1}{6}\left(\frac{0.462 + 1.134}{2}\right)\left(\frac{28.617 \times 10^6}{4.04 \times 10^6}\right) \times 0.153$$

$$\Delta P = 0.144$$

$$\text{Av. loss} = \left(\frac{n - 1}{2}\right) \Delta P = \left(\frac{6 - 1}{2}\right) \times 0.144 = 0.360$$

∴ Initial forces (after wedge set and elastic shortening are:

$$P_o = 27.95 - 0.360 = 27.59 \text{ k (180.3 ksi)}$$

$P_x = 28.92 - 0.360 = 28.56$ k (186.7 ksi) ←

Stress at c.g.s. due to superimposed dead load

$$= \frac{100 \times 50^2 \times 12}{8 \times 1038.1} = -361.2 \text{ psi}$$

Initial stress at c.g.s. due to prestressing

$$= \frac{186700 \times 0.918}{363} + \frac{186700 \times 0.918(12.09)^2}{363 \times 34.5758}$$

$$= 2468.2 \text{ psi}$$

$$\Delta f_{cgs} = \frac{-\Delta f_s}{186.7} \times 2468.2 = -13.22\ \Delta f_s \text{ (psi)}$$

Stress at c.g.s. due to girder dead load

$$= \frac{M}{S_e} = \frac{wl^2}{8S_e} = \frac{378 \times 50^2 \times 12}{8 \times 1038.1}$$

$$= -1365.5 \text{ psi}$$

$2468.2 - 1365.5 = 1102.6$ psi ←

Creep Loss

$$C = e_i \alpha_f \beta_f \phi_o \xi \rho_{time}$$

$$d_m = \frac{18 \times 9.5}{(18 + 9.5)} = 6.22$$

(use d_m for stem only because this is where prestressing steel is located)

$\alpha_f = 0.75$

$\beta_f = 0.85$

$\phi_o = 3.2$ (mean for 40% relative humidity)

$$C = 0.75 \times 0.85 \times 3.2 \xi \rho_{time} e_i$$

$$C = 2.04 \xi \rho_{time} e_i$$

$$f_{sc} = 2.04 \times \frac{28.617 \times 10^3}{4,040,000} f_{cgs} \xi \rho_{time} \text{(ksi)}$$

$$f_{sc} = 1.445 \times 10^{-2} f_{cgs} \xi \rho_{time} \text{ (ksi)}$$

Shrinkage Loss

$$s = \psi \alpha_r \beta_r (1 - 10 \rho_p)$$

$\psi = 400 \times 10^{-6}$ (mean for 40% relative humidity)

$\alpha_r = 0.76$

$\beta_r = 1.2$ (mean for 0.5 w/c ratio)

$S = 400 \times 10^{-6} \times 0.76 \times 1.2 \times (1 - 10 \times 5.464 \times 10^{-4})$

$S = 3.628 \times 10^{-4}$

$f_{ss} = 3.628 \times 10^{-4} \times 28.617 \times 10^{3} \times \rho_{time}$

$f_{ss} = 10.382 \rho_{time}$ (ksi)

Relaxation Loss (for stress relieved strand)

TIME (HOURS)	MAX	MIN	MEAN
7 x 24 = 168	0.047	0.029	0.038
14 x 24 = 336	0.054	0.034	0.044
30 x 24 = 720	0.062	0.039	0.0505
90 x 24 = 2160	0.074	0.048	0.061
360 x 24 = 8640	0.087	0.058	0.0725
1825 x 24 = 43,800	0.104	0.071	0.0875

$\therefore$ at 7 days:

$f_{sc} = 1.445 \times 10^{-2} \times 1102.6 \times 1.2 \times 0.21 = 4.015$ ksi

$\Delta f_{sc} = 4.015$ ksi

$f_{ss} = 10.382 \times 0.34 = 3.53$ ksi

$\Delta f_{ss} = 3.53 - 3.11 = 0.42$

$\Delta f_{st} = 186.7 \times 0.038 = 7.09$ ksi

$f_{st} = 186.7 - 7.09 = 179.6$ ksi

$\Delta f_s = 4.015 + 0.42 + 7.09 = 11.52$ ksi

$\Delta f_{cgs} = -13.22 \times 11.52 = -152.3$ psi

$f_{cgs} = 1102.6 - 152.3 = 950.3$ psi

at 14 days:

$\Delta f_{sc} = 1.445 \times 10^{-2} \times 950.3 \times 1.2 \times (0.3 - 0.21)$

$= 1.483$ ksi

$\Delta f_{ss} = 10.382\ (0.4 - 0.34)$

$= 0.62$ ksi

$\Delta f_{st} = 179.6(0.044 - 0.038) = 1.08$ ksi

$f_{st} = 179.6 - 1.08 = 178.5$ ksi

$\Delta f_s = 1.483 + 0.62 + 1.08 = 3.183$ ksi

$\Delta f_{cgs} = -13.22 \times 3.183 = -42.08$ psi

$f_{cgs} = 950.3 - 42.08 = 908.2$ psi

See Table B-1 for summary of calculations.

Calculation of Percentage Loss*:	
Elastic shortening	$\frac{0.360}{28.92} = 1.24\%$
Shrinkage	$\frac{0.99}{28.92} = 3.42\%$
Creep	$\frac{1.70}{28.92} = 5.88\%$
Relaxation	$\frac{2.42}{28.92} = 8.36\%$
Subtotal	$\frac{5.47}{28.92} = 18.91\%$
Friction	$\frac{0.966}{28.92} = 3.34\%$
Anchorage	$\frac{1.588}{28.92} = 5.49\%$
Friction + Anchorage	8.83%
All losses	27.74%

*All losses in percentage of nominal stress at transfer which is equal to $0.7f_{pu}$. (See Table 4.5 for maximum, minimum and mean losses.)

$$\sigma_{fric+anch} = \frac{\max(\text{fric + anch})\text{loss} - \min(\text{fric + anch})\text{loss}}{6}$$

$$= \frac{12.48 - 4.74}{6} = 1.29\% \text{ of nominal transfer stress}$$

$$\sigma_{jacking} = \begin{bmatrix}\text{Coefficient of Variation} \\ \text{of ratio of Actual to} \\ \text{Specified Jacking Force}\end{bmatrix}\begin{bmatrix}\text{ratio of jacking} \\ \text{to transfer force}\end{bmatrix}$$

Table B-1

MEAN LOSSES FOR POST-TENSIONED BEAM WITH STRESS RELIEVED STRAND.

Time† Days	ρ_{time} (Shrinkage)	f_{ss} ksi	Δf_{ss} ksi	ρ_{time} (Creep)	ξ	f_{sc} ksi	Δf_{sc} ksi	Δf_{st} ksi	f_{st} ksi	Δf_s ksi	Δf_{cgs} psi	f_{cgs} psi
0	0.3	3.11	--	--	--	0	--	0	186.7	--	0	1102.6
7	0.34	3.53	0.42	0.21	1.2	4.015	4.015	7.09	179.6	11.52	-152.3	950.3
14	0.4	4.15	0.62	0.3	1.2	4.943	1.483	1.08	178.5	3.18	-42.08	908.2
				(0.21)	(1.2)	3.460						
30	0.5	5.19	1.04	0.41	1.2	6.456	1.732	1.16	177.3	3.93	-51.98	856.1
				(0.3)	(1.2)	4.724						-361.2
												494.9
90	0.61	6.33	1.14	0.6	1.2	5.149	1.630	1.86	175.4	4.63	-61.17	433.7
				(0.41)	(1.2)	3.518						
360	0.8	8.30	1.98	0.8	1.2	6.016	1.504	2.02	173.4	5.50	-72.76	360.9
				(0.6)	(1.2)	4.512						
1825	0.92	9.55	1.25	0.92	1.2	5.758	0.751	2.60	170.8	4.60	-60.82	300.1
				(0.8)	(1.2)	5.007						
			6.45				11.12	15.81		33.36		
			×0.153				×0.153	×0.153		×0.153		
			=0.99kips				=1.70kips	=2.42kips		=5.10kips		

†Time is from time of stressing (14 days after concrete cast)

$= 1.316 \left(\frac{109}{100}\right) = 1.43\%$ of nominal transfer stress

$f_{transfer} = \alpha_{tr} \cdot f_{jacking}$

Mean stress at transfer = Nominal Value

= 0.7 × specified ultimate ←

$\sigma_{transfer} = \left[\left(\frac{1.29}{100}\right)^2 + \left(\frac{1.43}{100}\right)^2\right]^{\frac{1}{2}}$

= 1.93% × Mean stress at transfer ←

Mean value of losses = $\frac{18.91}{100}$ × Mean stress at transfer

= 0.19 × Mean stress at transfer ←

$\sigma_{losses} = \frac{\text{max. loss - min. loss}}{6}$

$= \frac{26.90 - 8.95}{6}$

= 3.00% of Mean stress at transfer

= 0.03 × Mean stress at transfer ←

$f_{se} = f_{transfer}$ - losses

APPENDIX C

FLOW DIAGRAMS OF THE MONTE CARLO PROGRAM

This appendix contains flow diagrams of the Monte Carlo Program used in this study including:

The Main Program

Subroutine THEORY

MONTE CARLO PROGRAM

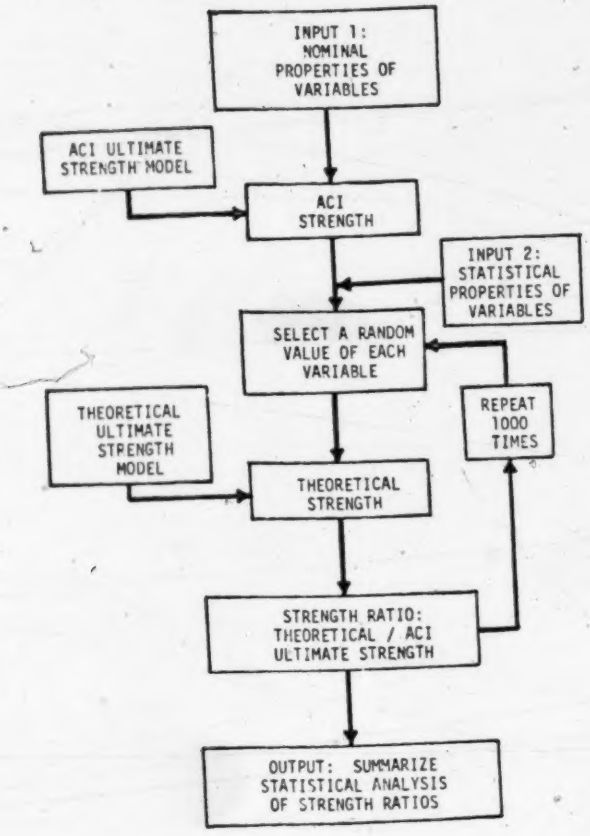

SUBROUTINE THEORY

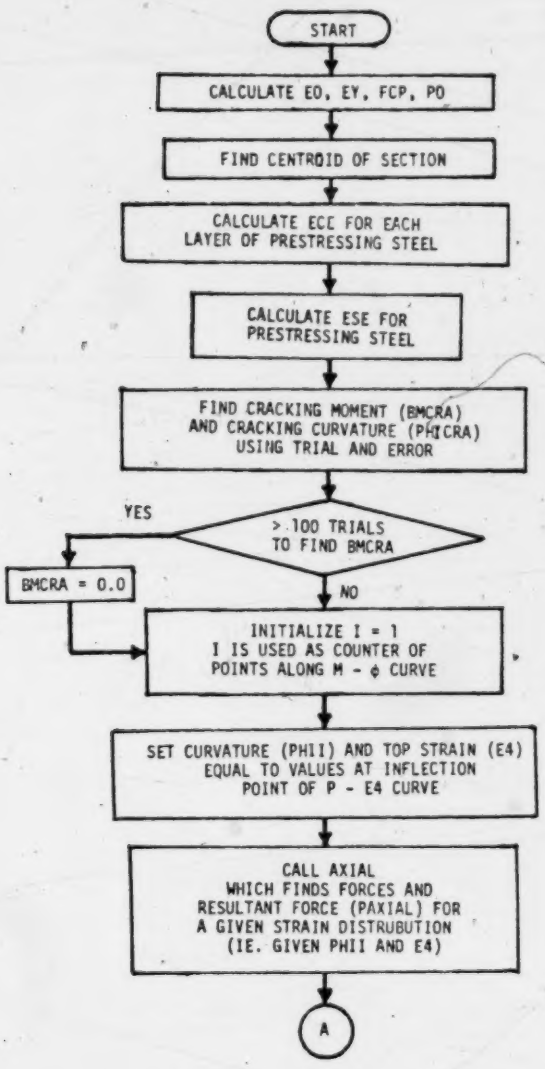
START
CALCULATE EO, EY, FCP, PO
FIND CENTROID OF SECTION
CALCULATE ECC FOR EACH LAYER OF PRESTRESSING STEEL
CALCULATE ESE FOR PRESTRESSING STEEL
FIND CRACKING MOMENT (BMCRA) AND CRACKING CURVATURE (PHICRA) USING TRIAL AND ERROR
YES
> 100 TRIALS TO FIND BMCRA
NO
BMCRA = 0.0
INITIALIZE I = 1
I IS USED AS COUNTER OF POINTS ALONG M - ϕ CURVE
SET CURVATURE (PHII) AND TOP STRAIN (E4) EQUAL TO VALUES AT INFLECTION POINT OF P - E4 CURVE
CALL AXIAL
WHICH FINDS FORCES AND RESULTANT FORCE (PAXIAL) FOR A GIVEN STRAIN DISTRUBUTION (IE. GIVEN PHII AND E4)
A

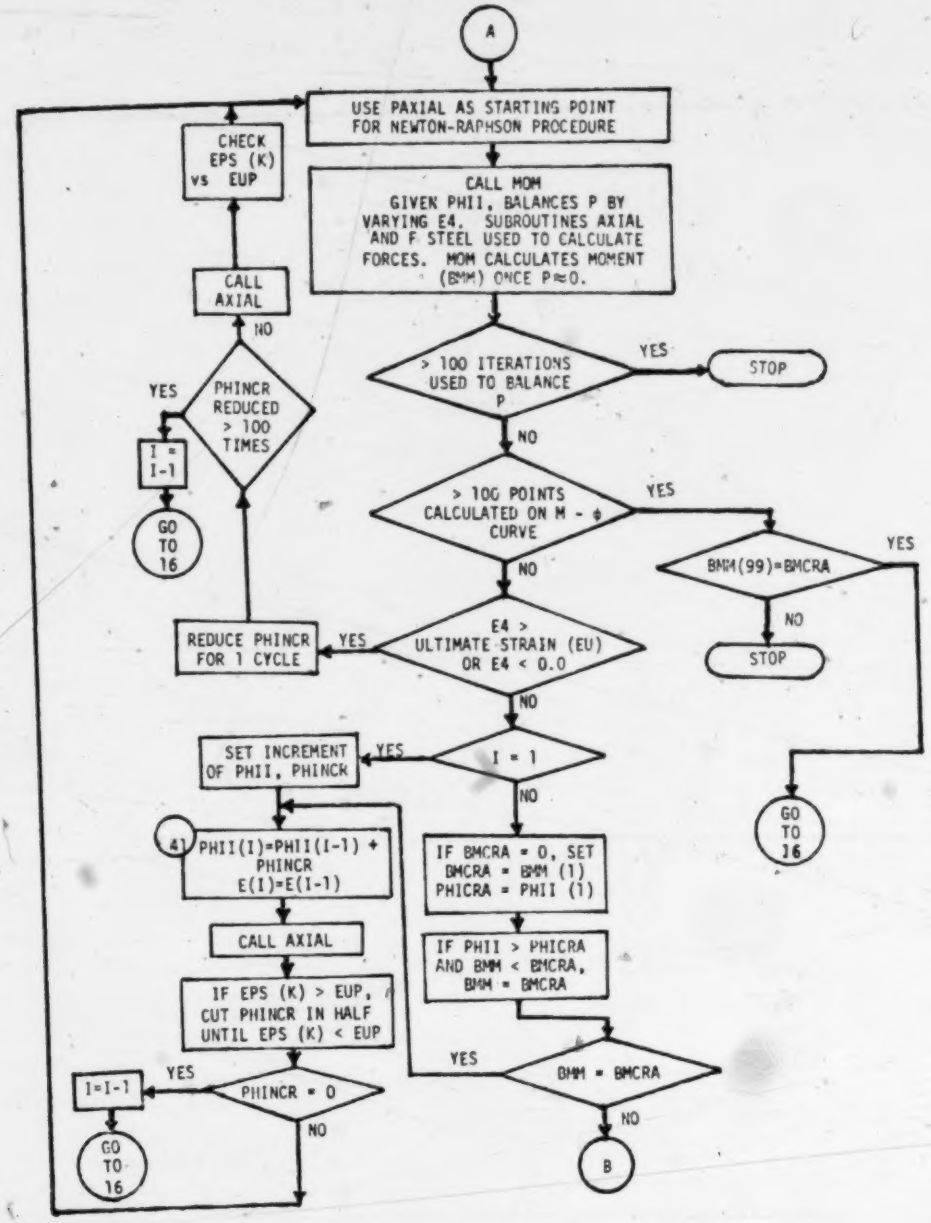
A
USE PAXIAL AS STARTING POINT FOR NEWTON-RAPHSON PROCEDURE
CALL MOM GIVEN PHII, BALANCES P BY VARYING E4. SUBROUTINES AXIAL AND F STEEL USED TO CALCULATE FORCES. MOM CALCULATES MOMENT (BMM) ONCE P≈0.
> 100 ITERATIONS USED TO BALANCE P
YES
STOP
NO
> 100 POINTS CALCULATED ON M - φ CURVE
YES
BMM(99)=BMCRA
YES
NO
STOP
NO
E4 > ULTIMATE STRAIN (EU) OR E4 < 0.0
YES
REDUCE PHINCR FOR 1 CYCLE
NO
I = 1
YES
SET INCREMENT OF PHII, PHINCK
NO
IF BMCRA = 0, SET BMCRA = BMM (1) PHICRA = PHII (1)
IF PHII > PHICRA AND BMM < BMCRA, BMM = BMCRA
YES
BMM = BMCRA
NO
B
GO TO 16
4
PHII(I)=PHII(I-1) + PHINCR
E(I)=E(I-1)
CALL AXIAL
IF EPS (K) > EUP, CUT PHINCR IN HALF UNTIL EPS (K) < EUP
YES
PHINCR = 0
NO
I=I-1
GO TO 16
CHECK EPS (K) vs EUP
CALL AXIAL
NO
YES
PHINCR REDUCED > 100 TIMES
I = I-1
GO TO 16

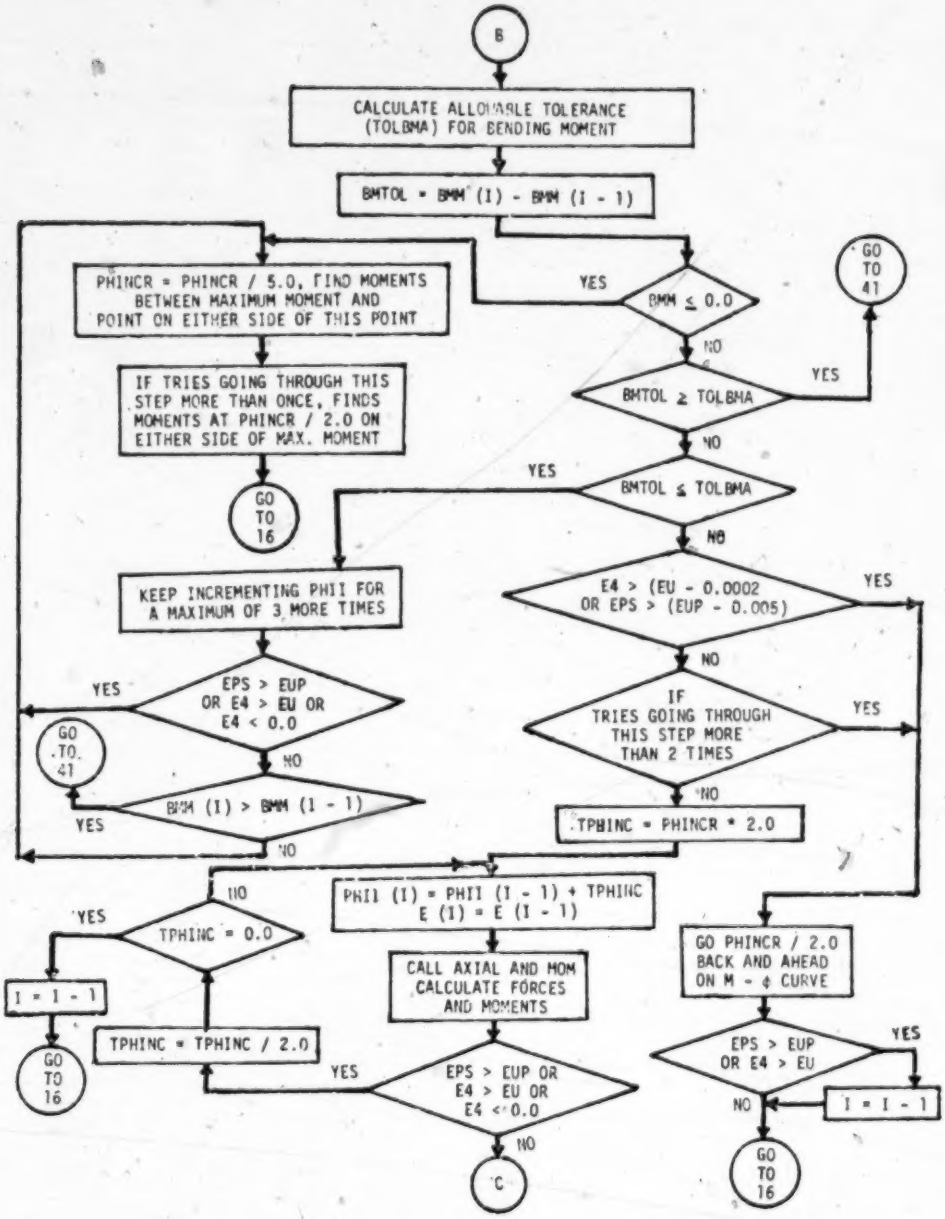
B
CALCULATE ALLOWABLE TOLERANCE (TOLBMA) FOR BENDING MOMENT
BMTOL = BMM (I) - BMM (I - 1)
PHINCR = PHINCR / 5.0, FIND MOMENTS BETWEEN MAXIMUM MOMENT AND POINT ON EITHER SIDE OF THIS POINT
IF TRIES GOING THROUGH THIS STEP MORE THAN ONCE, FINDS MOMENTS AT PHINCR / 2.0 ON EITHER SIDE OF MAX. MOMENT
GO TO 16
BMM ≤ 0.0
YES
GO TO 41
NO
BMTOL ≥ TOLBMA
YES
NO
BMTOL ≤ TOLBMA
YES
NO
KEEP INCREMENTING PHII FOR A MAXIMUM OF 3 MORE TIMES
E4 > (EU - 0.0002 OR EPS > (EUP - 0.005)
YES
NO
EPS > EUP OR E4 > EU OR E4 < 0.0
YES
GO TO 41
NO
BMM (I) > BMM (I - 1)
YES
NO
IF TRIES GOING THROUGH THIS STEP MORE THAN 2 TIMES
YES
NO
TPHINC = PHINCR * 2.0
NO
TPHINC = 0.0
YES
I = I - 1
GO TO 16
TPHINC = TPHINC / 2.0
PHII (I) = PHII (I - 1) + TPHINC
E (I) = E (I - 1)
CALL AXIAL AND MOM CALCULATE FORCES AND MOMENTS
EPS > EUP OR E4 > EU OR E4 < 0.0
YES
NO
C
GO PHINCR / 2.0 BACK AND AHEAD ON M - ϕ CURVE
EPS > EUP OR E4 > EU
YES
NO
I = I - 1
GO TO 16

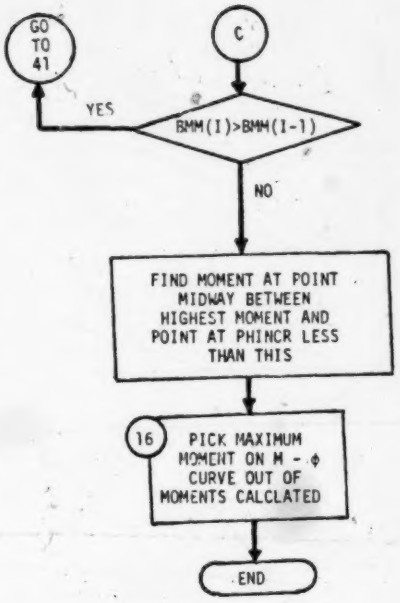
GO TO 41
C
YES
BMM(I)>BMM(I-1)
NO
FIND MOMENT AT POINT MIDWAY BETWEEN HIGHEST MOMENT AND POINT AT PHINCR LESS THAN THIS
16
PICK MAXIMUM MOMENT ON M - φ CURVE OUT OF MOMENTS CALCLATED
END

APPENDIX D

NOMENCLATURE

Alphabetic Symbols

a	depth of equivalent rectangular stress block
A_s	area of conventional reinforcement steel, sq. in.
A_{sp}	area of prestressing steel, sq. in.
b	cross section width on compression face, in.
b_w	width of web, in.
c	depth to neutral axis
C_c	compressive force in concrete, lb.
C_{cs}	compressive force that would have been exerted by concrete that is displaced by compression steel, lb.
C_s	compressive force due to compression reinforcing steel, lb.
d	effective depth, in.
d	depth to tension reinforcing steel, in.

d'	depth to compression reinforcing steel, in.
d_p	depth to prestressing steel, in.
d_t	depth of tension stress block in concrete.
e	eccentricity
E	modulus of elasticity of concrete (used with subscripts given later), psi, (mean value = $\bar{E}$)
E_c	modulus of elasticity of concrete, psi
E_s	modulus of elasticity of reinforcing steel, psi
E_{sp}	modulus of elasticity of prestressing steel, psi
f	strength of concrete (used with subscripts given later), psi, (mean value = $\bar{f}$)
f_{bot}	stress at the bottom of the section
f'_c	specified compressive strength of concrete, psi
f''_c	maximum stress in Hognestad (1952) stress-strain curve for concrete, psi
f_{cu}	the effective stress of the concrete in the compression zone, psi

$f_{jacking}$	stress in the prestressing steel due to the jacking force, psi
f_{ps}	calculated stress in the prestressing steel at design load, psi
f_{pu}	ultimate stress in prestressing steel, psi
f_r	modulus of rupture of concrete, psi
f_{se}	effective stress in prestressing steel, after losses, psi
$f_{specified}$	specified ultimate stress of prestressing steel, psi
f_{su}	prestressing steel stress at ultimate moment, psi
f_{top}	stress at the top of the section
$f_{transfer}$	stress in prestressing steel at transfer
f_y	yield strength of reinforcing steel, psi
F	strain compatibility factor
h	overall depth of cross section, in.
h_f	depth of flange, in.
I	moment of inertia
M	Moment

M_{cr}	cracking moment
M_{dl}	moment due to dead load, psi
M_u	ultimate moment, psi
n	number of prestressing tendons
P	resultant force acting on a cross section, lb.
P_o	prestress force at transfer
P_x	steel force at any point x
T_c	tension force in concrete, lb.
T_{sp}	tensile force due to prestressing steel, lb.
T_{sr}	tensile force due to tension reinforcing steel, lb.
V	coefficient of variation (used with subscripts given later)
$V_{in\text{-}batch}$	in-batch variability
V_s	coefficient of variation of the ratio of test strength to theoretical strength
V_{test}	variability due to different people testing and the errors implicit in the test itself
V_{theo}	variability of the theoretical model

y	distance from mid-height to the resultant compressive force in concrete
y_f	distance from mid-height to the resultant compressive concrete force in the flange
y_w	distance from mid-height to the resultant compressive concrete force in the web
Z_b	section modulus with respect to the bottom fiber of a cross section
Z_t	section modulus with respect to the top fiber of a cross section

In addition, the following symbols are used in subscript:

c	refers to "compressive" in conjunction with strength and elastic modulus
ccyl	refers to "compressive cylinders" in conjunction with strength
ci	refers to "initial tangent" in conjunction with modulus of elasticity
g	gross
r	refers to "modulus of rupture with third point loading"
R	refers to "rate of loading R psi/sec" corresponding to strength or modulus of elasticity

str	refers to "in-structure or *in-situ*" in conjunction with strength and modulus of elasticity
35	refers to "rate of loading 35 psi/sec" corresponding to compressive strength and modulus of elasticity

Greek Symbols

β	safety index
β	ratio of stress at 1 percent strain to ultimate stress for prestressing steel
β_1	a constant defined in Section 10.2.7 of the ACI Code (1971a)
Δ	prediction errors
Δ	increment
ε	strain, in./in.
ε_{ce}	the compressive strain in the concrete due to the prestressing force
ε_{cu}	the strain in the extreme concrete fiber in compression at ultimate moment
ε_{ps}	the total strain in the prestressing steel, in./in.
ε_r	cracking strain in concrete

ε_{se}	effective prestrain in prestressing steel after losses have taken place
ε_{su}	prestressing steel strain at ultimate moment
ε_t	strain at the level of the prestressing tendons
ε_y	yield strain of reinforcing steel
ε_u	ultimate strain in concrete
ε_{up}	ultimate strain in prestressing steel
ε_0	the strain in concrete that corresponds to the maximum stress in Hognestad's (1952) stress-strain curve for concrete
ε_1	the strain at the bottom of the section
ε_3	the strain at the bottom of the flange
ε_4	the strain at the top of the section
λ	overload factor
$\bar{\mu}$	mean value
ρ	ratio of nonprestressed tension reinforcement (= A_s/bd)
ρ'	ratio of nonprestressed compression reinforcement (= A'_s/bd)

ρ_p	ratio of prestressed reinforcement (= A_{sp}/bd)
σ	standard deviation
σ	stress
σ_1	stress at 1 percent strain for prestressing steel
ϕ	understrength factor
ϕ	curvature
ϕ_{cr}	cracking curvature
ω	= $\rho f_y/f'_c$
ω'	= $\rho' f_y/f'_c$
ω_p	= $\rho_p f_{ps}/f'_c$
$\omega_w, \omega_{pw}, \omega'_w$	reinforcement indices for flanged sections computed as for $\omega, \omega_p, \omega'$ except that b is the web width, and the steel area is that required to develop the compressive strength of the web only.

Units

The Monte Carlo study was carried out using the basic units of pounds and inches. Thus, the forces were in pounds, the dimensions were in inches, the stress was in psi, and the moment was in in-lbs.